

DESIGN, CALIBRATION, AND EXPERIMENTS TO IMPROVE THE FEASIBILITY
OF STUDENT-BUILT MAGNETOMETERS FOR HELIOPHYSICS RESEARCH

By

Austin David Cohen, B.S.

A Master's Thesis Submitted in Partial Fulfillment of the Requirements

for the Degree of

Master of Science

in

Physics

University of Alaska Fairbanks

August 2023

APPROVED:

Dr. Dogacan Ozturk, Committee Chair

Dr. Don Hampton, Committee Member

Dr. Peter Delamere, Committee Member

Dr. Michael Hull, Committee Member

Liya Billa, Graduate Coordinator

Dr. Martin Truffer, Chair

Department of Physics

Dr. Karsten Hueffer, Dean

College of Natural Science and Mathematics

Dr. Richard Collins, Director

The Graduate School

Abstract

Dynamic interactions between the solar wind and the Earth's magnetosphere can create strong geomagnetic field disturbances and trigger geomagnetically induced currents. Geomagnetically induced currents may cause damage to infrastructure such as damage to high-voltage power transformers and increased corrosion of pipelines. Ground observations of geomagnetic fields are widely used for geomagnetically induced current studies; however, there is insufficient information on the spatial extent of the localized geomagnetically induced current events due to a lack of spatial coverage. The Space Weather UnderGround is an education and outreach program, first initiated by Dr. Charles Smith at the University of New Hampshire and expanded to the University of Alaska Fairbanks. The Space Weather UnderGround program is aimed to educate high school students on space weather phenomena while equipping them with STEM skills. Students who participate learn to build a semi-professional magnetometer kit which is then used by researchers as a cost-effective and research-capable array of magnetometers across Alaska and New Hampshire. The Space Weather UnderGround magnetometer array provides high resolution geomagnetic field data with 1nT/s accuracy, and the data is made publicly available for improving our understanding and prediction of geomagnetically induced currents. Several University of Alaska Fairbanks Space Weather UnderGround magnetometer designs have been developed between 2021 and 2023, and various experiments and calibrations have been conducted to improve their applicability towards heliophysics research. This thesis will give a brief introduction to magnetometers and space weather, while focusing on the Simple Aurora Monitor and its use in the Space Weather UnderGround program. Next, sensor and deployment experiments will be described, including deployment vessels developed by the University of Alaska Fairbanks Space Weather UnderGround team. Finally, the data acquisition process, along with the educational outcomes of the project, will be discussed.

Table of Contents

	Page
Abstract	i
Table of Contents.....	ii
List of Figures	v
List of Tables.....	vii
List of Appendices	viii
Chapter 1 Introduction to Magnetometers	1
1.1 History and Background	1
1.2 Types of Magnetometers.....	1
1.2.1 Search-coil Magnetometers	1
1.2.2 Superconducting Quantum Interference Device.....	3
1.2.3 Hall Effect Magnetometers	4
1.2.4 Fluxgate Magnetometers	4
1.3 Goals of the Thesis.....	7
Chapter 2 Introduction to Space Weather.....	7
2.1 Sun-Earth Interactions.....	7
2.2 Introduction to the Magnetosphere.....	8
2.3 Introduction to the Ionosphere.....	10
2.3.1 Types of Ionospheric Current Systems	10
2.3.2 Substorm Current Wedge.....	11
2.3.3 Auroral Electrojets	12
2.3.4 Induced Current Systems	13
Chapter 3 Simple Aurora Monitor III Magnetometer	14
3.1 History and Introduction	14
3.1.1 Technical Specifications, Applications, and Properties.....	14
3.2 Construction Procedure	16
3.2.1 Required Tools	17
3.2.2 Begin Assembly	18

3.2.3 Keyboard Construction.....	19
3.2.4 Main Printed Circuit Board	19
3.2.5 Serial and Display.....	23
3.2.6 Software Installation.....	24
Chapter 4 SAM-III Sensor Experiments.....	25
4.1 Introduction to the Experiments.....	25
4.2 Proximity Experiments to Determine Crosstalk Distance.....	26
4.3 Accuracy/Validation Experiment with Known Rate of Change.....	28
4.4 Temperature Experiments for Calibration	29
4.4.1 Temperature Data Loggers Used During Calibrations.....	30
4.4.2 Roof Experiment Using Polynomial Fit Methods	32
4.4.3 Cooler Experiment with Known Rate of Change.....	33
Chapter 5 Deployment Experiments.....	35
5.1 Considerations for Alaska Specific Deployments.....	35
5.2 Deployment Types.....	36
5.2.1 Anchor and L-Types.....	36
5.2.2 Box Types	37
5.2.3 Multiple Deployment Vessel	39
Chapter 6 UAF SWUG Data Acquisition.....	41
6.1 Computer and Initial Set-up	41
6.2 UAF SWUG Network System.....	42
6.3 UAF SWUG Data Center	43
Chapter 7 Educational Applications.....	44
7.1 Introduction to SWUG	44
7.1.1 Similar Projects.....	45
7.2 UAF Programs.....	45
7.2.1 Summer High School Student Internship Program	46
7.2.2 Educator Development Program	47
Chapter 8 Conclusion and Outlook	50

8.1 Conclusion.....	50
8.2 Outlook	50
References.....	51

List of Figures

	Page
Figure 1.1: Search-coil used in THEMIS spacecraft.....	3
Figure 1.2: SQUID Schematic.....	4
Figure 1.3: Sketch of basic fluxgate.....	6
Figure 2.1: Parker spiral.....	8
Figure 2.2: Simplified magnetosphere diagram.....	9
Figure 2.3: Current system graphs.....	11
Figure 2.4: Substorm current wedge from Figure 1a of Kepko et al. (2014).	12
Figure 2.5: Geoelectric field from magnetic field using time domain method.	13
Figure 3.1: Completed SAM-III kit.....	14
Figure 3.2: Narod photo.	15
Figure 3.3: SAM-III kit step-by-step construction flow.	17
Figure 3.4: Main SAM-III PCB.	19
Figure 3.5: Power cable procedure overview.....	20
Figure 3.6: Finished power cable.	21
Figure 3.7: Power supply test voltage guide.....	22
Figure 3.8: Finished main PCB.	23
Figure 3.9: Serial port cable.....	23
Figure 3.10: SAM-III ready for software setup.....	24
Figure 3.11: Final screen.....	25
Figure 4.1: Original separation distance experiment.....	27
Figure 4.2: The new separation distance experiment.....	28
Figure 4.3: Disco ball setup and results.....	29
Figure 4.4. Reichardt roof magnetometer data with the temperature data.	30
Figure 4.5: Options tested for temperature data collection.....	31
Figure 4.6: Elegoo Uno R3 and DS18B20.....	32
Figure 4.7: Applied linear fit.	33
Figure 4.8: Disco motor temperature experiment setup.....	34

Figure 4.9: Disco ball temperature experiment data.....	35
Figure 5.1: In order from left to right: L-Type, MDV, A-Type, and B-Type.	36
Figure 5.2: A-Type (Left) and L-Type (Right).....	37
Figure 5.3: B1-Type.....	38
Figure 5.4: Location of the power source on the B1-Type from Reyes (2021).	38
Figure 5.5: Red B1-Type.	38
Figure 5.6: Inside MDV (left) and outside sideview (right).	39
Figure 6.1: Example data from mini-PC.....	42
Figure 6.2: Example of a directory from SWUG Atlas.	43
Figure 6.3: GIMA Poker Flat data compared to UAF SWUG Poker Flat data.	44
Figure 7.1: Students working in the laboratory.	46
Figure 7.2: Satellite by Savion (14) & Aurora by Bethany (17).	47
Figure 7.3: Educator Development Program 2021.	48
Figure 7.4: Educator Development Program 2022.	48
Figure 7.5: Students working on kits during their lab time.	49

List of Tables

Table 2.1: Ionospheric regions with distance and density peak height.....	10
Table 3.1: SAM-III Technical Specifications.....	16
Table 3.2: Required and optional tools.....	18
Table 4.1: Temperature device price comparison.....	31
Table 5.1: Type price comparison.....	40
Table 5.2: Supply list with cost breakdown.....	40

List of Appendices

Appendix A: Temperature sensor Arduino code.....	55
Appendix B: Polynomial fit python code.....	57
Appendix C: UAF SWUG SAM Student Manual.....	59
Appendix D: UAF SWUG Deployment Manual.....	98
Appendix E: Comprehensive Manual for the SWUG Multi-Deployment-Vessel.....	144

Chapter 1 Introduction to Magnetometers

1.1 History and Background

The magnetometer's inception is attributed to Carl Friedrich Gauss (of Gauss' Law) in 1834, where he used only a bar magnet and gold suspension wire, to measure the period of the oscillations of the magnet to determine magnetic field strength (Schumacher, 1836). Over the course of about 200 years, magnetometer technology has been improved upon and has become an important instrument to include in ground-based observatories or space-based missions. While used for detecting magnetic perturbations, magnetometers have a variety of aeronomy, education, hobby, and military applications. This chapter will briefly outline several popular types of magnetometers.

1.2 Types of Magnetometers

Edelstein (2007) separates magnetometers into two different types: vector and scalar. Vector magnetometers are designed to measure the components of the magnetic field, while a scalar magnetometer will measure the magnitude of the local field. Scalar magnetometers, or more commonly referred to as total field magnetometers, are invariant to variations occurring from movement and rotations. This design allows smoother measurements when collected on a moving object. However, since vector magnetometers allow measurements along multiple components, they can provide more information than their magnitude gathering counterparts (Edelstein, 2007).

1.2.1 Search-coil Magnetometers

A search-coil magnetometer is a vector magnetometer that uses a magnetically permeable rod wrapped in a conductive coil to measure the time dependent change in the magnetic flux. The magnetic flux within the coil changes if exposed to time varying magnetic fields, rotation through uniform fields, or moved through a non-uniform field. A voltage is then seen across the sensor that is proportional to the rate of change of flux

that passes through the coil. Depending on the coil's ratio of its inductance to its resistance, a frequency response will be produced from this voltage within the range between 1 Hz to 1 MHz (Edelstein, 2007).

Roux et al. (2008) provides a fundamental formulation for the search coil principle. Lenz's law states that induced current and magnetic flux flow in a direction to go against the change of flow within a circuit (Jackson, 1999). Using this principle:

$$e = -N \left(\frac{d\phi}{dt} \right) \quad 1.1$$

where e is the electromotive force, N is the number of wraps around the core, and ϕ is magnetic flux across a loop. From this, the electromotive force, which is the measure of the work done per unit charge (Griffiths, 2017), becomes:

$$e = NS \left(\frac{1}{L} \int_0^L \mu_{app}(l) dl \right) B_{ext} \omega \quad 1.2$$

where S is the cross section of the core, L is the length of the core, ω is the frequency response, B_{ext} is the external magnetic induction, and μ_{app} is the apparent field given by:

$$\mu_{app}(m) = \frac{B_{core}}{B_{ext}} = \frac{\mu_r}{[1 + (\mu_r - 1) N_z(m)]} \quad 1.3$$

where B_{core} is the core magnetic induction, μ_r is the relative permeability, and $N_z(m)$ is the coefficient of the demagnetizing field as a function of m , the ratio of the length and the diameter of the core. If $\mu_r \gg 1$, then equation 1.3 can be simplified to:

$$\mu_{app}(m) = \frac{1}{N_z(m)}, \text{ if } \mu_r \gg 1 \quad 1.4$$

From equation 1.4, minimizing $N_z(m)$ will increase $\mu_{app}(m)$, and thus increase magnetic amplification since $\mu_{app}(m) = \frac{B_{core}}{B_{ext}}$. Figure 1.1 shows an example of a search-coil used in the Time History of Events and Macroscale during Substorms (THEMIS) spacecraft. The coil has yet to be installed inside a deployment vessel.

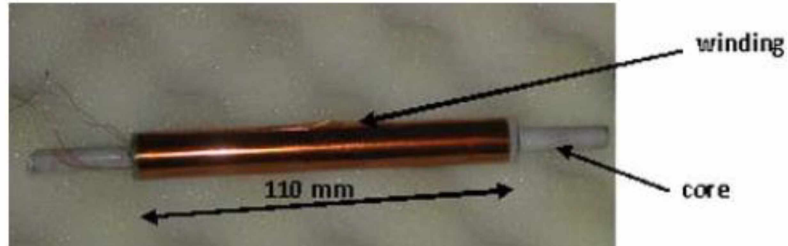


Figure 1.1: Search-coil used in THEMIS spacecraft before insulation and mounting. *Adapted from Roux et al. (2008).*

1.2.2 Superconducting Quantum Interference Device

The superconducting quantum interference device (SQUID) is a very sensitive vector magnetometer used in measuring magnetic fields at frequencies less than 1 Hz. Magnetic flux through a superconducting ring (see Figure 1.2) becomes quantized and experiences periodic flux variations (Edelstein, 2007). These variations are examined to measure the current in the superconductor. The ring is coupled inductively to a radio frequency tuned circuit which provides a known magnetic field and is used as the detector's output. The changes in the field are measured by calculating the peaks resulting from flux quantization or alternatively by applying a feedback loop in order to keep the radio frequency tuned circuit at a single peak. The current generated from this feedback is then used to measure the magnetic field (Edelstein, 2007).

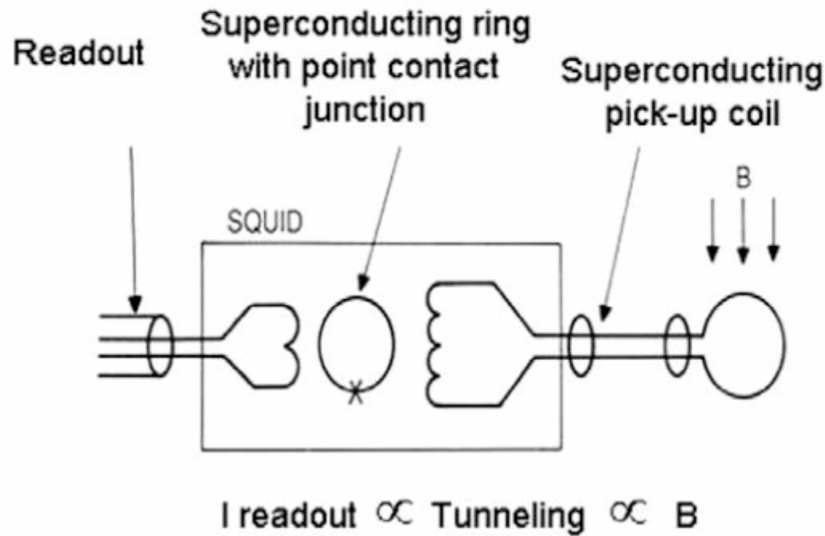


Figure 1.2: SQUID Schematic. Magnetic flux through ring quantizes and experiences flux variations which is used for measurement. *Adapted from* Figure 2 of Edelstein (2007).

1.2.3 Hall Effect Magnetometers

Hall effect sensors are low-cost vector magnetometers that use semiconductors to boost the strength of the Hall effect and from this determine a Hall voltage (Edelstein, 2007). Jackson (1999) explains that the Hall effect occurs when an electric field and transverse magnetic field are applied to a conductor or a semiconductor. Current will then flow through the conductor and induce an electric field in an orthogonal direction to both the applied magnetic and electric field. The result of this induction is a voltage difference between the sides of the conductor. Depending on the material used, the magnetic sensitivity lies between 10^{-3} and 10^3 Gauss or 10^2 nT and 10^8 nT with an upper-frequency limit of 1 MHz (Edelstein, 2007).

1.2.4 Fluxgate Magnetometers

Fluxgate sensors are commonly used in part due to their sensitivity, stability, and robustness, which is why they are used in ground-based observatories and used on sounding rockets, low-altitude satellites, and this study. They are even used in flagship NASA missions like THEMIS (Roux et al., 2008), the Magnetospheric Multiscale

(MMS) (Russel, 2016), and the Radiation Belt Storm Probes (RBSP) (Kletzing, 2013). Primdahl (1979) illustrates a simple example of the flux gate principle. A fluxgate sensor (see Figure 1.3) contains a ferromagnetic core that is wrapped with a conducting pick-up coil. An external magnetic field (such as Earth's field) along the core's axis induces magnetic flux within the core, changing the core's magnetization. The magnetic field inside the core is:

$$H = \frac{B}{\mu_0} - M \quad 1.5$$

where B is the magnetic induction, μ_0 is the permeability of free space, and M is the magnetization with $M = \chi H$ and $\chi = \mu_r - 1$, where μ_r is the relative permeability. Due to the magnetization change, the permeability changes which, induces a voltage on the pick-up coil:

$$V_{sec} = nA \frac{dB}{dt} \quad 1.6$$

where A is the cross-sectional area of the core and n is the number of wraps. B is proportional to the external induction B_{ex} if it is small. Thus, B inside the core can be expressed as:

$$B = \mu_0 (H + M) = \mu_a B_{ex} \quad 1.7$$

where μ_a is the apparent magnetization. Using $M = \chi H$, where $H = H_{ex} - DM$, where D is the demagnetizing factor, and $H_{ex} = \frac{B_{ex}}{\mu_0}$, substitute into equation 1.7:

$$B = \frac{\mu_r B_{ex}}{1 + D (\mu_r - 1)}. \quad 1.8$$

Now substituting equation 1.8 into equation 1.6:

$$V_{sec} = \frac{nAB_{ex} (1 - D)}{[1 + D(\mu_r - 1)]^2} \left(\frac{d\mu_r}{dt} \right). \quad 1.9$$

Primdahl (1979) calls equation 1.9 the basic fluxgate equation.

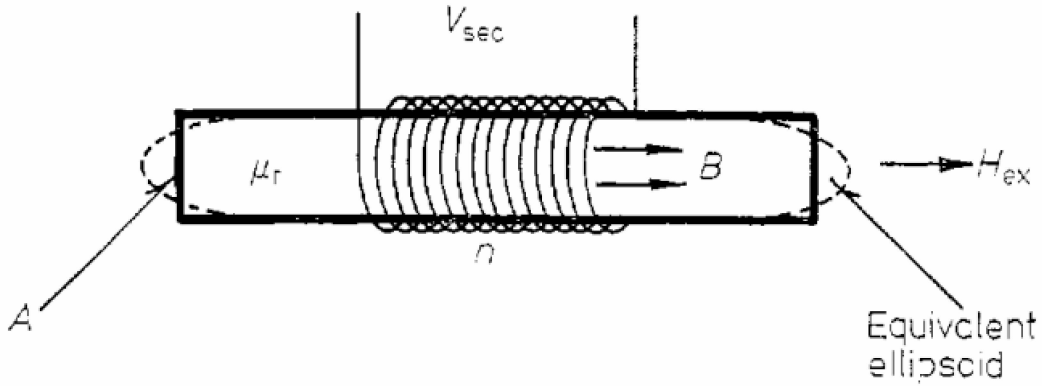


Figure 1.3: Sketch of basic fluxgate where A is the cross-sectional area of the core, B is the magnetic induction inside the core, n is the number of wraps of the pick-up coil, μ_r is the relative permeability of the core which is equivalent to $1 + \chi$ where χ is the susceptibility, H_{ex} is the external magnetic field, and V_{sec} is the induced voltage. *Adapted from* Figure 1 of Primdahl (1979).

Edelstein (2007) describes the typical fluxgate magnetometer as containing a ferromagnetic core that has a drive coil and sense coil wrapped around it. An alternating current is applied to the drive coil in order to saturate the core to a prespecified magnetization. Once saturated, the core becomes resistant to the external magnetic field which makes it difficult for the field to pass through the core. The change in the field ($\frac{dB}{dt}$) from this resistance is then detected by the sense coil. An output voltage produced by the sense coil is then used for the measurement.

Standard fluxgate magnetometers are sensitive to temperature changes (Primdahl, 1970). While Ripka (2001) and Primdahl (1979) explain that more sensitive devices can be designed to be temperature stable, modern commonly available fluxgates like the FG3+ (see chapter 4) have explicit sensitivity to temperature changes. According to Primdahl (1970), this dependence is linearly proportional to the measured magnetic field.

1.3 Goals of the Thesis

Magnetometers are key in gathering information on Sun-Earth interactions, Earth's magnetic field, solar wind, and ionospheric current systems (Menk et al., 2013). These observatories are used to study geomagnetic variations which can aid in the study of geomagnetically induced currents (GIC) (Menk et al., 2013).

This thesis aims to answer the following questions regarding the use of magnetometers across Alaska:

1. Can the spatial coverage of magnetometers be increased across Alaska where infrastructure is limited (Chapter 7)?
2. If so, can these magnetometers be procured in a cost-effective manner (Chapter 3)?
3. Are the magnetometer sensors able to perform well at detecting magnetic fields (Chapter 4)?
4. Could these cost-effective magnetometers be optimized to perform in Alaska specific conditions (Chapter 5)?
5. Can they perform on par with the more expensive science grade magnetometers (Chapter 6)?
6. Can they detect geomagnetic disturbances (GMDs) and be used for geomagnetically induced current (GIC) research (Chapter 2)?

Chapter 2 Introduction to Space Weather

2.1 Sun-Earth Interactions

The Sun and its atmosphere are made up of plasma (Cravens, 1997). Plasma is continuously ejected from the Sun and streams towards the Earth in a spiral motion due to the Sun's rotation around its own axis called the Parker spiral (see Figure 2.1) (Parker 1958). This continuous stream is known as the solar wind. The solar wind flows supersonically, on the order of a few hundred kilometers per second, and carries with it the interplanetary magnetic field. The interplanetary magnetic field (IMF) is the

magnetic field that has become embedded, or frozen-in, into the solar wind that reaches from the Sun into interplanetary space (Menk et al., 2013).

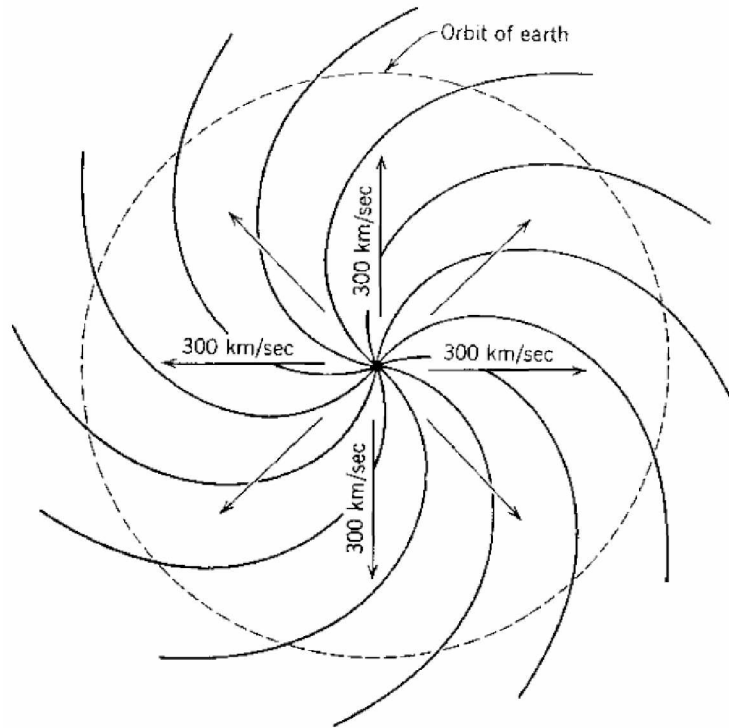


Figure 2.1: Parker spiral. Plasma is ejected from the Sun and forms a spiral pattern called the Parker spiral. *Adapted from Cravens (1997).*

2.2 Introduction to the Magnetosphere

The Earth's magnetosphere occurs as a result of the interaction between the Earth's magnetic dipole field and the solar wind. Protons and electrons from the solar wind are not able to penetrate through the magnetic field and become deflected which creates a boundary called the magnetopause. Because the solar wind flow speed is supersonic, a bow shock is created upstream. Downstream, the plasma slows down to subsonic speeds and rises in temperature which creates a region known as the magnetosheath (Cravens, 1997). Even though the solar wind plasma is confined inside the magnetosheath, when geomagnetic and interplanetary field lines merge in a process called magnetic reconnection, the solar wind magnetic field lines are able to penetrate into the magnetosphere (Gombosi, 1998). Figure 2.2 shows a visual representation of the magnetosphere.

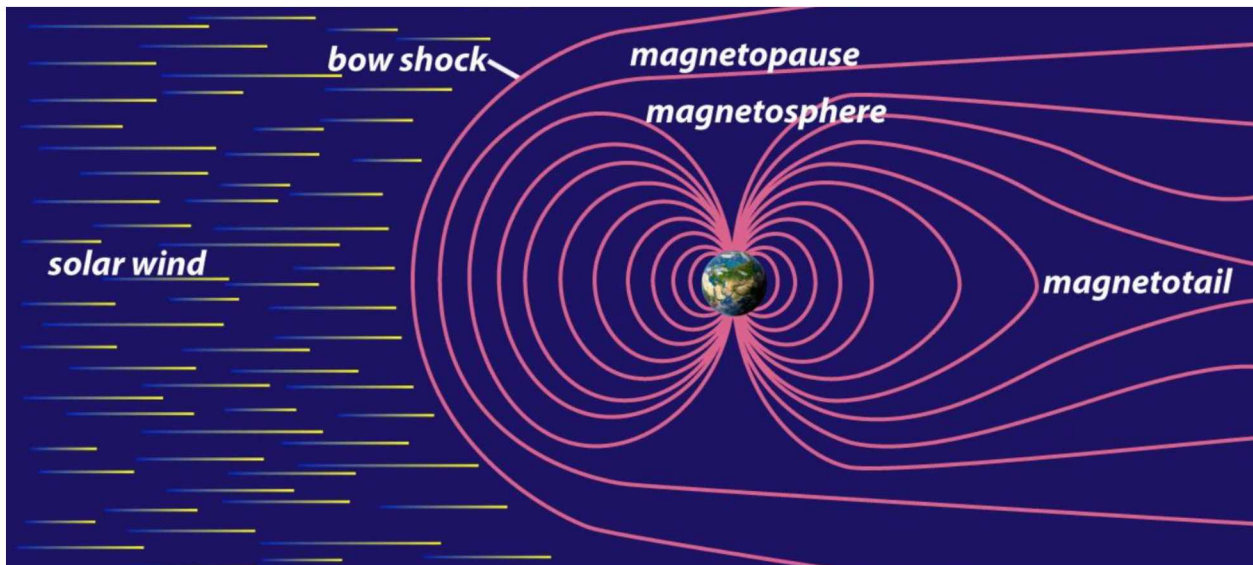


Figure 2.2: Simplified magnetosphere diagram that shows the basic structure of Earth's magnetosphere. *Adapted from Study.com.*

The solar wind particles can directly enter the Earth's upper atmosphere by being deposited into the cusp region on the dayside through open magnetic field lines (Schunk and Nagy, 2009). This cusp region is a funnel-like boundary layer that extends into the magnetosphere (Cravens, 1997). In addition, solar wind can even be deposited along the magnetotail, the night side region where the magnetic field lines are elongated. Solar wind from the tail will then fill up the center region of the night side known as the plasmashet. Some particles in the plasmashet have direct access to Earth's upper atmosphere through magnetic field lines that have a narrow latitudinal band at low altitudes, but a wide longitudinal band around the Earth. These field lines combine to form the auroral oval (Schunk and Nagy, 2009). The auroral oval forms in both the north and south and is the region where aurorae and significant magnetic field disturbances can be observed (Kivelson and Russel, 1997)

2.3 Introduction to the Ionosphere

The Earth's ionosphere is the ionized region of the atmosphere located about sixty to a thousand kilometers above the surface of the Earth. The ionosphere is characterized by large numbers of free electrons and ions created by the photoionization of neutral molecules from solar photons (Schunk and Nagy, 2009). There are four regions of the ionosphere (see Table 2.1). However, at night the D and F_1 regions disappear. Each region is determined by their respective electron density (Gombosi, 1998)

Region	Distance (in km) from surface of the Earth (approximate)	Electron density peak height (in km) (approximate)
D	60 — 90	90
E	90 — 140	110
F_1	140 — 200	200
F_2	200 — 500	300

Table 2.1: Ionospheric regions with distance and density peak height. Distances are approximate values. *Adapted from Gombosi (1998).*

2.3.1 Types of Ionospheric Current Systems

Pressure from the solar wind compresses Earth's magnetic field on the dayside which gives rise to the magnetopause current system known as the Chapman-Ferraro current system which flows across the magnetopause. The nightside is subsequently stretched giving rise to magnetotail currents. This tail current system flows in the center of the magnetotail from dawn to dusk while also creating current loops around the magnetotail's center, thus, closing the current within the magnetopause (Ganuskina et al., 2018).

Charged particles gyrate along the magnetic field lines, reflect near the poles, which causes them to bounce back and forth from the Northern and Southern Hemisphere, and will then drift azimuthally due to the curvature of the magnetic field.

Ions will drift westward while electrons will drift eastward. This drift in conjunction with the gyromotion gives rise to the ring current system (Ganushkina et al., 2018). In addition, electrons carrying current along the magnetic field lines connect with magnetospheric currents to give rise to the field-aligned current systems called Region 1 and Region 2 (Ganushkina et al., 2018). Region 1 current system is a downward dawnside and upward duskside field aligned current system that is the result of the connection between open magnetic field lines from the solar wind and magnetopause with the polar cap ionosphere, while Region 2 is the result of the connection between the plasmasheet to the ionosphere along the closed magnetic field lines (Cravens, 1997). Figure 2.3 from Ganushkina et al. (2018) gives a three-dimensional representation of each previously mentioned current system.

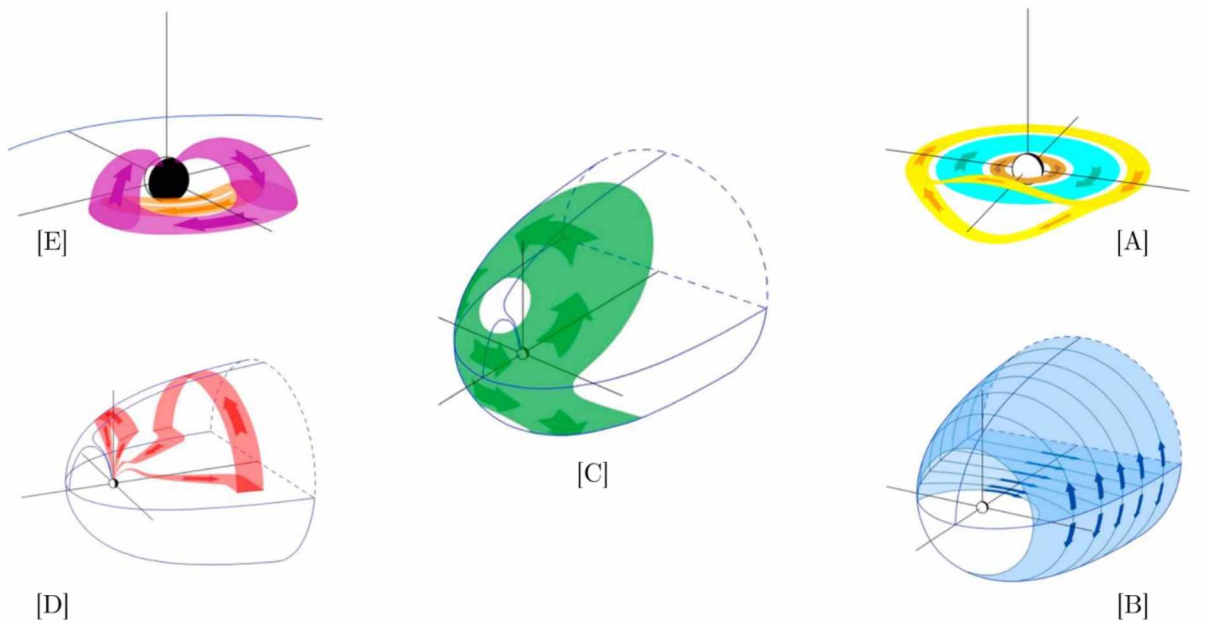


Figure 2.3: Current system graphs. [A] ring current system. [B] tail current system. [C] Chapman-Ferraro current system. [D] Region 1 current system. [E] Region 2 current system. *Adapted from* Ganushkina et al. (2018).

2.3.2 Substorm Current Wedge

Magnetic field measurements taken from ground-based observatories show variations during presence of strong auroral activity (Kepko et al., 2014). When enough energy is deposited into the magnetosphere and is released into the ionosphere, this

creates a significant auroral event known as an auroral substorm (Schunk and Nagy, 2009). Patterns of ionospheric current systems drive the substorms' growth (Kepko et al., 2014). However, the patterns are not yet identified. One of the proposed scenarios from Kepko et al. (2014) is through one-cell and two-cell convection patterns that occur during different phases of a substorm. Kepko et al. (2014) call this resulting pattern the substorm current wedge (see Figure 2.4).

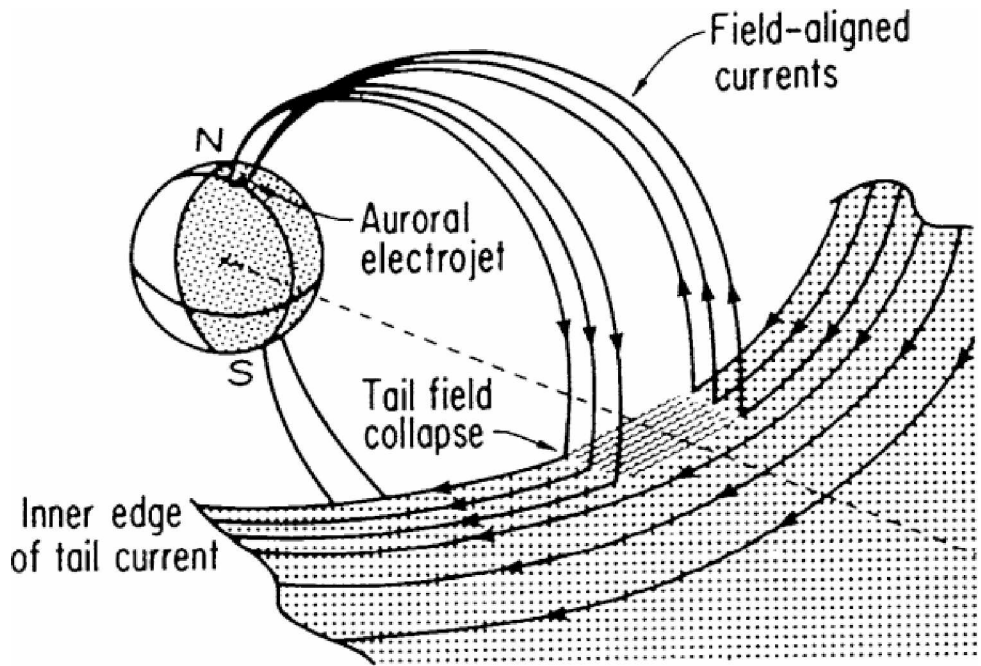


Figure 2.4: Substorm current wedge from Figure 1a of Kepko et al. (2014). The tail current is being diverted from the northern and southern ionospheres. *Adapted from* Kepko et al. (2014).

2.3.3 Auroral Electrojets

The auroral electrojets are Hall currents (currents perpendicular to both the electric and magnetic field) flowing eastward in the dusk sector and westward in the dawn sector around the auroral oval. The closure of the substorm current wedge feeds the westward electrojet and allows the electrojet to enhance in the midnight sector. This enhancement occurs predominantly in the winter in the Northern Hemisphere, giving rise to more substorm activity (Guo et al., 2014). Electrojet current densities from

these enhancements have been reported to be around 1 to 30 $\mu\text{A}/\text{m}^2$, leading to $\frac{dB}{dt}$ values on the order of several hundred nT/min.

2.3.4 Induced Current Systems

High-latitude regions experience geomagnetic field disturbances when the auroral electrojet currents intensify during auroral substorms. These disturbances, when accompanied by a large time rate of change in the geomagnetic field, will produce significant geoelectric fields resulting in geomagnetically induced currents (GIC) (Kappenman, 2003). GICs along power lines reduce the reliability of an electrical network by damaging transformers, and potentially causing outages (NERC, 2013). According to Beggan (2015), there are three activities needed to compute GIC within an electrical network. These activities are: modelling the region's conductivity structure, gathering temporal and spatial magnetic field measurements, and gathering information regarding the electrical network's topology and electrical properties.

GIC modeling can be used to further understand forecasting, occurrences, and causes of GIC. Observational GIC data are crucial for validating and deriving these models. Suggested means of forecasting is done by collecting magnetic observatory data and conducting magnetotelluric surveys to estimate the geoelectric field (Pulkkinen, 2017). The geoelectric field could be calculated using magnetic field data. Collecting a time series of magnetic field values, an applied Fast Fourier Transform (FFT) obtains the frequency spectrum of the magnetic field variations. From this, the geoelectric field spectral values ($E(\omega)$) are obtained by multiplying the magnetic field spectral values ($H(\omega)$) with the surface impedance values ($Z(\omega)$). Applying an inverse Fast Fourier Transform (IFFT) over the geoelectric field spectral values yields a time series of geoelectric field values (see Figure 2.5) (NERC, 2013).

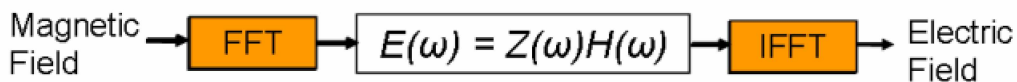


Figure 2.5: Obtaining geoelectric field values from magnetic field values using time domain method. *Adapted from* NERC (2013).

3.1 History and Introduction

The Simple Aurora Monitor (SAM) magnetometer systems are a family of magnetometer systems where the iteration of each system is based on the number of maximum coordinate axis the system can support. Thus, the SAM-II magnetometer can support up to a two-axis configuration, while the SAM-III magnetometer can support up to a three-axis configuration. The hardware and software were designed by Dirk Langenbach and Karsten Hansky respectively. The sensors at the core of the system are the three-axis fluxgate magnetometer or FG-3 sensors from Speake & Co Llanfapley (Reeve, 2018). The SAM-III kits are the topic of discussion in this chapter.

3.1.1 Technical Specifications, Applications, and Properties

Whitham Reeve, of Reeve's Engineers, published a comprehensive guide and construction manual that details the method for one to craft their own SAM-III kit. The user has the option to purchase a printed circuit board (PCB) with all the components already installed or to solder all the mounted components such as resistors, capacitors, and diodes. The kit can be purchased from Reeve's Engineers for approximately \$300-\$400 depending on part availability. Figure 3.1 shows a completed SAM-III kit.



Figure 3.1: Completed SAM-III kit. As of May 2023, this is the latest optional enclosure for the SAM-III.

The device has a measurement range of approximately ± 50000 nT with a resolution of 1—2 nT at 1 Hz (Reeve, 2018). This resolution of 1 nT differs greatly from the pico-Tesla order Narod ring-core fluxgate magnetometer (named after Barry Narod) that the Geophysical Institute Magnetometer Array (GIMA) uses (Osborn, 1991) (see Figure 3.2). While the accuracy is significantly different by three orders of magnitude, according to Zou et al. (2022) resolutions within 1 nT to 5 nT can detect geomagnetic disturbances that are used in the study of current induced ground perturbations (Engebretson et al., 2019).



Figure 3.2: Narod photo. The lid has been removed to show the internal components of the device. *Adapted from* Osborn (1991).

It is also useful to note the price difference. The price of the Narod magnetometer system is approximately \$82,000 USD (Osborn, 1991). Though no longer available, when adjusted for inflation, the price becomes approximately \$180,000 USD. This is about five hundred times that of the SAM-III. The cheaper price of the SAM-III kits makes them more accessible to students, teachers, and citizen scientists. Table 3.1 lists the important

technical specifications for the SAM-III which can be found explicitly in the SAM-III construction manual (Reeve, 2018).

Magnetic field magnitude range	approximately ± 50000 nT
Magnetic field resolution	1—2 nT
Connectors /Connections	8-pin pluggable terminal block (input/output) 10-pin pluggable terminal block (sensors) EIA-232: DB-9M (serial port) DC coaxial 2.1 mm x 5.5 mm, center + (power)
Real-time clock	16 MHz clock controlled by microprocessor with backup battery
Display	4x20 STN LCD
Power	12 V DC power at 60—100 mA (depends on the number of sensors)
Keyboard	Compatibility via surface mounted ribbon plugs

Table 3.1: SAM-III Technical Specifications. All adapters and cables are included with the kit. *Adapted from* Reeve (2018).

3.2 Construction Procedure

The SAM-III kits come with a comprehensive construction manual that is written by Whitham Reeve (Reeve, 2018). Construction of the SAM-III requires tasks such as soldering, crimping, taking voltage and current readings with multimeters, and careful component placement. Many of the components are small and unfamiliar to students and teachers. This creates a barrier that raises the entry-level required for building these kits.

Appendix C contains the University of Alaska Fairbanks Space Weather Underground (UAF SWUG) student manual written by Austin Cohen as part of the

physics bachelors capstone project requirements. This manual contains adaptations and additions to the Reeve Engineering construction manual to make it accessible to high school students. Figure 3.3 shows the fundamental steps for the SAM-III construction process. The first step is to gather all the equipment needed (see Table 3.2), find the main PCB, and separate the parts. The second step is to solder all the parts. Lastly, put all the cables together and insert them into the optional enclosure (see Reeve (2018) for information regarding the enclosure).

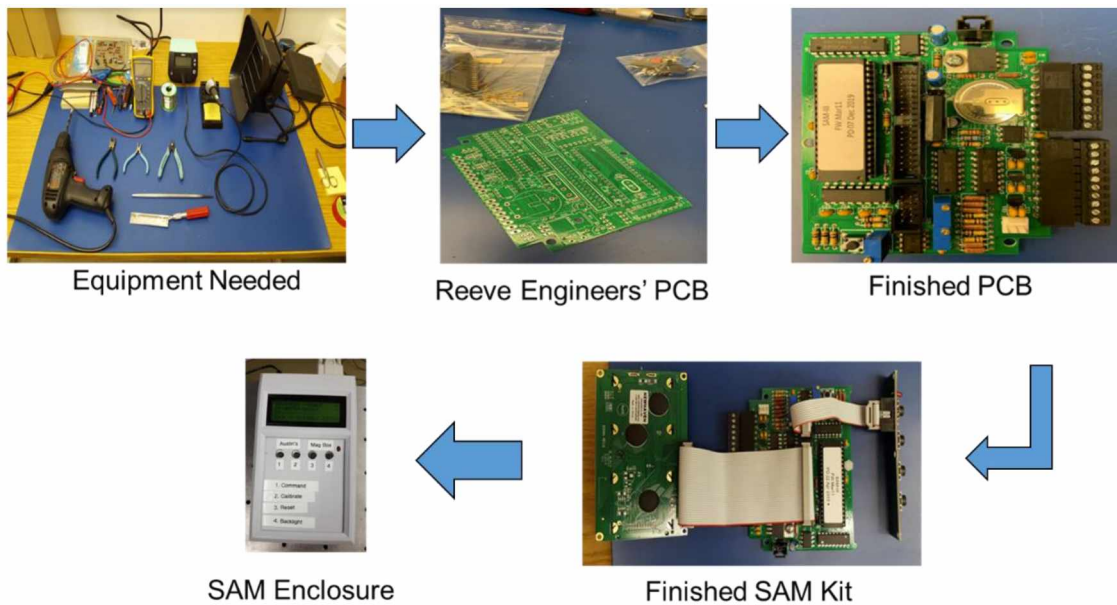


Figure 3.3: SAM-III kit step-by-step construction flow. Through the SWUG program, supplies, tools, and kits are provided.

3.2.1 Required Tools

Several tools are required to fully construct the SAM-III device, but not all of the tools are provided as part of the SAM-III kit. Table 3.2 is a comprehensive list of all the tools an individual needs to acquire before constructing a kit (with some optional tools that will help). If participating in a UAF SWUG summer program, tools will be provided to participants.

Required	Optional
Soldering iron	Electrical tape or heat shrink tubes
Solder	Heat gun or hot hair dryer
Wire stripper (16-24 AWG)	Vise or helping hands
Wire cutter (micro)	Needle nose pliers, or crimping tools
Multimeter	Soldering mat
Small flat-head screwdriver (approx. 0.25 mm x 1.5 mm head)	Jumper wires
Computer with USB plugin	Desoldering tools (wick, suckers, etc.)

Table 3.2: Required and optional tools. Optional tools are still highly recommended, but the process can be done without them.

3.2.2 Begin Assembly

After gathering the necessary tools, the SAM-III construction process begins. Refer to the SAM-III Construction Manual (Reeve, 2018) from Whitham Reeve from his website or the UAF SWUG SAM Student Manual (Appendix C) for detailed, step-by-step instructions. The PCB's has been labeled for each component making it easier to determine where each part needs to be soldered.

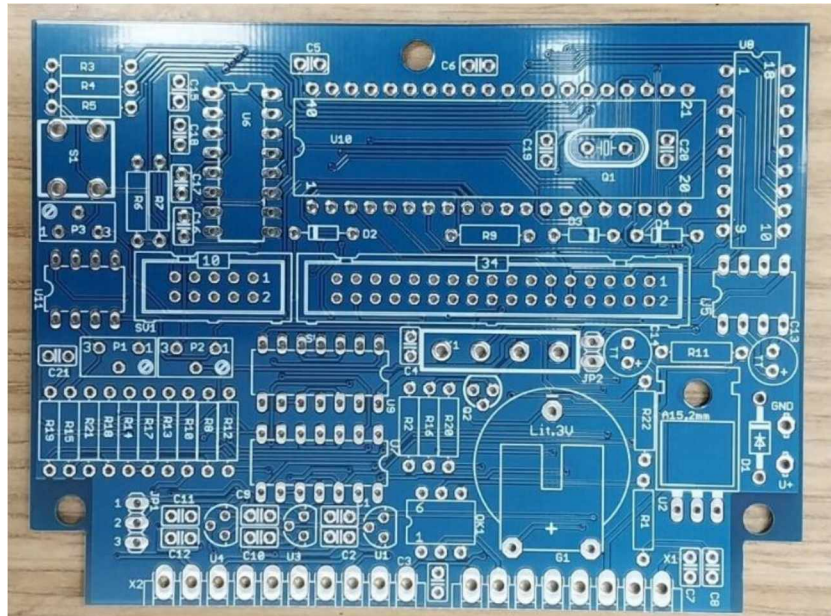


Figure 3.4: Main SAM-III PCB. All the parts are labeled on the PCB, making it clear to determine which part goes where.

3.2.3 Keyboard Construction

The keyboard is the first recommended piece to be constructed as it has large solder pads. Larger solder pads provide sufficient practice before trying to solder components onto the smaller pads of the main circuit board. However, in our experience, the small LED component orientation on the keyboard has been the first question raised by participants in the SWUG Educator Program (Section 7.2). To help with this, the use of learn-to-solder LED kits is highly recommended. This way, individuals understand certain components have orientation dependencies.

3.2.4 Main Printed Circuit Board

The next component to be constructed is the main printed circuit board (PCB). This is where the majority of time will be spent. The resistors are the first to be soldered. Each resistor is either color-coded or has an ohmic reference number to identify the component. A resistor chart is provided in the manuals, but the resistors still incite problems. For beginners in electronics and circuits, becoming familiar with the resistor chart could take some time. The effective use of a multimeter eliminates the need for charts and reference numbers. Thus, instructions on multimeter use, as well as

resistor charts are included in the UAF SWUG SAM Student Manual (Appendix C) to give the student a choice of which method to use.

The capacitors and the diodes are the next components to be soldered after the resistors have been successfully installed. The 100 nF ceramic capacitors require no orientation while being soldered on the board, but the diodes need to be placed with the correct orientation. Even though the diodes have indicators that match up with the board, it could still be confusing for students and teachers attempting to find the correct placement. Having an instructor overseeing the construction process alleviates this issue.

The resistors, capacitors, and diodes constitute the majority of small components that need to be soldered. Larger components such as the voltage regulators, voltage converters, electrolytic capacitors, and the terminal blocks still need to be installed next. At this point in the construction process, participants will become more familiar with the orientation of the components. However, flipped or other incorrect component placements may still occur through the construction process.

The longest section of the construction process lies with constructing the power supply components and its respective adapters. To begin the process, the battery must be soldered. However, the battery can be damaged if a significant static charge is applied while handling. To avoid damage, it is instructed to either wear the provided grounding bracelets or solder the battery on an insulating surface (i.e., wood tables, insulating soldering mats, etc.). Next, the power supply cable and its adapters must be assembled. Figure 3.5 shows an overview of the procedure.

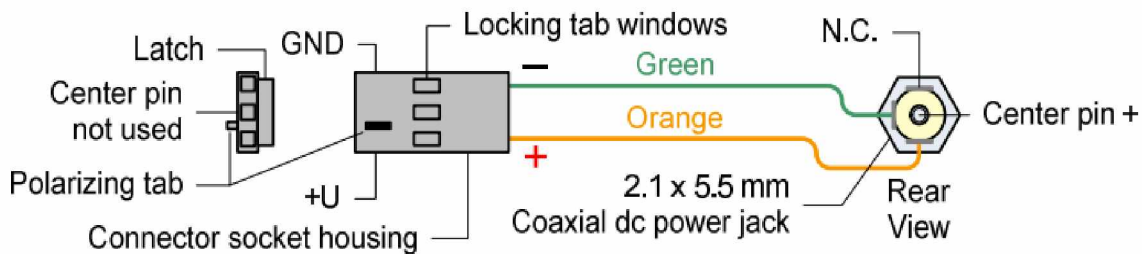


Figure 3.5: Power cable procedure overview. All these parts are included. Orientation is important. See Figure 3.8 for the finished product. *Adapted from* Reeve (2018).

The cable construction process is more straightforward compared with the PCB assembly. Most issues arise during the crimping portion of the terminal contacts for the wires. This process may be difficult for those who have no prior experience. However, to overcome this difficulty, it is recommended to acquire and use Arduino (or similar) jumper wires instead of crimps, as shown in Figure 3.6.

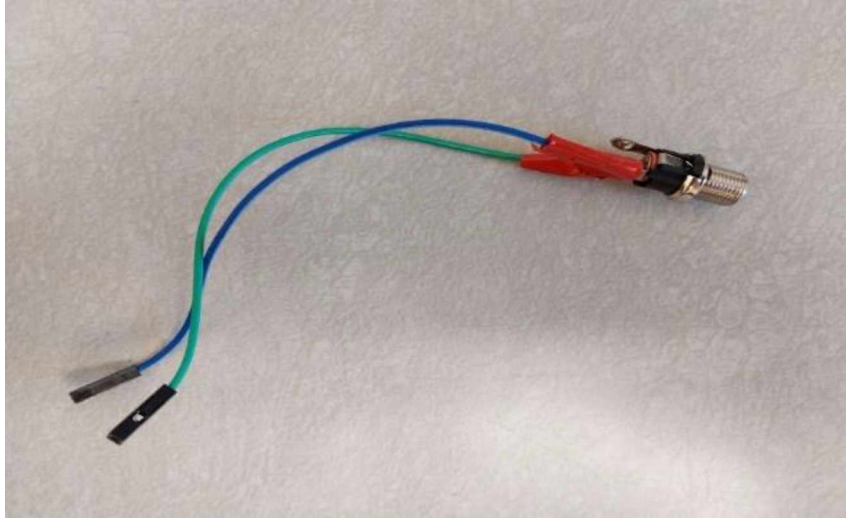


Figure 3.6: Finished power cable. This cable was created using Arduino jumper cables. This is optional and not provided with the kit.

The construction of the power supply designates the half-way point in the construction process. At this stage, the power supply will need to be tested. A multimeter with a minimum of 20 V DC range is required. The grounded lead needs to be situated on the reference ground labeled in Figure 3.5. All the locations marked in Figure 3.7 will need to be checked and have the voltages match accordingly (to within ± 0.25 V).

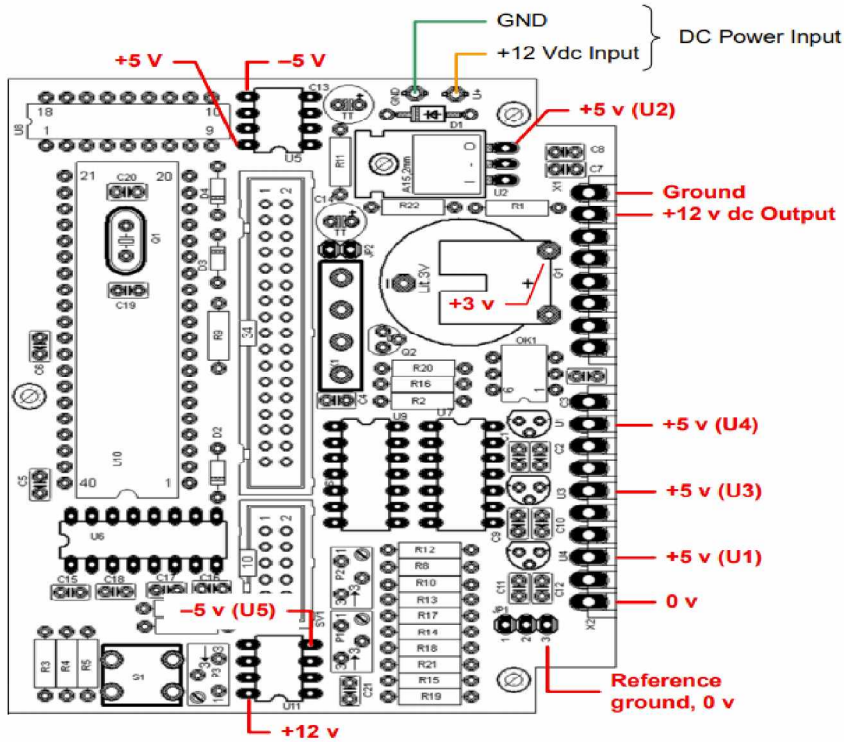


Figure 3.7: Power supply test voltage guide. With the ground lead on the reference ground, place the other lead on one of the spots with the red lettering and the multimeter should read the value. *Adapted from Reeve (2018).*

If the test proved successful, the forty-pin and PCB header sockets, the polarized and two-pin header blocks, the variable resistors, and the reset pushbutton will be the next in installation. The forty-pin socket is used for the microprocessor, while the PCB header sockets are used for the sensors and input/output. The polarized header block is used to connect the serial port connector to the PCB while the two-pin header block will be connected with a header shorting block (later on in the construction process) to activate the real-time clock battery. Lastly, the variable resistors change the gamma factor on the provided LCD screen during initial setup, while the reset push button allows a hardware reset during initial setup and operation.

The final components for the main PCB include the reed relay, integrated circuits, a transistor, an opto-coupler, a 16 MHz quartz crystal, a microprocessor, and some final capacitors. These components are very static shock sensitive. All these parts

together allow the SAM-III to have its own display and data transfer capabilities. Figure 3.8 shows the PCB with all the components soldered.



Figure 3.8: Finished main PCB. Some of the older boards are green, while the newer boards are blue.

3.2.5 Serial and Display

The last cable which needs to be constructed is the serial port cable. This cable allows the SAM-III to receive the initialization software and send data to a connected computer. Figure 3.9 shows a completed serial port cable.

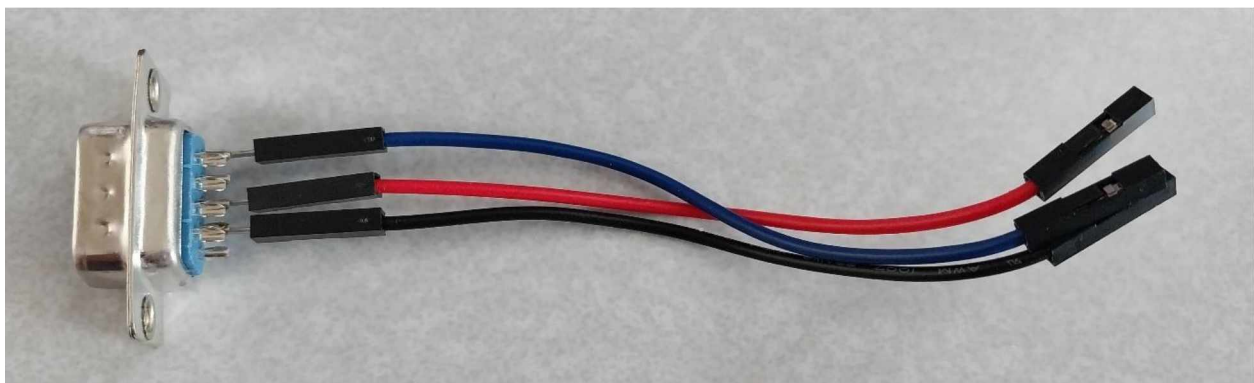


Figure 3.9: Serial port cable. This cable was made using optional Arduino jumper cables. These cables are not included with the kit.

Next, the LCD display will be constructed. A set of pre-assembled ribbon display cables and a display module are included in the SAM-III kit. The only installation requirement for the display is simply plugging the ribbon cables into the LCD and the display port on the board. Lastly, the header shorting block will be installed over the two-pin block to activate the internal clock. After applying power to the board, the LCD's gamma settings will need to be adjusted. This adjustment can be done by changing the resistance on the variable resistor. Text will appear on the LCD to indicate the completion of the hardware portion of the construction process.

3.2.6 Software Installation

If everything was constructed correctly, then the text on the LCD will read "Keyboard: Successively Press F1-F4". The SAM-III is now ready to begin the software setup. The LCD will show in sequence all the tests it requires before it will begin overwriting the initialization software with the SAM-III operation software. Figure 3.10 shows the SAM-III ready for software setup.



Figure 3.10: SAM-III ready for software setup. The steps will need to be followed on the LCD.

To begin, all the push buttons on the keyboard need to be pressed to ensure the working functionality of the keyboard. Now a computer needs to be connected to the SAM-III via the serial port. A serial port reading software is needed (e.g., Tera Term, an open-source product) to ensure the working functionality of the serial port connection. Next, the system time and date need to be set.

Following these steps, a faint chirp will begin to sound after all the previous tests have been completed. If chirps occur every one second, then the test is successful. Before proceeding, the voltage needs to be tested. By following the on-screen instructions, tune the other variable resistors (different from the one used for the LCD) to maintain proper voltage levels. This step is best performed with an instructor (see Appendix C, pg 33 of manual). Lastly, the software will be installed. This is done by using the provided PIC downloader .exe file while the computer and SAM-III are connected via serial cable. If all previous steps were done correctly, then construction is finished, and the LCD should resemble Figure 3.11.



Figure 3.11: Final screen. None of the sensors are installed at this point in the construction process, so the readings should be empty at this moment.

Chapter 4 SAM-III Sensor Experiments

4.1 Introduction to the Experiments

Several experiments were conducted to ensure the quality of data acquisition. These experiments were designed to explore the utilization of SAM-III kits for space weather research. This chapter is separated into three experiment types: accuracy/validation, proximity, and temperature. The motivation for proximity

experiments stems from crosstalk feedback discovered when the FG-3 sensors (section 3.1) were within a certain distance from each other. This causes the data to become noisy. An accuracy/validation experiment was needed to determine if the sensors will be able to measure a known rate of change. Lastly, significant temperature changes can alter the data. Insulation assists in the protection of this alteration, yet effects can still be seen even when buried underground. Therefore, the temperature dependence of the sensors needed to be examined further prior to deployment.

4.2 Proximity Experiments to Determine Crosstalk Distance

During the initial stages of preliminary deployment vessel construction, the optimization of sensor proximity was examined. Reeve (2018) mentions that six inches (about 15 cm) is the closest the sensors can be operated without significant crosstalk and feedback. This significantly limits the size of deployment vessels that can be built. Thus, the UAF SWUG team decided to perform some experiments to determine if this separation distance is indeed the minimum.

The first experiment was performed in the spring of 2021. The objective was to determine if the sensors can be placed within a closer distance than six inches. Two sensors were placed on an optical rail starting at two inches apart and were moved away two inches from each other every thirty minutes until the six inch distance was reached. This process was then repeated in reverse back to a two inch separation. Figure 4.1 shows the original experiment performed in 2021 where only data from one sensor was examined. At four inches, the data is consistent in time indicating a lack of crosstalk and feedback. Furthermore, at two inches, the data experiences inconsistencies in time indicating evidence of feedback and/or cross talk. While this experiment was not very rigorous, the experiment was meant to qualitatively determine a safe distance between the sensors to avoid feedback or crosstalk, in this case roughly four inches.

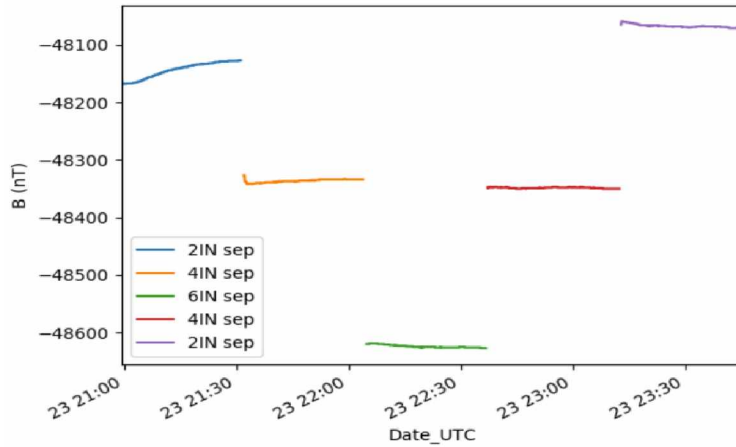


Figure 4.1: Original separation distance experiment. The separation started at two inches and the sensor was moved by two inches every thirty minutes. Consistent data was observed at four inches of separation, but data was inconsistent at two inches.

In 2023, the experiment was performed again, with more rigor, to show that the sensors can be closer than initially anticipated. This experiment was conducted by keeping two FG-3 sensors parallel to each other and kept at a starting distance of six inches apart. The sensors, dubbed “Still” and “Moved” respectively, were secured within a wooden block to keep them in place and positioned on an optical rail to be able to slowly move the sensors closer to each other. Every thirty minutes, the “Moved” sensor was moved half an inch closer to the “Still” sensor. This was done until the sensors reached two inches. As seen in Figure 4.2, feedback between each sensor is very minimal until the 2.5 inch mark. At this location, the “Still” sensor experiences significant variations indicating crosstalk. From this, we conclude that the sensors can reliably be about three inches apart with very little feedback or crosstalk. This is half of the distance indicated in Reeve (2018).

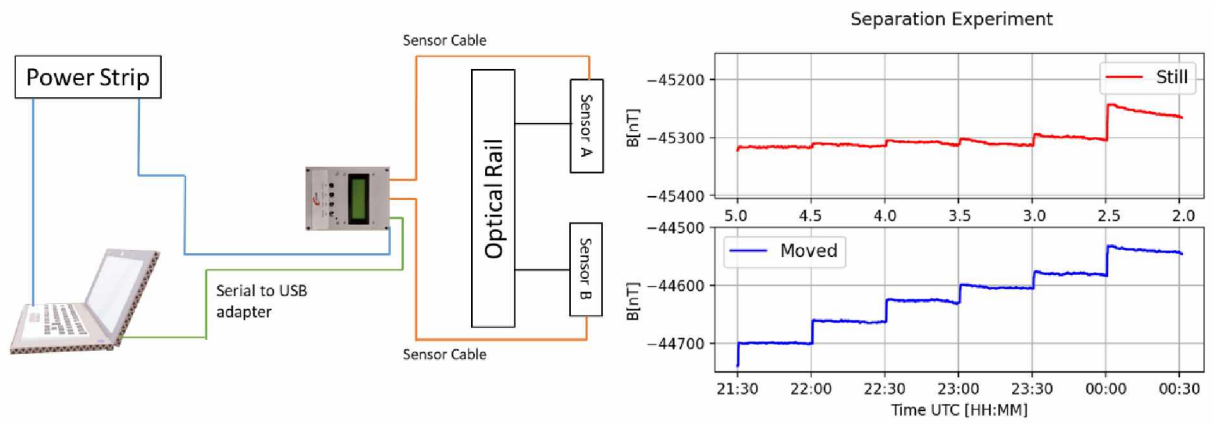


Figure 4.2: The new separation distance experiment started at six inches and moved one sensor half an inch closer every thirty minutes. The 6 in and 5.5 in were removed due to the SAM needing to be saturated beforehand, causing error early in the data.

4.3 Accuracy/Validation Experiment with Known Rate of Change

An accuracy experiment was designed and conducted to determine if the FG-3 sensors would be able to measure a known rate of change in the magnetic field. For this experiment the known rate of change is about 400 nT per minute. Three sensors were placed in an orthogonal cartesian orientation where the x-axis was placed one foot away directed at a rotating magnet. The rotating magnet completes a full rotation every sixty seconds in the X-Y plane with the magnets pole horizontal to the X and Y sensors. Being within the direct line of sight of the rotating magnet, the x-sensor experienced more variation than the y-sensor and z-sensor. As seen in Figure 4.3, the x-sensor experienced explicit periodicity with a period of sixty seconds and a maximum change of about 400 nT, indicating that the sensors are able to measure a known rate of change in the magnetic field.

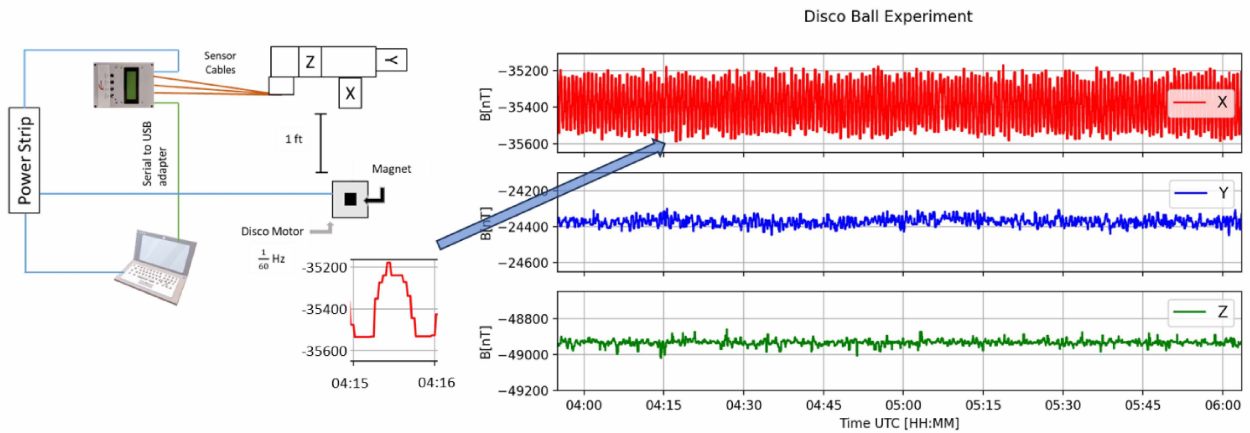


Figure 4.3: Disco ball setup and results. The disco ball motor with the magnet is rotating at one rotation every sixty seconds.

4.4 Temperature Experiments for Calibration

During initial testing, the UAF SWUG team noticed variations in the SAM-III data that correlate to changes in temperature. The magnetometer data displayed in Figure 4.4 was taken from the deployment vessel (nicknamed Icarus) located on the roof of UAF's Reichardt building. These data are compared to the GIMA magnetometer at the Poker Flat Research Range. A temperature data logger was placed inside (T_{in}) and outside (T_{out}) the deployment vessel to gather temperature data to see if there is a correlation between the temperature and magnetometer data. The magnetometer data variations are, to a good approximation, linearly proportional to temperature variations. As shown in Figure 4.4, the blue line (Icarus) shows similar magnetic perturbations to the orange line (GIMA Poker Flat). However, the Icarus (or SAM-III) measurements' slope deviates approximately 0.38 nT/min with a $mx + n$ shape (see section 4.4.2) from the GIMA measurements, especially in the D component (2nd from the top), in a manner that echoes the temperature deviation, (bottom panel). Thus, it is important to calibrate the deviation of the SAM-III magnetometer data with the temperature data.

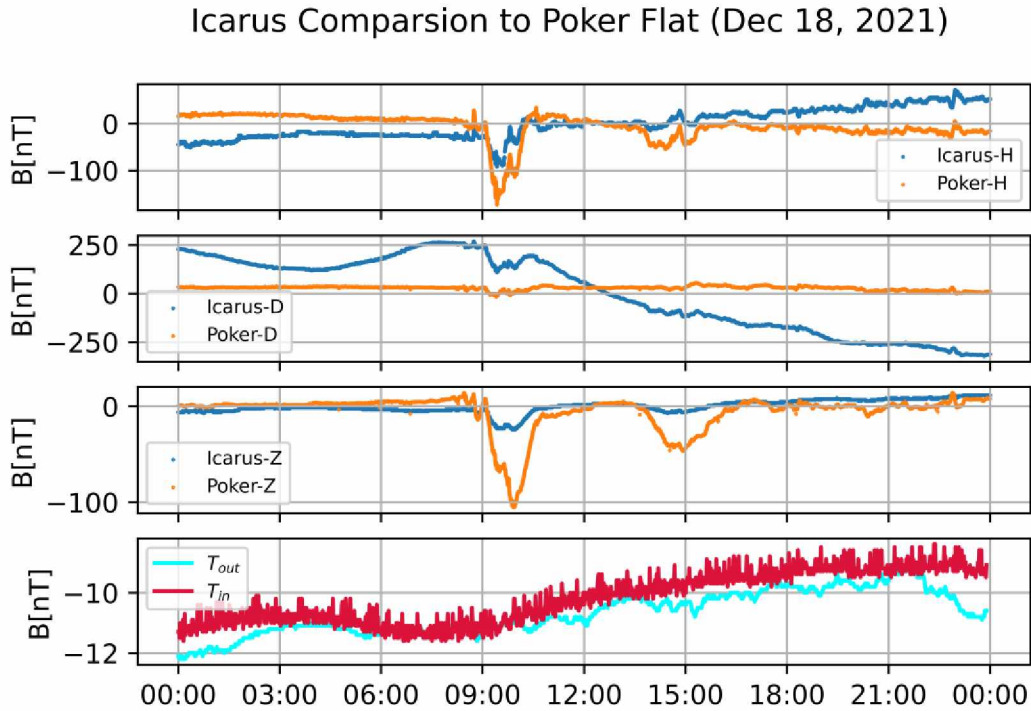


Figure 4.4. Reichardt roof magnetometer data with the temperature data. The roof data are compared to the Geophysical Institute Magnetometer Array (GIMA) Poker magnetometer.

4.4.1 Temperature Data Loggers Used During Calibrations

Fluxgate sensors are temperature dependent (Primdahl, 1970). For the FG3+ sensors used in this study, there is no documentation on what type of temperature dependence (linear, logarithmic, etc.) these sensors have. Placing temperature sensors alongside the magnetometer sensors will tell us their dependencies.

Several iterations of temperature sensors were used in deployments. The Elitech GSP-6 was the first sensor used. This device runs off a rechargeable lithium battery which is charged through a micro-USB. The shortcoming of this device is that it must be started and stopped manually. Therefore, it is not a viable solution for remote deployments. Data also has to be collected by connecting the device to a computer and downloading the resulting .txt file.

The next iteration of temperature experiments made use of the Lascar EL-USB-1. This device can be plugged into a computer while collecting temperature data. With a Windows based Operating System (OS) remote screen viewing software, one can send

the data from a remote location as long as an internet connection is established. However, this device only runs on a 3.6 V battery. During the winter, the battery would lose charge rapidly and the device would become unusable. With a price tag of about eighty USD, this device costs about four times that of less expensive alternatives.

To find the most suitable temperature sensor for various deployment methods, we considered several alternatives. However, the proprietary software or lack of documentation about the device make them impractical to use. Figure 4.5 illustrates the different options of temperature sensors used and Table 4.1 gives a cost comparison.



Figure 4.5: Options tested for temperature data collection. [Top left] Lascar EL-USB-1. [Bottom left] Taidacent MODBUS. [Bottom Middle] TEMPer Gold. [Right] Elitech GSP-6.

Device	Price
Elitech GSP-6	\$45.99
Lascar EL-USB-1	\$86.49
Taidacent MODBUS	\$23.58
TEMPer Gold	\$18.99
Elegoo Uno R3 and DS18B20	\$18.31

Table 4.1: Temperature device price comparison. Prices are shown at the time of purchase.

The latest iteration of temperature experiments made use of the Elegoo Uno R3 (similar to the Arduino) and the DS18B20 temperature sensor. The Uno R3 must first be programmed with the Arduino IDE (or similar). Appendix A details the Arduino code.

The jumpers need to be soldered to the board to ensure a stable connection. The jumpers are provided with the temperature sensor. The soldered connections need to go in GND (ground), 8 (data port), and 5V (power) which are labelled on the board. Figure 4.4 shows a fully assembled temperature sensor.

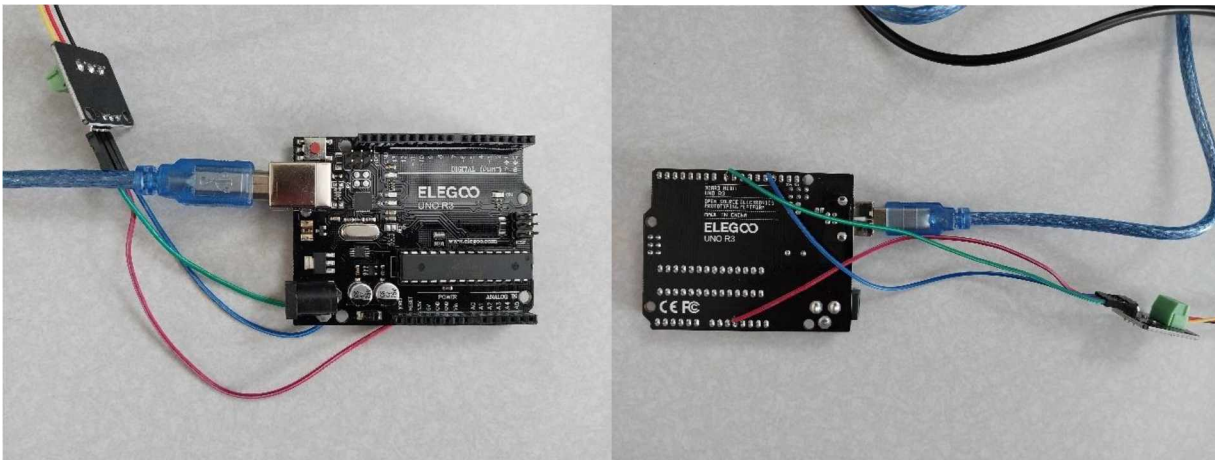


Figure 4.6: Elegoo Uno R3 and DS18B20. Some set-up is required. The code needs to be uploaded to the Elegoo, the cables need to be soldered to the main board, and the correct cable placement needs to be checked.

Next, the jumper cable receptacle can be connected to the provided terminal piece. The wire soldered to the board will be connected accordingly (Appendix A). A serial port reading software, such as Tera Term, can determine if data are being read. Using the cat command in a Linux machine (Appendix A), data will then be stored on the computer. The Uno R3 has been established as the baseline temperature sensor for UAF SWUG, using the design described above.

4.4.2 Roof Experiment Using Polynomial Fit Methods

During December of 2021, a UAF SWUG deployment vessel was stationed on the roof of the Reichardt building on the UAF campus. A temperature sensor was installed inside the vessel. Data were collected over a month before analysis to ensure some form

of geomagnetic variations, as shown previously in Figure 4.4. The UAF SWUG team took the temperature data and applied a linear fit (See Appendix B) on top of the magnetometer data in order to remove temperature effects. The green line in Figure 4.7 is the fitted data which is compared to the orange line GIMA Poker Flat magnetometer. Each component of the magnetic field is compared. The fit removed most of the offset caused by the temperature in the Icarus data which indicates that this fit is a good approximation to use to calibrate magnetometer data. The environment, however, was not controlled, giving rise to interference, thus more tests are required.

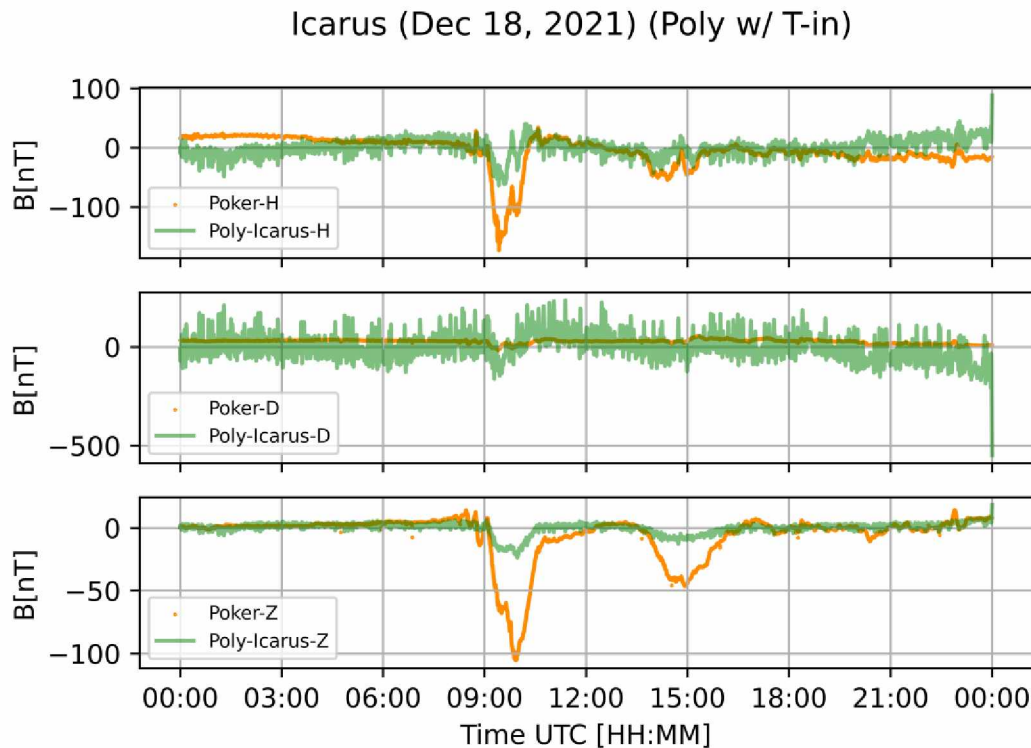


Figure 4.7: Applied linear fit. Comparison with Poker Flat magnetometer. Data correlation has improved from the fit, but more calibration is needed.

4.4.3 Cooler Experiment with Known Rate of Change

Using an Alpicool C15 portable cooler, the UAF SWUG team placed two FG-3 sensors inside the cooler parallel to each other. This was done to ensure each sensor experiences the same temperature variations and does not require to be serialized and

calibrated separately. The cooler was set to the lowest temperature of -15 C. The disco ball motor with the magnet from section 4.2 was included in this experiment to ensure a known rate of change in the magnetic field. Figure 4.8 shows the experiment setup.

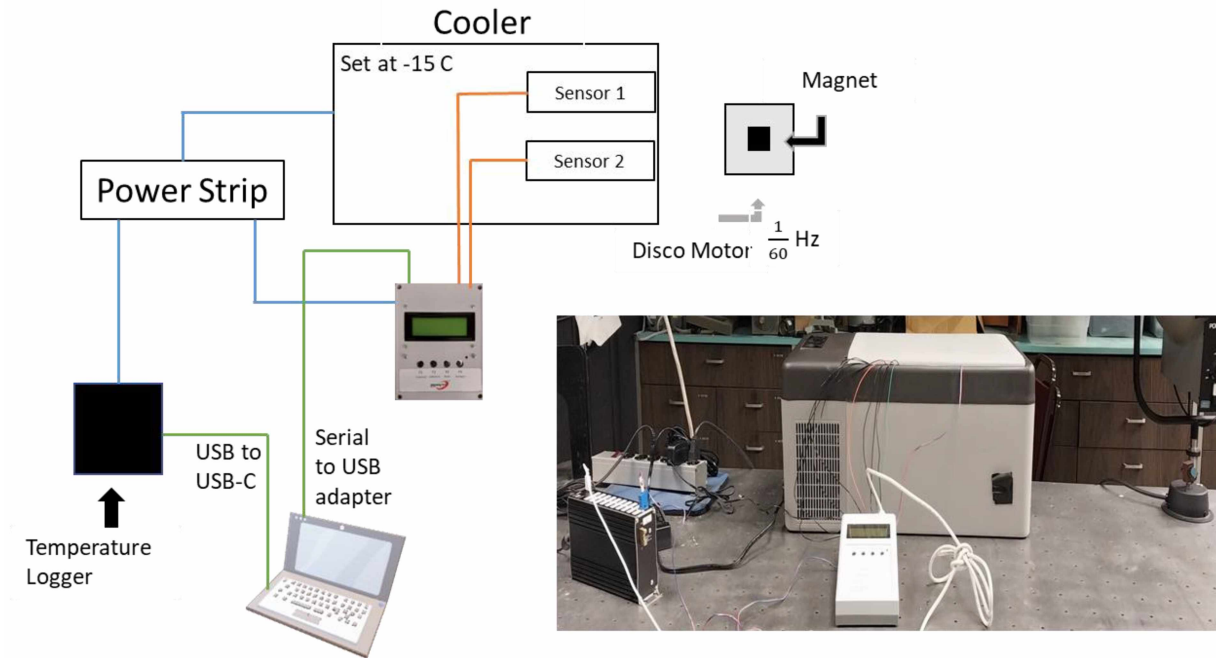


Figure 4.8: Disco motor temperature experiment setup. The two sensors will experience temperature change while also being exposed to a known magnetic field change rate.

Once the cooler reaches the designated temperature, it will turn off. Then, once the temperature rises to a certain threshold, designated by the cooler, it will turn back on to cool to the designated temperature again. Using a Campbell Scientific Temp-120 data logger for the temperature data, the cooler has a periodic temperature cycle as seen in Figure 4.9. A Fast Fourier Transform was applied over the data to remove higher frequencies. The sensor data follows the same cyclic pattern as the cooler. Both Sensor 1 and Sensor 2 experience an average $\left| \frac{dB}{dt} \right|$ of about 705 nT and 675 nT respectively every temperature transition from -13°C to -15°C and from -15°C to -13°C. The magnetic field profiles follow the temperature profile as $\frac{1}{T}$ where T is the temperature.

Disco Ball Temperature Experiment (2023)

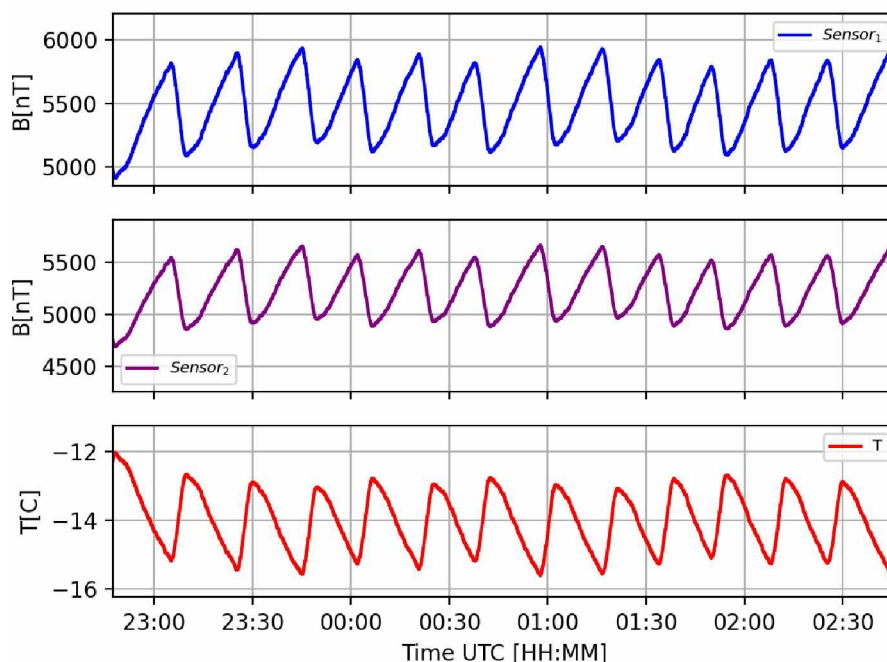


Figure 4.9: Disco ball temperature experiment data. A Fast Fourier Transform was used to remove the higher frequencies. The sensor's magnetic field change is linear to the temperature change.

Chapter 5 Deployment Experiments

5.1 Considerations for Alaska Specific Deployments

Careful deployments are crucial to ensure the continuity and reliability of data collection. The environment, location, seasonal conditions, and wildlife play important roles in deployment success. For example, does the deployment site have any metal objects? Is the ground at the site permafrost? Is the site frequented by large wildlife? These and many other questions need to be asked before a deployment is conducted.

Alaska has unique problems when it comes to magnetometer deployments. Due to Alaska's size and lack of infrastructure, finding a source of power and internet is a difficult task. Power from solar panels will work during the summer but can quickly become obsolete during the winter and fail to provide ample power even with a

substantial battery supply. Most remote Alaska village schools have both power and internet and thus can be used for deployment sites.

In the event that the power and internet issues are successfully resolved, wildlife may interact with the device and destroy it in the process. The best way to prevent wildlife interaction is to either bury the device or have it secured within a resilient structure. Since the latter can be rather expensive, burying the device has become a common approach. However, the ground in many parts of Alaska is frozen for most of the year, and the time to bury the device is limited.

5.2 Deployment types

Since the summer of 2021, there have been several different types of UAF SWUG deployment vessels. They are categorized by A-Type, B-Type, L-Type, and the MDV or Multi-deployment-vessel. Appendix D delves deep into the history of the earlier vessel types (A-, L-, and B-Types), while Appendix E details the MDV, the current model in production. Figure 5.1 illustrates all the types.



Figure 5.1: In order from left to right: L-Type, MDV, A-Type, and B-Type. Each type is available; however, the MDV is the current model in production.

5.2.1 Anchor and L-Types

The A- and L-Types are labeled according to their shape of construction. The A- or “Anchor” Type loosely resembles a ship anchor, while the L-Type resembles that of the letter “L”. Both types are displayed in Figure 5.2. These vessels are designed to be

buried underground and have long sensor cables that run from the top of the vessel back to a computer inside a building. Once the device is buried, it becomes extremely difficult to retrieve or repair if there are any issues. They must be deployed when the ground is completely thawed, so the deployment window is about four months instead of any time of year.



Figure 5.2: A-Type (Left) and L-Type (Right). All the cabling required for operation is shown in the background.

5.2.2 Box Types

The “Box” type vessel or B-Type is separated into two types all on its own. The Type-I Box Type or B1-Type contains an L-Type sensor arrangement but is placed inside a durable storage box (see Figure 5.3). Everything needed for data collection is contained inside the box. The device is powered by plugging in a long power extension cable on the outside of the box (see Figure 5.4). This device was designed to be placed above ground. Thus, the device can be deployed any time of year and it can be relocated if the situation arises.

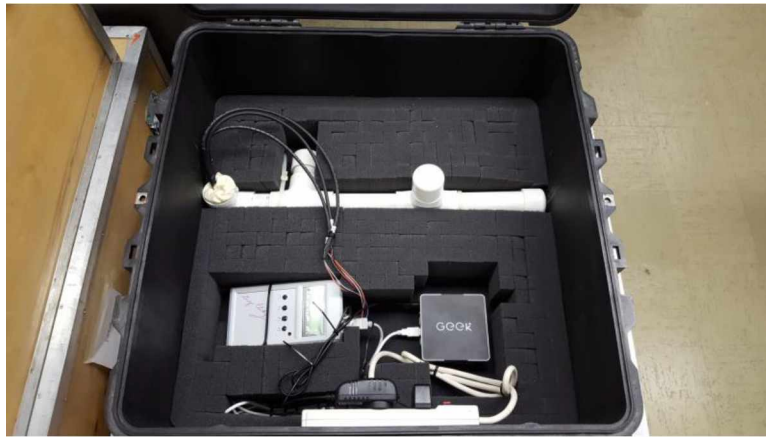


Figure 5.3: B1-Type. All the components fit inside, and power will need to be applied to begin operation.

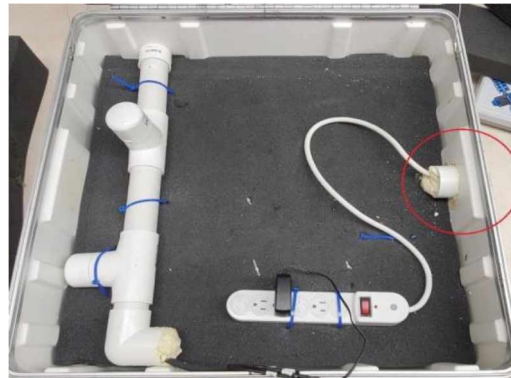


Figure 5.4: Location of the power source on the B1-Type from Reyes (2021). The power plug is inserted into a PVC tube and filled with insulation foam. A hole is drilled into the box to have the pipe fit through and is glued and cemented to maintain structural integrity.



Figure 5.5: Red B1-Type. Smaller than the black boxes. These boxes are not as expensive and are durable.

The main downside to this design is its bulkiness and weight. The box itself can weigh about 9 kg (about 20 lbs). The weight hinders the mobility of the devices and hinders access for remote hosts. New box designs were used to help reduce the weight (see Figure 5.5), but the overall issue remained.

5.2.3 Multiple Deployment Vessel

The Multiple Deployment Vessel, or MDV, is the most recent iteration of deployment vessel developed by the UAF SWUG team. Most of the devices structural components are gathered from home improvement or hardware stores. The only components that cannot be purchased from a store are the SAM-III and the special made 3D printed components designed by the SWUG team (Barkley-Griggs, 2023) (see Figure 5.6). The files for these components are publicly available on the UAF SWUG Atlas website.

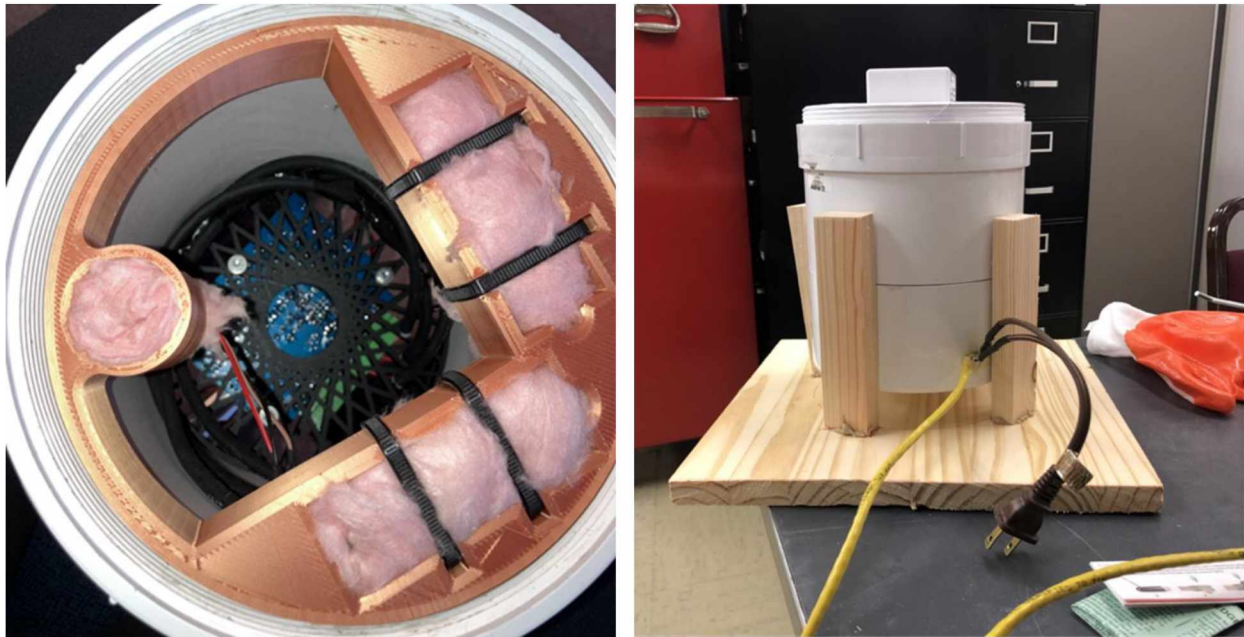


Figure 5.6: Inside MDV (left) and outside sideview (right). 3D printed components are used to house the sensors and hold the SAM-III in place.

This device is designed to be watertight and able to withstand the large snow melt that occurs during the springtime in Alaska. The MDV can either be completely buried as deep as necessary or remain above ground, depending on the needs of the host

site. With its “plug-and-play” design, deployments can be facilitated by teachers without the worry of complex deployment techniques. This in turn saves time and money on making trips to deployment sites. Table 5.1 gives a price comparison between each type while Table 5.2 lists all the supplies and tools with a cost breakdown needed for the MDV.

Type	Approximate Price
L-Type	\$2000
A-Type	\$2000
B-Type	\$1400
MDV	\$740

Table 5.1: Type price comparison. The UAF SWUG team was able to reduce the cost of the MDV to about half of the B-Type.

Cost Breakdown:

Variable Costs (per Item Unit):		Variable Costs (Estimated Maximum):		Fixed Costs (Exact; per Device):	
Item	Unit cost	Item	\$ per Device	Item	Cost \$
Gloves	0.26 \$/pair	PVC primer	0.10	Solderless jumper wires	0.78
Thread tape	0.52 \$/roll	Thread tape	0.26	Zip ties	0.80
Heat-Shrink	0.55 \$/piccc	Pipe dope	0.45	Temperature Sensor	1.33
PVC Cement	0.64 \$/oz	Silicone	0.49	RJ45 to RJ45 adapter	1.83
Fiberglass Insulation	0.82 \$/ft ²	Gloves	0.52	Power cable	2.51
Silicone	0.99 \$/oz	PVC Cement	0.64	3d printed components	3.89
PVC Primer	1.19 \$/oz	Heat-Shrink	3.29	Short CAT 5 cable	9.97
Electric tape	1.83 \$/roll	6inØ PVC Pipe	3.52	6inØ PVC threaded lid	10.98
Pipe dope	2.70 \$/oz	Insulated cable	15.27	Micro Controller Board	16.98
Insulated cable	5.09 \$/ft	Labor	~ 65.00	6inØ PVC end cap	17.98
PVC 6inØ Pipe	7.04 \$/ft	Fiberglass Insulation	<0.01	6inØ PVC adapter	23.28
Labor	~ 5hrs	Electric tape	<0.01	Power extension cord	28.57
				150 ft CAT 5 cable	46.97
				Computer	82.79
				SAM PCB kit	400.00
Total cost: ~738 USD (as of April 2023)					

Table 5.2: Supply list with cost breakdown. Prices are shown at the time of their purchase. *Adapted from Barkley-Griggs (2023).*

6.1 Computer and Initial Set-up

Miniature PCs are used as the key component for data acquisition. Due to inflation in Raspberry-pi and other similar devices prices during 2021 to 2023, mini-PCs became a more cost-effective option. The computers typically have 2 GB of RAM and 32 GB of storage. The data collected from the SAM-III is only about 100 Bytes per second or about 8.5 MB per day, which yields about 3 GB a year. Thus, in about 10 years, the device will need to be cleaned of old data. However, a data center has been developed to host all this data (see section 6.3).

Each computer runs a version of CentOS-7 operating system that does not have a graphical user interface (GUI). Code and configuration files have already been developed by the Geophysical Institute Magnetometer Array (GIMA) to collect, store, and transfer data. Alterations have been made to the original code to support the SAM-III. Adapted remote configuration files and code are downloaded onto each miniature PC. Thus, the data collection can begin.

The command “`$ service gima_launch start`” needs to be run each time the computer is booted to ensure data collection and transfer or can be programmed as part of the startup script. After this command is run, data from the SAM-III will be collected into a .dat file, which is then transferred to the UAF SWUG data center (see section 6.3). Figure 6.1 illustrates what the .dat file contains. H, D, and Z represent the components of the magnetic field. RIOM is unused but stands for Remote Interactive Observing Module. IRIG D is unused, but stands for Inter-Range Instrument Group time code D. Decimal time is calculated by:

$$hour + \frac{minute}{60} + \frac{second}{3600} \tag{6.1}$$

Narod byte number is unused and only pertains to the Narod magnetometers. Record count is unused and must be a value between 1 and 3600.

```

===== UAF SWUG Magnetometer Array =====
-----

Poker Alaska Magnetometer System
Version # 0.1 gima_mag.py

May 9 2023 Site Clock is ntp
-----

H          D          Z          RIOM    IRIG D    DECIMAL TIME    NAROD    RECORD
-----    -----    -----    ----    -
-7594.0    680.0    -44267.0    0        0        17.000000        0        1
-7594.0    680.0    -44267.0    0        0        17.000278        0        1
-7595.0    680.0    -44267.0    0        0        17.000556        0        1
-7595.0    678.0    -44267.0    0        0        17.000833        0        1
-7595.0    678.0    -44267.0    0        0        17.001111        0        1
-7596.0    678.0    -44267.0    0        0        17.001389        0        1
-7596.0    678.0    -44267.0    0        0        17.001667        0        1
-7596.0    678.0    -44267.0    0        0        17.001944        0        1
-7597.0    678.0    -44267.0    0        0        17.002222        0        1
-7597.0    678.0    -44267.0    0        0        17.002500        0        1
-7597.0    678.0    -44267.0    0        0        17.002778        0        1
-7597.0    678.0    -44267.0    0        0        17.003056        0        1
-7597.0    677.0    -44267.0    0        0        17.003333        0        1
-7597.0    677.0    -44267.0    0        0        17.003611        0        1
current_1hz.dat

```

Figure 6.1: Example data from mini-PC. This example is from the Poker Flat Research Range deployment site.

6.2 UAF SWUG Network System

Each computer can be remotely accessed via a predetermined password using a virtual VPN provider. The VPN provider provides connection statuses for the computers as well as virtual IP addresses to access the computers as long as an internet connection is established. As of this writing, only cabled ethernet connections can be made with the deployment vessels.

On boot, the computers will immediately try to connect to the VPN. This allows for quick deployment updates when a new vessel is deployed. For example, on March 10th, 2023, a deployed vessel on the roof top of the Soldotna Public Library was updated to be able to access the UAF SWUG data center (see section 6.3). A temperature sensor and a new computer were added. As soon as the device received power and ethernet, the

UAF SWUG team was able to remotely access from the roof and start the data collection within five minutes.

6.3 UAF SWUG Data Center

When a proper internet connection is established and the launch service has been initialized, data will then be sent to the UAF SWUG data center SWUG Atlas. From the SWUG Atlas website, hourly .dat files, full day .csv files, and .png files can be retrieved from a directory. Figure 6.2 shows an example directory.

Index of /DATA/www/2023/04/21/soldotna


<u>Name</u>	<u>Last modified</u>	<u>Size</u>	<u>Description</u>
 Parent Directory		-	
 sol2023-11100fgt.dat	2023-04-21 16:02	292K	
 sol2023-11101fgt.dat	2023-04-21 16:02	292K	
 sol2023-11102fgt.dat	2023-04-21 16:02	292K	
 sol2023-11103fgt.dat	2023-04-21 16:02	292K	
 sol2023-11104fgt.dat	2023-04-21 16:02	292K	
 sol2023-11105fgt.dat	2023-04-21 16:02	292K	
 sol2023-11106fgt.dat	2023-04-21 16:02	292K	
 sol2023-11107fgt.dat	2023-04-21 16:02	290K	
 sol2023-11108fgt.dat	2023-04-21 16:02	288K	
 sol2023-11109fgt.dat	2023-04-21 16:02	286K	
 sol2023-11110fgt.dat	2023-04-21 16:02	287K	
 sol2023-11111fgt.dat	2023-04-21 16:02	288K	
 sol2023-11112fgt.dat	2023-04-21 16:02	288K	
 sol2023-11113fgt.dat	2023-04-21 16:02	288K	
 sol2023-11114fgt.dat	2023-04-21 16:02	288K	
 sol2023-11115fgt.dat	2023-04-21 16:02	288K	
 sol2023-11116fgt.dat	2023-04-21 16:02	291K	
 sol2023-11117fgt.dat	2023-04-21 16:02	295K	
 sol2023-11118fgt.dat	2023-04-21 16:02	295K	
 sol2023-11119fgt.dat	2023-04-21 16:02	295K	
 sol2023-11120fgt.dat	2023-04-21 16:02	295K	
 sol2023-11121fgt.dat	2023-04-21 16:02	295K	
 sol2023-11122fgt.dat	2023-04-21 16:02	295K	
 sol2023-11123fgt.dat	2023-04-21 16:00	295K	
 soldotna_2023_04_21.csv	2023-04-21 16:02	3.4M	
 soldotna_2023_04_21.csv.tar.gz	2023-04-21 16:02	953K	
 soldotna_2023_04_21.dat.tar.gz	2023-04-21 16:02	364K	
 soldotna_2023_04_21.nc.tar.gz	2023-04-21 16:02	464K	
 soldotna_2023_04_21.png	2023-04-21 16:02	45K	

Figure 6.2: Example of a directory from SWUG Atlas. The hourly .dat files are seen first, then the daily .csv file, along with the combined .tar files, and finally the .png file which shows a pictorial representation of data from that day.

Figure 6.3 shows a comparison between the north component data from the GIMA Poker Flat magnetometer compared to north component data from the UAF SWUG magnetometer deployed at Poker Flat. The GIMA data were taken from the Geophysical Institutes website and the UAF SWUG data were taken from SWUG Atlas. The magnitude and variability of the geomagnetic disturbance was well captured. Only the $\frac{dB}{dt}$ values are of interest for this thesis due to $\frac{dB}{dt}$ being of significance in GIC studies (Dimmock et al., 2020).

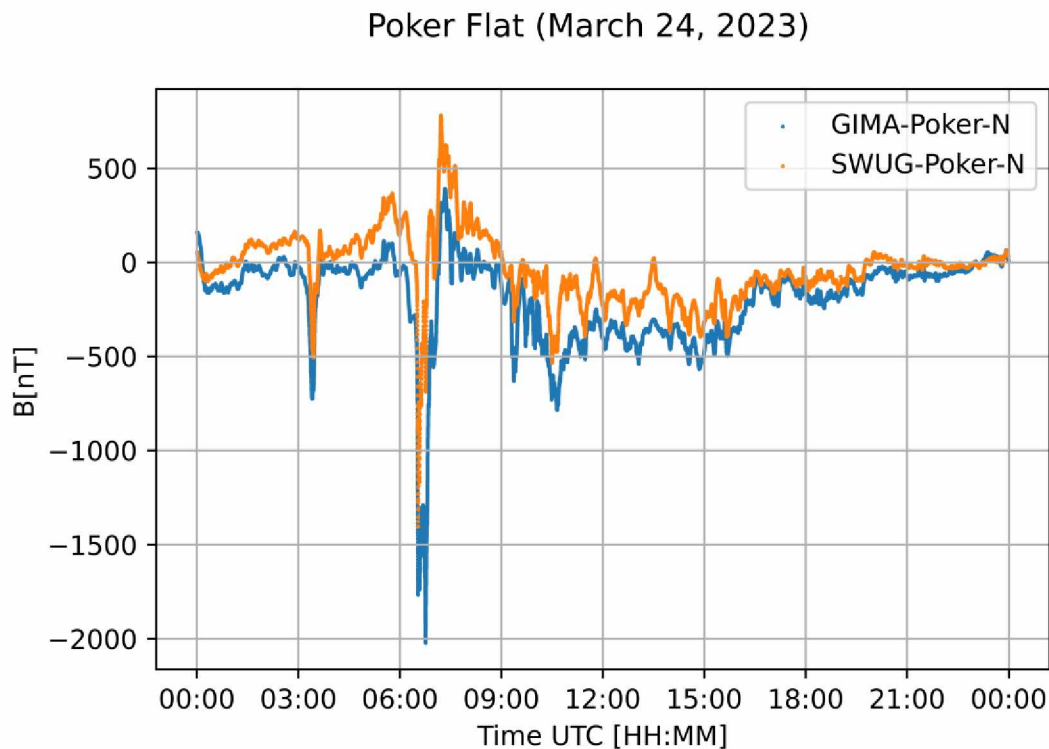


Figure 6.3: GIMA Poker Flat north component data compared to UAF SWUG Poker Flat north component data.

Chapter 7 Educational Applications

7.1 Introduction to SWUG

Space Weather UnderGround (SWUG) is an education and outreach program, first initiated by Dr. Charles Smith at the University of New Hampshire and expanded to the University of Alaska Fairbanks (UAF) (Smith, 2019). The SWUG program is

aimed to educate high school students on space weather phenomena while equipping them with STEM skills. Students who participate learn to build a semi-professional magnetometer kit which is used by researchers to deploy a cost-effective and research-capable array of magnetometers across Alaska and New Hampshire.

7.1.1 Similar Projects

There are similar projects that involve citizen interaction with space weather research. Odenwald (2021) describes that modern phones (devices past iPhone 3GS and post 2009) have built-in Hall Effect magnetometers. Using many types of phones, Odenwald (2021) concludes that most modern phones can detect magnetic field changes resulting from geomagnetic storms with a resolution of about 1 μT . Operational issues can still arise however, if there are changes in temperature, moving the phone around, or a presence of magnetic materials, noise can become significant and drown out the geomagnetic storm variations.

There are various other ways magnetic field signatures can be used for citizen science and education. One such example, Archer et al. (2022) used online surveys to choose audio clips based off the ULF wave spacecraft data from THEMIS compressed using different sonification methods. Participants were recruited, rather than randomly selected. People of interest for recruitment were people with music experience or those familiar with science communication. Participants were tasked to pick a method based off sound quality. Archer et al. (2022) used these data as recommendations to determine which methods of sonification to use for future research.

7.2 UAF Programs

The UAF SWUG teams hosts two summer programs: one for middle school to high school aged students and another for educators. These programs are the Summer High School Student Internship Program and the Educator Development Program.

7.2.1 Summer High School Student Internship Program

During the summer of 2021 and 2022, the UAF SWUG team invited students aged fourteen to eighteen to participate in the Summer High School Student Internship Program. This program allows students to develop Science Technology Engineering and Mathematics (STEM) skills by building their own SAM-III kit and learn about space weather in the process. The student pick a schedule and participate in up to two sessions each week. Each session lasts about three hours. This program is free for the students. Figure 7.1 shows a session in progress.



Figure 7.1: Students working in a UAF Geophysical Institute (GI) laboratory to start on sensor proximity experiments.

Overall, this program gives students the opportunity to develop engineering skills through soldering, physics knowledge through discussions on space weather, and computer science skills through basic programming needed for the device. Students are also encouraged to express their artistic skills. In Figure 7.2, a couple of the students decorated their SAM-III kits using markers (left) and acrylic paints (right).



Figure 7.2: Satellite by Savion (14) & Aurora by Bethany (17). These two were students from the 2021 Summer Student Program.

7.2.2 Educator Development Program

During the summer of 2021, the UAF SWUG team recruited educators from the local Fairbanks North Star Borough to participate in the Educator Development Program. This program provided continuing education credits to teachers who attended the two-week class. Attendees are tasked with constructing a SAM-III kit during week one and completing an asynchronous homework assignment during week two. Lectures on space weather are given throughout the first week to complement the laboratory portion. Figure 7.3 shows the participants from the 2021 class.



Figure 7.3: Educator Development Program 2021 (photo courtesy of Doga Ozturk). From left to right: four teachers from the local Fairbanks North-Star Borough, the laboratory lead, and the physics laboratory director.

In the summer of 2022, the UAF SWUG team hosted educators from outside the local Fairbanks North Star Borough to participate in the Educator Development Program. All ten participants were from rural Alaskan schools. The class has received positive feedback and many students expressed interest in hosting magnetometers. Figure 7.4 shows the participants of the 2022 class.



Figure 7.4: Educator Development Program 2022 (photo courtesy of Doga Ozturk). All the teachers are from small Alaskan communities.

Once the educators finish their SAM-III kit, the device is placed within a deployment vessel which they can choose to take back to their school to start a satellite SWUG program. If the teachers wish to take back a device, a memorandum of understanding is signed, and deployment instructions are given. Contact is maintained between the teacher and the UAF SWUG team during this process in order to ensure correct deployment. In addition, educators are encouraged to start their own SWUG clubs at their respective schools. Kits and equipment are provided for the teachers. It is suggested to have this class as either a club activity or used as laboratory time. In Figure 7.5, two Eagle River students are working on their own SAM-III kits during their physics laboratory section.



Figure 7.5: Students working on kits during their lab time. Supplies are provided to the students.

As of May 2023, deployment sites in Utqiagvik and Illiamna, Alaska have been secured through this program.

Chapter 8 Conclusion and Outlook

8.1 Conclusion

This thesis demonstrated that semi-professional magnetometers can detect geomagnetic disturbances and can be used to study geomagnetically induced currents. The SAM-III is one such magnetometer that can detect these geomagnetic disturbances while being cost-effective and commercially available. Experiments described in this thesis have shown that the sensors accompanying the SAM-III, can perform as expected from a fluxgate sensor, while also having the ability to be optimized to withstand Alaska specific conditions, and perform on par with more expensive science grade magnetometers. Finally, this thesis also explained how the UAF SWUG team is actively increasing the spatial coverage of magnetometers across Alaska through the use of educational and outreach programs.

8.2 Outlook

To accomplish UAF SWUG goals, the team will working on improving the measurements as well as investing in education and outreach programs. One of the planned improvements is the more precise calibration of the measurements with temperature data. Temperature sensors will be included with every new deployment and data from these sensors will be added to the data center's data files for automatic acquisition. This new data will be used to calibrate the magnetometer sensors by establishing a temperature-dependent baseline value by inspecting the measurements.

The SWUG team plans various future deployments. There are still plenty of locations in Alaska that do not have any magnetometers, especially in the West and North sectors. UAF SWUG will keep collaborating with Alaskan high schools to extend the coverage of magnetometers.

The Educator Development Program and the Summer Student Program will continue as long as demand, funding, and staffing are available. Teachers will always have the option to take back a deployment vessel as was done in previous years.

References

- Archer, M. O., Cottingham, M., Hartinger, M. D., Shi, X., Coyle, S., Hill, E., Fox, M. F. J., Masongsong, E. V. (2022). Listening to the magnetosphere: How best to make ULF waves audible. *Frontiers in Astronomy and Space Physics*. Retrieved from <https://doi.org/10.3389/fspas.2022.877172>.
- Barkley-Griggs, J. (2023). Comprehensive Manual for the SWUG Multi-Deployment-Vessel. University of Alaska, Fairbanks.
- Beggan, C. (2015). Sensitivity of geomagnetically induced currents to varying auroral electrojet and conductivity models. *Earth Planets Space*, 67, 24. Retrieved from [doi:10.1186/s40623-014-0168-9](https://doi.org/10.1186/s40623-014-0168-9)
- Cohen, A. (2023). UAF SWUG SAM Student Manual (V1.2). University of Alaska, Fairbanks.
- Cravens, T. E. (1997). *Physics of Solar System Plasmas*. Cambridge University Press.
- Dimmock, A. P., Rosenqvist, L., Welling, D. T., Viljanen, A., Honkonen, I., Boynton, R. J., & Yordanova, E. (2020). On the regional variability of dB/dt and its significance to GIC. *Space Weather*, 18, e2020SW002497. Retrieved from <https://doi.org/10.1029/2020SW002497>
- Edelstein, A. (2007). Advances in magnetometry. *Journal of Physics: Condensed Matter*, 19, 165217. <http://dx.doi.org/10.1088/0953-8984/19/16/165217>.
- Engebretson, M. J., Pilipenko, V. A., Ahmed, L. Y., Posch, J. L., Steinmetz, E. S., Moldwin, M. B., Connors, M. G., Weygand, J. M., Mann, I. R., Boteler, D. H., Russell, C. T., & Vorobev, A. V. (2019). Nighttime magnetic perturbation events observed in Arctic Canada: 1. survey and statistical analysis. *Journal of Geophysical Research: Space Physics*, 124(9), 7442–7458. Retrieved from <https://doi.org/10.1029/2019ja026794>.

- Fortunato, M., Ravanelli, M., & Mazzoni, A. (2019). Real-Time Geophysical Applications with Android GNSS Raw Measurements. *Remote Sensing*, 11(18), 2113. MDPI AG. Retrieved from <http://dx.doi.org/10.3390/rs11182113>.
- Ganushkina, N. Y., Liemohn, M. W., & Dubyagin, S. (2018). Current systems in the Earth's magnetosphere. *Reviews of Geophysics*, 56, 309-332. Retrieved from <https://doi.org/10.1002/2017RG000590>.
- Gombosi, T. I. (1998). *Physics of the Space Environment*. Cambridge University Press.
- Griffiths, D. (2017). *Introduction to Electrodynamics (4th ed.)*. Cambridge University Press.
- Guo, J., Pulkkinen, T. I., Tanskanen, E. I., Feng, X., Emery, B. A., Liu, H., Liu, C., and Zhong, D. (2014). Annual variations in westward auroral electrojet and substorm occurrence rate during solar cycle 23. *J. Geophys. Res. Space Physics*, 119, 2061–2068. Retrieved from doi:[10.1002/2013JA019742](https://doi.org/10.1002/2013JA019742).
- Jackson, J. D. (1999) *Classical Electrodynamics (3rd ed)*. John Wiley & Sons, Inc.
- Kappenman, J. G. (2003). Storm sudden commencement events and the associated geomagnetically induced current risks to ground-based systems at low-latitude and midlatitude locations, *Space Weather*, 1(3), 1016.
doi:10.1029/2003SW000009.
- Kepko, L., McPherron, R.L., Amm, O., *et al.* (2015). Substorm current wedge revisited. *Space Sci Rev* 190, 1–46. Retrieved from <https://doi.org/10.1007/s11214-014-0124-9>.
- Kivelson, M.G., Russell, C. T. (1997). *Introduction to Space Physics*. Cambridge University Press.

- Kletzing, C.A., Kurth, W.S., Acuna, M. et al. (2013). The electric and magnetic field instrument suite and integrated science (EMFISIS) on RBSP. *Space Sci Rev* 179, 127–181. Retrieved from <https://doi.org/10.1007/s11214-013-9993-6>
- Menk, F. W., Waters, C. L. (2013). *Magnetoseismology*. Wiley-VCH.
- NERC Application Guide: Computing Geomagnetically-Induced Current in the Bulk-Power System. (2013). North American Electric Reliability Corporation. Retrieved from https://www.nerc.com/comm/PC/Geomagnetic%20Disturbance%20Task%20Force%20GMDTF%202013/GIC%20Application%20Guide%202013_approved.pdf
- Odenwald, S. F. (2022). Can smartphones detect geomagnetic storms? *Space Weather*, 20, e2020SW002669. <https://doi.org/10.1029/2020SW002669>.
- Osborn, D. L. (1991). NAROD Ring-Core Magnetometer Manual. University of Alaska, Fairbanks.
- Parker, E. N., (1958). Dynamics of the interplanetary gas and magnetic fields. *Ap J*, 128, 664.
- Primdahl, F. (1970). Temperature compensation of fluxgate magnetometers. *IEEE Transactions on Magnetics*, 6(4), 819-822. doi: 10.1109/TMAG.1970.1066971.
- Primdahl, F. (1979). The fluxgate magnetometer. *Journal of Physics E: Scientific Instruments*, 12(4), 241.
- Pulkkinen, A., et al. (2017). Geomagnetically induced currents: Science, engineering, and applications readiness. *Space Weather*, 15, 828–856. doi:10.1002/2016SW001501
- Reeve, W. D. (2018). SAM-III Construction Manual. Anchorage, AK: SAM.

- Reyes-Mora, J. (2021). Capstone Report: Optimization techniques in the assembling, testing, and deployment for SAM IV Magnetic induction Data Collection Vessels. University of Alaska, Fairbanks.
- Ripka, P. (2001). *Magnetic sensors and magnetometers*. Artech House.
- Roux, A., Le Contel, O., Coillot, C., Bouabdellah, A., de la Porte, B., Ruocco, S., Vassal, M. C. (2008). The search coil magnetometer for THEMIS. *Space Sci Rev* 141, 265-275. Retrieved from <https://doi.org/10.1007/s11214-008-9455-8>.
- Russell, C.T., Anderson, B.J., Baumjohann, W. et al. (2016). The Magnetospheric Multiscale magnetometers. *Space Sci Rev* 199, 189–256. Retrieved from <https://doi.org/10.1007/s11214-014-0057-3>
- Schumacher, H. C. (1836). ‘Erdmagnetismus und Magnetometer’. *Jahrbuch für 1836*. Tübingen: J.G.Cotta'sche Buchhandlung, pg 1-47.
- Schunk, R., Nagy, A. (2009). *Ionospheres: Physics, Plasma Physics, and Chemistry (2nd ed)*. Cambridge University Press.
- Smith, W. C., et al. (2019). The Space Weather Underground: A Student-Built Array of Ground Based Fluxgate Magnetometers in Northern New England. University of New Hampshire.
- Zou, Y., Dowell, C., Ferdousi, B., Lyons, L. R., Liu, J. (2022). Auroral drivers of large dB/dt during geomagnetic storms. *Space Weather*, 20, e2022SW003121. Retrieved from <https://doi.org/10.1029/2022SW003121>.

Appendix A

```
/*
 * Created by ArduinoGetStarted.com
 *
 * Modified my Austin Cohen
 *
 * This example code is in the public domain
 *
 * Tutorial page: https://arduinogetstarted.com/tutorials/arduino-temperature-sensor
 */

#include <OneWire.h>
#include <DallasTemperature.h>

const int SENSOR_PIN = 8; // Arduino pin connected to DS18B20 sensor's DQ pin

OneWire oneWire(SENSOR_PIN); // setup a oneWire instance
DallasTemperature tempSensor(&oneWire); // pass oneWire to DallasTemperature library

float tempCelsius; // temperature in Celsius
float tempFahrenheit; // temperature in Fahrenheit

void setup()
{
  Serial.begin(9600); // initialize serial
  tempSensor.begin(); // initialize the sensor
}

void loop()
{
  tempSensor.requestTemperatures(); // send the command to get temperatures
  tempCelsius = tempSensor.getTempCByIndex(0); // read temperature in Celsius
  tempFahrenheit = tempCelsius * 9 / 5 + 32; // convert Celsius to Fahrenheit

  //Serial.print("Temperature: ");
  Serial.println(tempCelsius); // print the temperature in Celsius
  //Serial.print("°C");
  //Serial.print(" ~ "); // separator between Celsius and Fahrenheit
  //Serial.print(tempFahrenheit); // print the temperature in Fahrenheit
  //Serial.println("°F");

  delay(500); //delay 0 is half a second and delay 1000 is two seconds
}
```

Using a linux machine, “`$ cat /dev/tty(source) | ts %Y-%m-%d\ \ %H:%M:%S`” will read the temperature sensor and time stamp. To write the temperature file: “`$ cat /dev/tty(source) | ts %Y-%m-%d\ \ %H:%M:%S > (filename)`” will create a text file. The file can then be sent remotely via ssh transfer.

Arduino temperature sensor setup: 8 into DAT, GND into GND, and 5V into VCO. The multi-colored cable will be screwed down into the housing as follows: yellow into DAT, red into VCO, and black into GND. The sensor will then be ready for testing. The board and sensor are powered via USB and transmit data this way.

Appendix B

The following is the polynomial fit used in Figure 4.7:

```
temp_filename = 'file_path_goes_here'

with open(temp_filename) as f_in:
    temp_data_lines = list(line for line in (l.strip() for l in f_in) if
line)

temp_data = {}
temp_data_keys = 't1 t2'.split(' ')

for key in temp_data_keys:
    temp_data[key] = np.zeros(len(temp_data_lines))

temp_data['time'] = np.zeros(len(temp_data_lines), dtype=object)

for i in range(len(temp_data_lines)):

    entry_line = temp_data_lines[i].split()
    date_line = temp_data_lines[i].split()[1].split('/')
    time_line = temp_data_lines[i].split()[2].split(':')

    if ((entry_line[3] == 'AM') and (int(time_line[0])!=12)):
        hour = int(time_line[0])
    elif ((entry_line[3] == 'AM') and (int(time_line[0])==12)):
        hour = 0
    elif ((entry_line[3] == 'PM') and (int(time_line[0])==12)):
        hour = time_line[0]
    else:
        hour = int(time_line[0])+12

    temp_data['time'][i] = dt.datetime(year = int(date_line[2]),
        month = int(date_line[0]),
        day = (int(date_line[1])),
        hour = (int(hour)),
        minute = int(time_line[1]),
        second = int(time_line[2]))

    temp_data['t1'][i] = entry_line[4]
    temp_data['t2'][i] = entry_line[5]

temp_df = pd.DataFrame(temp_data)

def poly_baseline(y,order):
    x = np.arange(0,len(y),1)
    z = np.polyfit(x,y,order)
    p = np.poly1d(z)

    return(p(x))

t_in_xtr = signal.resample(temp_df['t2'], len(sam_data1['X']))
m,n= np.polyfit(t_in_xtr, sam_data1['X']-poly_baseline(sam_data1['X'],0), 1)
```

```
t_cal_x = m*(t_in_xtr)+n

t_in_ytr = signal.resample(temp_df['t2'], len(sam_data1['Y']))
m,n= np.polyfit(t_in_ytr, sam_data1['Y']-poly_baseline(sam_data1['Y'],0), 1)
t_cal_y = m*(t_in_ytr)+n

t_in_ztr = signal.resample(temp_df['t2'], len(sam_data1['Z']))
m,n= np.polyfit(t_in_ztr, sam_data1['Z']-poly_baseline(sam_data1['Z'],0), 1)
t_cal_z = m*(t_in_ztr)+n
```


* Added in original format*

Appendix C: UAF SWUG SAM Student Manual

Introduction

This manual is structured into three main parts. Part 1 will give a short introduction to space weather and introduce the SWUG project. Part 2 introduces the SAM-III magnetometer kit and will familiarize the reader with important tools and components. In Part 3, a step-by-step guide is provided for construction and operation of a completed kit.

-Part 1-

Space Weather



Figure 1.1: Aurora (Photo courtesy of Annetta Atwell)

How does the aurora form? This manual will provide some information on space weather and how it ties into the formation of aurora. Is there really weather in space? Yes! The sun emits all sorts of electromagnetic radiation and energized particles in the form of solar flares, plasma particles produced by coronal mass ejections, and flows of plasma known as the solar wind (Gombosi, 1998).

Space weather, such as the solar wind, can even affect Earth's magnetic field (see image below). The Earth's magnetic field is a dipole magnetic field, which means that magnetic field lines flow from both the top and bottom of the earth (like a bar magnet). However, the solar wind

pushes against Earth's magnetic field and creates what is called the magnetosphere. The Earth's magnetic field now looks more like a spider than a bar magnet.

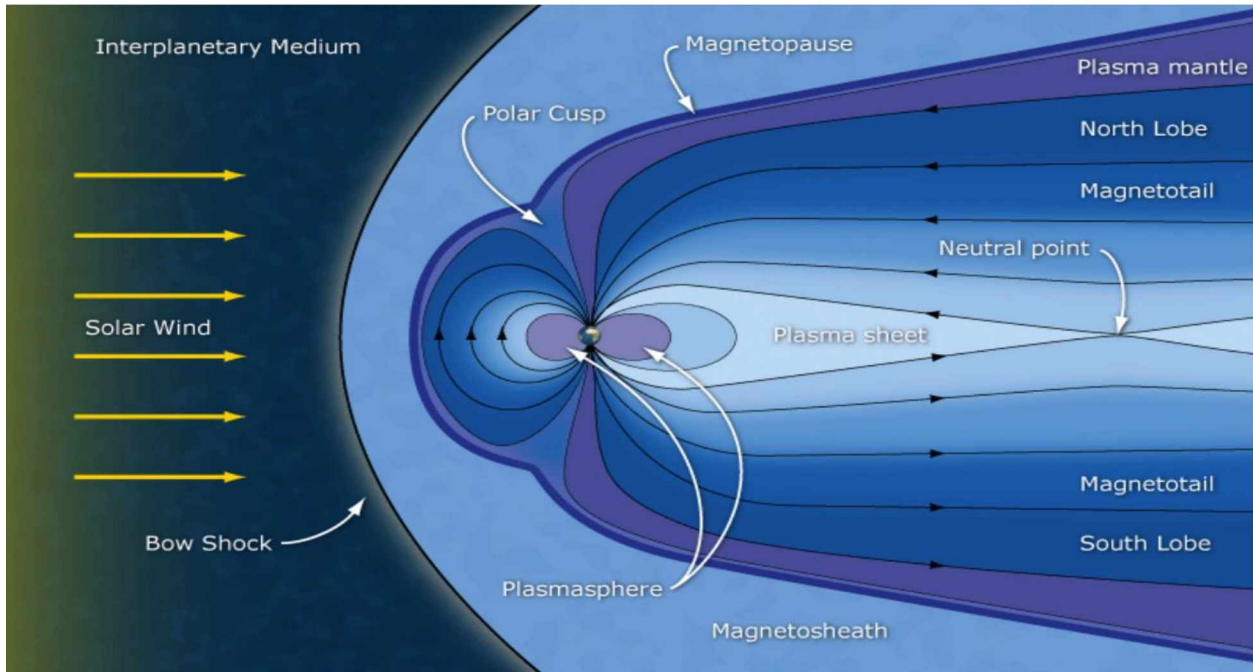


Figure 1.2: The Magnetosphere (Image courtesy of NASA (nasa.gov))

The solar wind occurs because there is a significant difference in pressure between the sun's corona and space surrounding it. The difference in pressure moves some plasma outward towards space even though gravity from the sun was keeping the plasma there in the first place. The solar wind is constant and thus occur more than CMEs and solar flares. (Kivelson et al, 1995).

What about other forms of space weather? What about the well-known solar flares? Solar flares are bundles of energy released suddenly from the sun. Flares occur near the upper atmosphere of the sun and are within the visual light and X-ray spectrum of electromagnetic radiation. They are even capable of traveling through space and interacting with earth's magnetic field. Large amount of material being ejected from the sun or coronal mass ejections (CMEs) are plasma particles and magnetic fields that can interact with Earth's magnetic field as well. CMEs are different from solar flares because flares have photons and CMEs have plasma. (Gombosi, 1998).

How does this tie into the aurora? Space weather carries light (photons) and energetic materials (charged particles). The aurora occurs when these charged particles and photons strike the Earth's ionosphere (between 90 km and 500 km from the ground). The gases in the ionosphere become photoionized (ionization of atoms from absorption of photons) to create an environment where there are as many ions as electrons. After collision with these gases, visible light is emitted and the creation of a beautiful auroral light display occurs.

SWUG Project



Figure 1.3: SWUG Team members Professor Don Hampton (left), undergraduate student Austin Cohen (middle), and PhD student Matt Blandin (right) discuss test results of the first SAM-4 magnetometer kit built in our laboratory.

The SWUG or Space Weather Underground project ([Space Weather Underground \(SWUG\)](#)) is a part of the National Science Foundation (NSF) Established Program to Stimulate Competitive Research (EPSCoR) project (grant #1920965) lead by Prof. Connor of the UAF Physics Department and Geophysical Institute. This project involves the construction of SAM-III (Simple Aurora Monitors 3rd edition) magnetometer kits to measure disturbances in Earth's magnetic field and provide the students constructing them experience in real world engineering, physics, and data analysis. During the summer time, this project provides educators the opportunity to learn how to construct these kits and in turn teach their students how to build them as well.



Figure 1.4: SWUG Team member and high school student Ian Lee working on his magnetometer kit.

-Part 2-

SAM-III Magnetometer

The SAM-III or Simple Aurora Monitoring (3rd edition) kit is purchased from Reeve engineers in Anchorage, AK (<http://www.reeve.com>). This manual is adapted from the original engineer construction manual to provide high school students and teachers a user-friendly approach. The kit comes with a motherboard, loads of components, a pre-built screen, and a hard plastic shell that hereafter referred to as “The Brick”. All the components are separated into recycled plastic bags. The kit also comes with 3 fluxgate magnetometers to measure magnetic field changes in a three-dimension cartesian (X-Y-Z) setup.

What is a fluxgate magnetometer? A magnetometer is a device that measures changes in magnetic fields. When a change in the magnetic field occurs, a current is produced. The fluxgate sensor notices this current and a voltage is applied. The sensor then sends a signal to the magnetometer to store the information to continue the cycle over again.

Tools and Components

The kit does not come with all the tools necessary for construction. Before beginning construction on the kit, make sure to have these tools at the ready:

--- Soldering Kit

--- Solder

--- Needle Nose Pliers

--- Drill

--- Wire Stripper / Cutter

--- Soldering Mat

--- Multimeter

--- Phillips and Small Flat Screwdriver

--- Computer (with USB plugin)

--- Null Modem Cable (Male) to USB

A soldering kit is required to connect most the components together. A soldering iron with a fine tip and operating temperature at 350 Celsius is recommended. If you are unfamiliar with soldering, the following link is a recommended soldering tutorial video (<https://youtu.be/oqV2xU1fee8>). Soldering is a useful skill to have for engineers or experimental scientists. The multimeter will be used to test your kit to make sure it is running properly. Each component should come in a recycled plastic bag. However, not all the resistors are the same. Each resistor should be marked based on its level of resistance. If it is not marked, then the resistance can be determined from the colored lines on the side (refer to the following image). The bands congregated together will determine the resistance, while the band by itself determines the tolerance. All that is needed is to determine the resistance. For example: A 1000-ohm resistor will have brown, black, and red stripe (in that order).

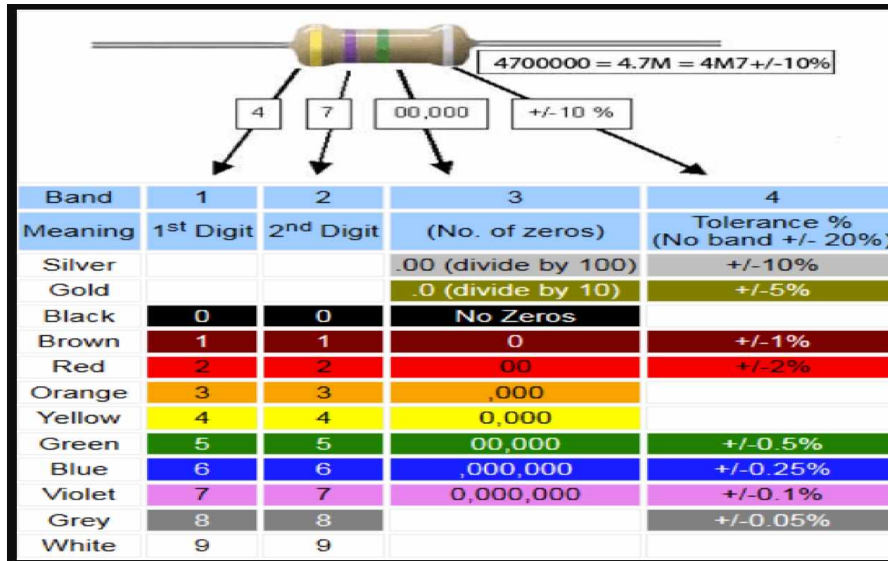


Figure 2.1: Resistor Chart (Courtesy of Learnabout-eletronics.org)

-Part 3-

This is where the fun begins. This section is structured to be a step-by-step guide to build the kit from the ground up. Images have been provided so that the reader has an idea of what component is needed for each step. Some figures, such as the components, have their image sources referenced in the footnotes. The motherboard has the part locations labeled, so that, a part labeled U2, for example, should be soldered on the board where the board is labeled 'U2'.

Be careful not to solder for too long. The board might break if a high heat is applied for an extended period. Have the soldering iron run at about 350 Celsius.

Step 1: Take out the motherboard.

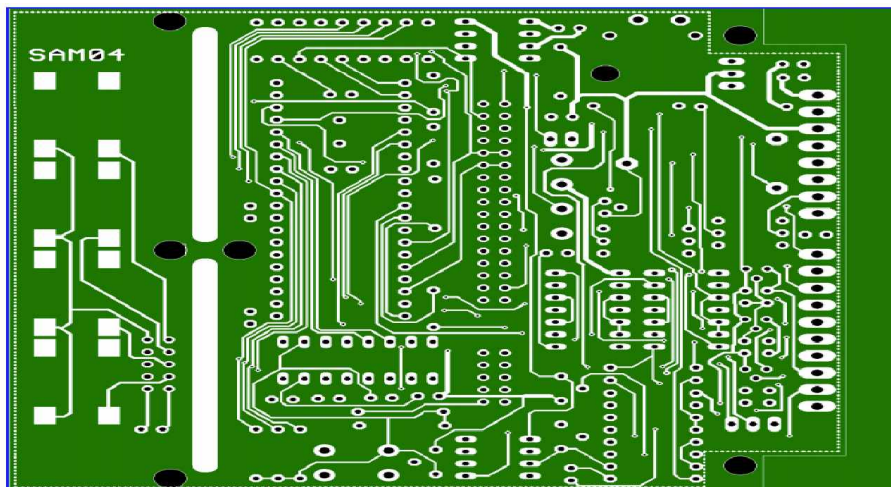


Figure 3.1: Motherboard (Image Courtesy of Reeve's Engineers)

Step 2: Saw between the slits in the board to have two separate pieces. The smaller piece will become the keyboard. NOTE: Some kits may already be in two pieces.

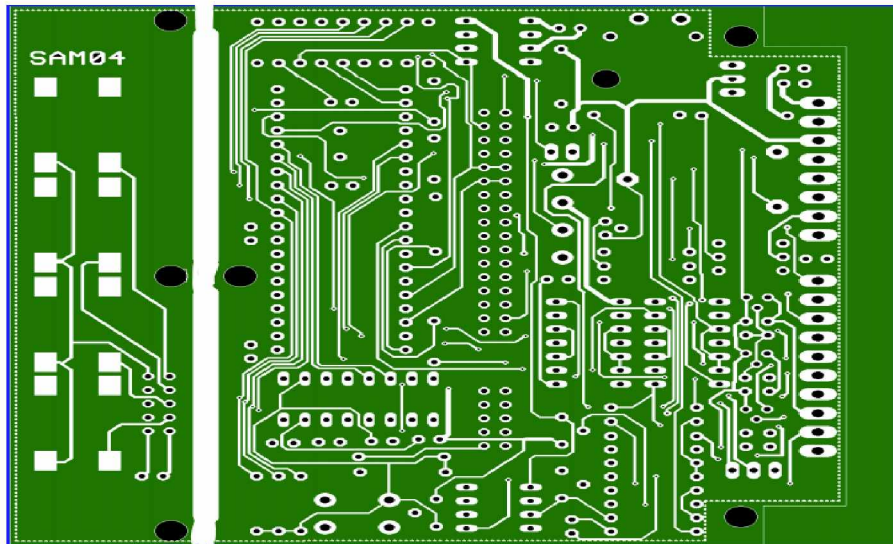


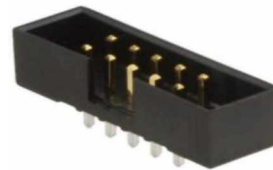
Figure 3.2: Split Motherboard (Image Courtesy of Reeve's Engineers)

Step 3: Find the parts for the keyboard

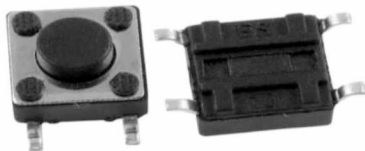
- Red LED (D5) ¹



- Black 10-Pin Header (SV3) ²



- (4) Pushbutton SMD (S2, S3, S4, S5) ³



¹ [3mm Red-6-1-2-800x800.jpg \(800x800\) \(cytron.io\)](#)

² [BE-01-1022-800x800.JPG \(800x800\) \(xcluma.com\)](#)

³ [s-11000.jpg \(1000x1000\) \(ebayimg.com\)](#)

- Put the short lead from the red LED through the top hole and solder it (the cathode is the short end).

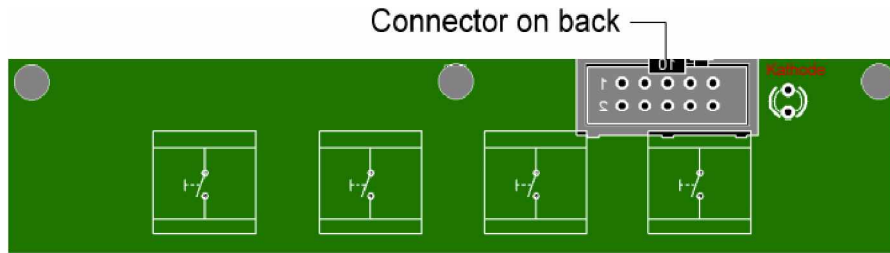


Figure 3.3: The Keyboard (Image Courtesy of Reeve's Engineers)

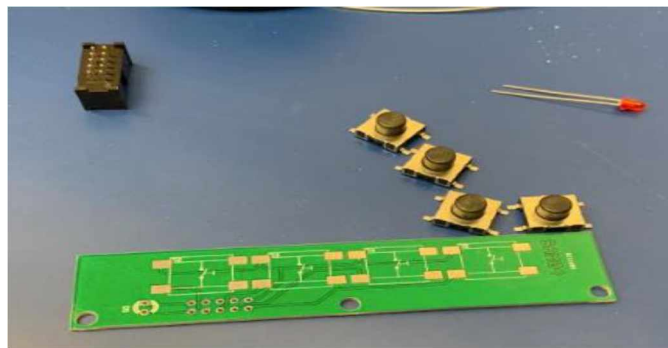
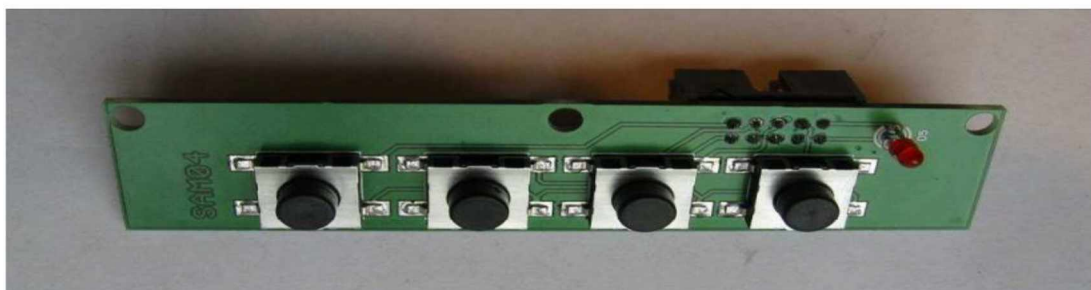


Figure 3.4: Keyboard Components (Image Courtesy of Dogacan Ozturk)

- Put the Black 10-Pin Header underneath the board and have the open slit face away from the keyboard. Solder it.
- Now solder the push buttons.⁴,⁵



Finished Keyboard

⁴ Zoomed view of a pushbutton (Images Courtesy of Reeve's Engineers)

⁵ Top view of the pushbuttons (Images Courtesy of Reeve's Engineers)

Now it is time to work on the motherboard. Remember to not keep the soldering iron on the board for very long or the board will start to warp and might break or become unusable.

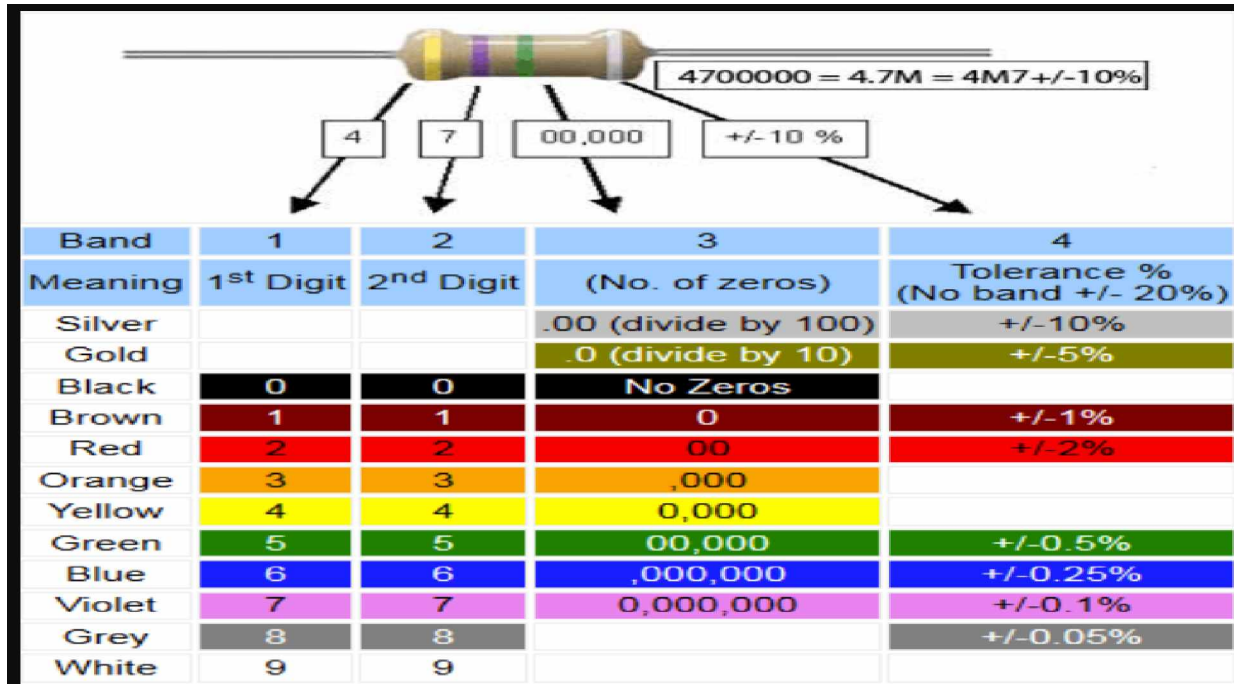


Figure 3.5: Resistor Chart (Courtesy of Learnabout-eletronics.org)

Step 4: Solder the resistors. You can use Figure 3.5 or a multimeter to find the resistance. Place both leads of the multimeter on the ends of the resistor and set to the Ω to the desired range.



Part	Quantity	Type
R16 □	1	Resistor, 68R1 1/4 w
R2 □, R7 □, R9 □	3	Resistor, 1k, 1/8 w (1001)
R20 □, R22 □	2	Resistor, 2k2, 1/8 w
R1 □, R8 □, R10 □	3	Resistor, 10k, 1/8 w (1002)
R12 □, R14 □	2	Resistor, 10k, 1/8 w (1002)
R15 □	1	Resistor, 39k, 1/8 w
R3 □, R4 □, R5 □	3	Resistor, 100k, 1/8 w (1003)
R6 □, R11 □, R13 □	3	Resistor, 100k, 1/8 w (1003)
R17 □, R18 □, R21 □	3	Resistor, 100k, 1/8 w (1003)
R19 □	1	Resistor, 470k, 1/8 w (4703)

Step 5: Solder the diodes (match the bar on the diode with the bar on the board)



6

Part	Quantity	Type
D1 <input type="checkbox"/>	1	Diode, 1N4007 ▶
D2 <input type="checkbox"/> , D3 <input type="checkbox"/>	2	Diode, 1N4148 ▶
D4 <input type="checkbox"/>	1	Diode, 1N5819 Schottky ▶

Step 6: Solder the capacitors (Orientation does not matter for the capacitors)



7

Part	Quantity	Type
C1 <input type="checkbox"/> , C2 <input type="checkbox"/> , C3 <input type="checkbox"/>	3	Capacitor, ceramic, 100 nF
C4 <input type="checkbox"/> , C5 <input type="checkbox"/> , C6 <input type="checkbox"/>	3	Capacitor, ceramic, 100 nF
C7 <input type="checkbox"/> , C8 <input type="checkbox"/> , C9 <input type="checkbox"/>	3	Capacitor, ceramic, 100 nF
C10 <input type="checkbox"/> , C11 <input type="checkbox"/> , C12 <input type="checkbox"/>	3	Capacitor, ceramic, 100 nF
C15 <input type="checkbox"/> , C16 <input type="checkbox"/> , C17 <input type="checkbox"/>	3	Capacitor, ceramic, 100 nF
C18 <input type="checkbox"/> , C21 <input type="checkbox"/>	2	Capacitor, ceramic, 100 nF

Step 7: Find U2 in one of the tinfoil bags. Take the three prongs and bend them so that the hole on the top lines up with the hole on the mother board (Refer to [final image](#) if needed). Next, a screw, washer, and nut should be in a small plastic bag (see image). Place the washer and the screw through the top hole and attach the nut on the bottom to secure U2. Solder U2.



8



9

⁶ [diodes2.jpg \(1024x768\) \(autodesk.com\)](#)

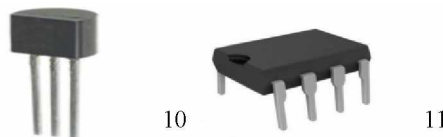
⁷ [dc930148-e56d-48bb-9a34-2f2ebc2ec2af.jpg \(600x600\) \(mikroelectron.com\)](#)

⁸ Plastic bag

⁹ [Voltage-regulator-7805-5v-800x800.jpg \(800x800\) \(potentiallabs.com\)](#)

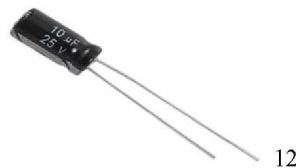
Part	Quantity	Type
U2 <input type="checkbox"/>	1	Voltage Regulator 7805, TO-220, +5 V/1 A
<input type="checkbox"/>	1	4-40 x 5/16 in. screw, washers & nut

Step 8: Solder U1, U3, U4, and U5. Make sure to orient them in the correct direction. The board will show you which way to place them. Read the top of U5 and make sure there is a 7660 and not a 358N.



Part	Quantity	Type
U1 <input type="checkbox"/> , U3 <input type="checkbox"/> , U4 <input type="checkbox"/>	3	Voltage Regulator 78L05, TO-92, +5 V/100 ma
U5 <input type="checkbox"/>	1	Voltage converter, ICL7660, -5 V out ▶

Step 9: Solder C13 and C14. Make sure to orient them properly. The longer lead goes into the + hole on the board.



Part	Quantity	Type
C13 <input type="checkbox"/> , C14 <input type="checkbox"/>	2	Capacitor, electrolytic, 10 μ F/25 V ▶

Step 10: Solder the pluggable terminal blocks (refer to following figure).



Part	Quantity	Type
XP1 <input type="checkbox"/>	1	Pluggable screw terminal block, 8-position
XP2 <input type="checkbox"/>	1	Pluggable screw terminal block, 10-position

¹⁰ [da78l05-250x250.jpg \(250x250\) \(hobbytronics.co.uk\)](#)

¹¹ [a-1385.jpg \(500x500\) \(taydaelectronics.com\)](#)

¹² [10uF-25V-Radial-Lead-Aluminum-Electrolytic-Capacitors.jpg \(1100x1100\) \(ardustore.dk\)](#)

¹³ [31137108_1_800x.jpg \(800x640\) \(shopify.com\)](#)

¹⁴ [s-l640.jpg \(640x495\) \(ebayimg.com\)](#)

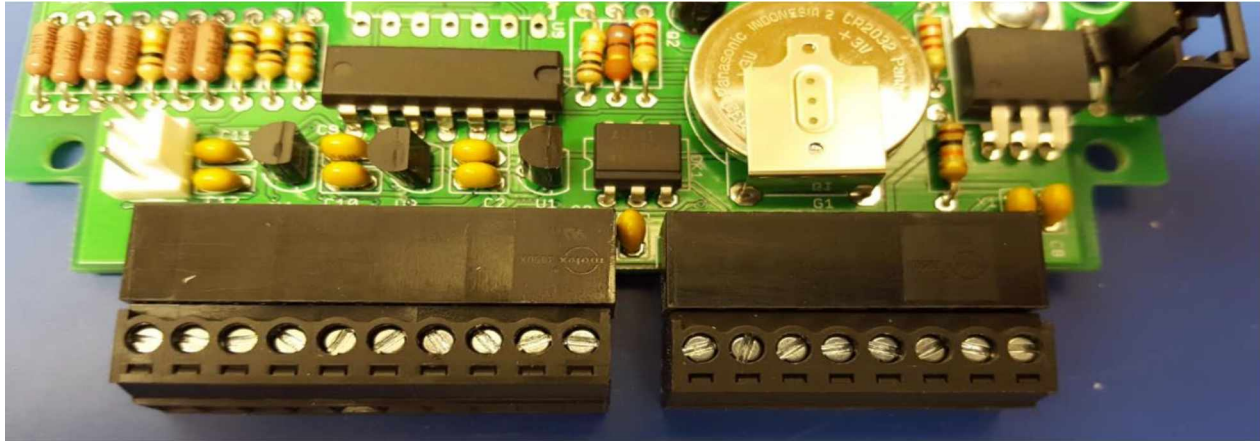


Figure 3.6: Terminal Blocks (Image Courtesy of Austin Cohen)

- After you solder them to the board, take a flat head screwdriver and screw in the pins until they are tight.

Step 11: Solder the 3-position, 2-pin power header next to the diode D1.

Part	Quantity	Type
□	1	PCB header, 3-position, 2 pin (1-0-1 configuration)

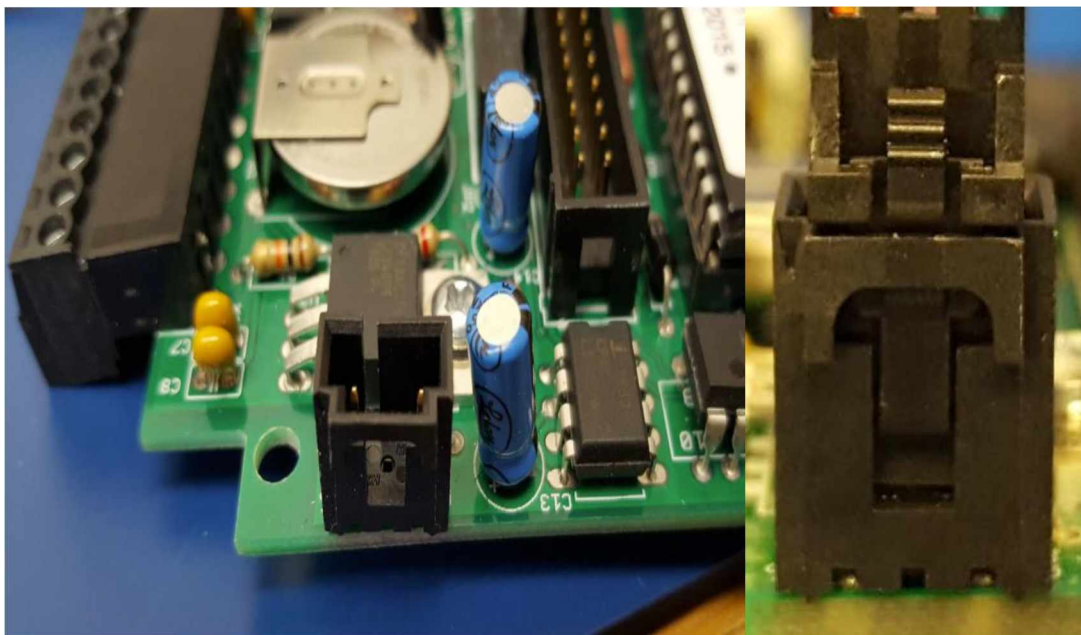


Figure 3.7: Location of the 2-Pin Header (Image Courtesy of Austin Cohen)

Step 12: Next is the battery. Make sure to avoid conductive surfaces or static electricity when handling the battery. Solder the battery G1.



15

Part	Quantity	Type
G1 <input type="checkbox"/>	1	Lithium battery, 3 V, 3-pin

Step 13: Assemble the power cable. Refer to the process laid out on the next page.



Housing¹⁶



Terminal Contact¹⁷



Power Jack¹⁸

Part	Quantity	Type
<input type="checkbox"/>	1	Connector socket housing, 3-position, black
<input type="checkbox"/>	2	Terminal socket contact, box type
<input type="checkbox"/>	1	24 AWG wire, 15 cm long, orange
<input type="checkbox"/>	1	24 AWG wire, 15 cm long, green
<input type="checkbox"/>	2	Heat shrink tubing, ~10 mm long
<input type="checkbox"/>	1	Coaxial power jack, 2.1 x 5.5 mm, panel mount

¹⁵ [CR2032_1GU_93872.1441763387.1280.1280.jpg \(800x800\) \(bigcommerce.com\)](https://www.bigcommerce.com/CR2032_1GU_93872.1441763387.1280.1280.jpg)

¹⁶ [0050579403 Molex | Connectors, Interconnects | DigiKey](https://www.digikey.com/product-detail/en/0050579403)

¹⁷ [Newark.com](https://www.newark.com)

¹⁸ [coaxial power jack, 2.1 x 5.5 mm, panel mount - Bing](https://www.bing.com)

- Strip about half an inch off both ends of the orange and green wires.



Figure 3.8: Stripped Wire for Power Cable (Image Courtesy of Austin Cohen)

- Place one end through a terminal contact. Use some needle nose pliers to squeeze the contact around the wire. **DO NOT SQUEEZE THE HEAD OF THE CONTACT.** Squeezing the head won't allow the contact to connect to the housing. Then solder the wire to the contact. Do this for both wires.



Figure 3.9: Terminal Contact Around Wire (Image Courtesy of Austin Cohen)

- Plug the wires into the housing as shown. Twist the wires to keep them together.



Figure 3.10: Terminal Contacted Wires into Housing (Image Courtesy of Austin Cohen)

- Now solder the wires to the power jack as shown in the next two figures.

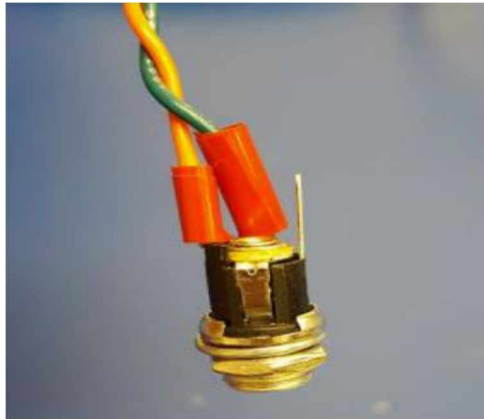


Figure 3.11: Power Jack with Insulation for Safety (Image Courtesy of Austin Cohen)

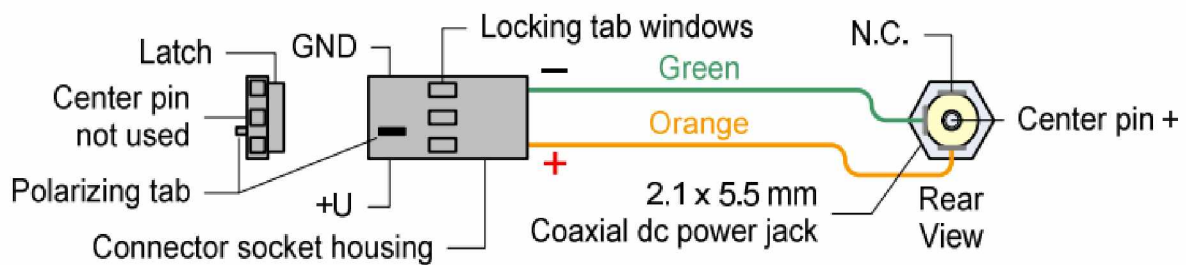


Figure 3.12: Overview of Procedure (Image Courtesy of Reeve's Engineers)

- The end result should look like the following image:



Figure 3.13: Finished Power Cable (Image Courtesy of Dogacan Ozturk)

Step 14: Test power supply

- Plug the housing on to the board and then plug in the AC adapter to an outlet.

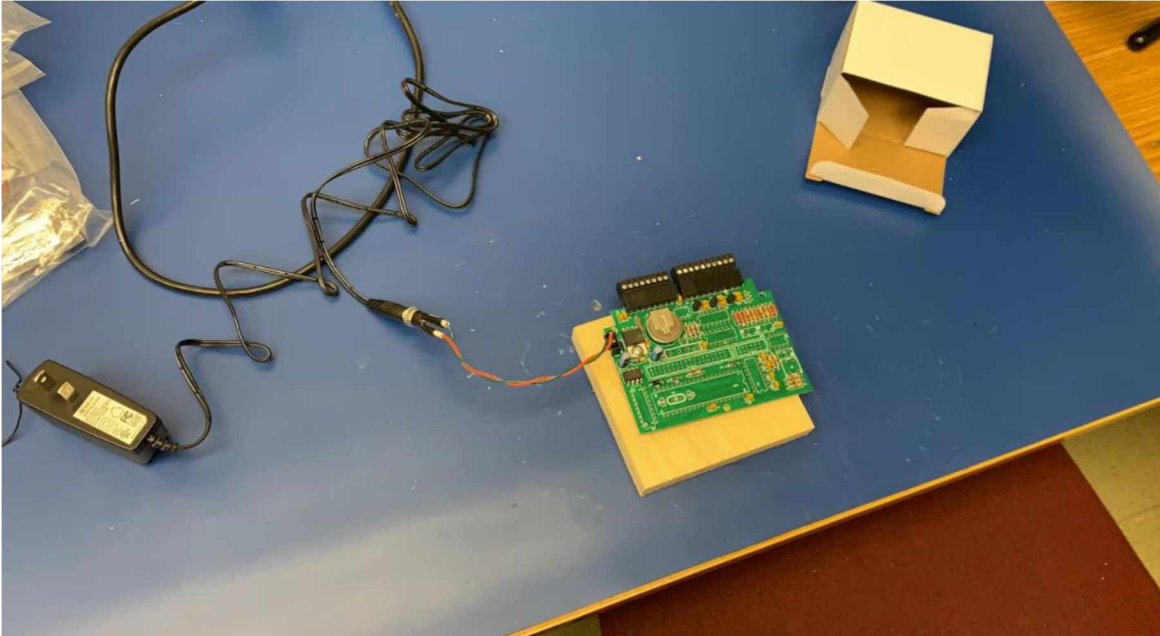


Figure 3.14: Testing Power Supply (Image Courtesy of Dogacan Ozturk)

- Take a multimeter and set it to the 20-volt range as shown.



Figure 3.15: Multimeter (Image Courtesy of Austin Cohen)

- Take the black cable from the multimeter and place the tip on the reference ground shown in the lower right hand corner of Figure 3.16.

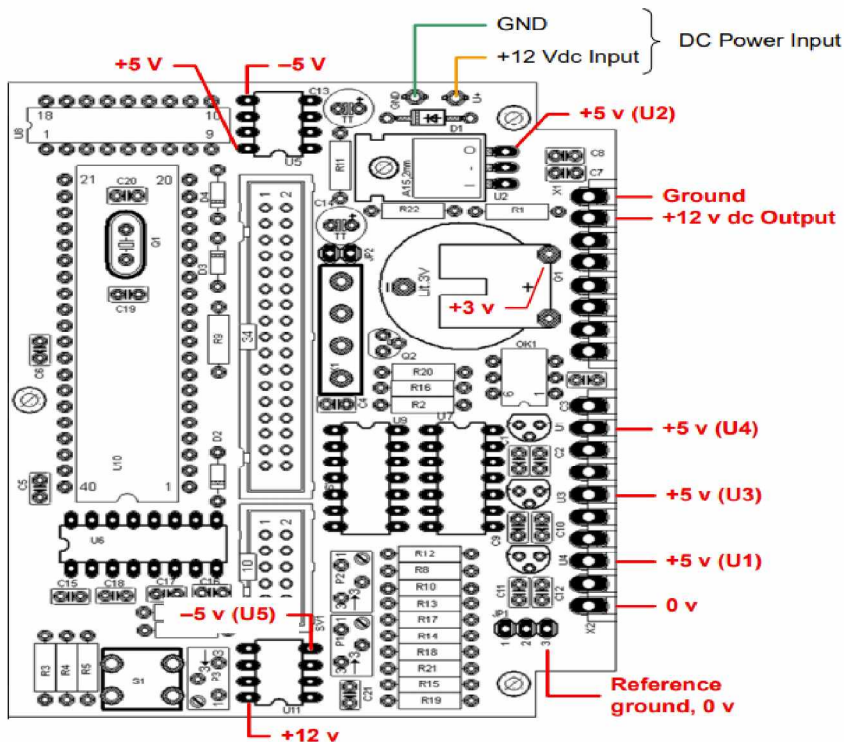


Figure 3.16: Motherboard Voltage Guide (Image Courtesy of Reeve’s Engineers)

- Keep the black cable on the reference ground and take the red cable and place the tip on each location shown in Figure 3.16. The voltage on the multimeter should be close to what is shown in Figure 3.16. Once finished, unplug the power.

Step 15: Solder the 40-pin socket. Make sure to line up the socket with image on the board. It has a specific orientation.



19

Part	Quantity	Type
□	1	DIL 40-pin IC socket

¹⁹ [dill-socket-40-wide-500x500.jpg \(500x500\)](http://dill-socket-40-wide-500x500.jpg) (hobbytronics.co.uk)

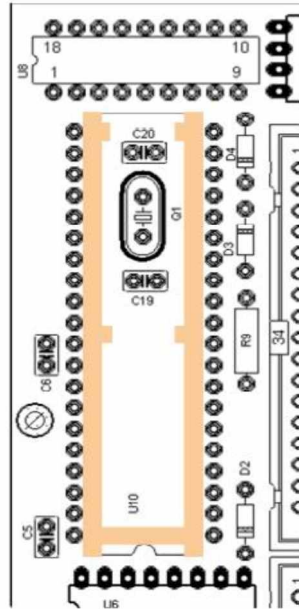
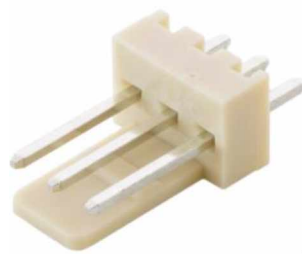
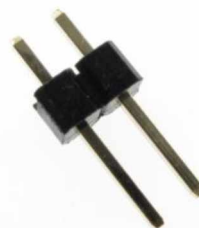


Figure 3.17: Location for 40-Pin Socket (Image Courtesy of Reeve's Engineers)

Step 16: Solder JP 1 and JP 2. For JP 1, put the shorter pins through the board and have the backplate face the battery. For JP 2, put the shorter pins through the board as well. You want the longer pins sticking up.



20



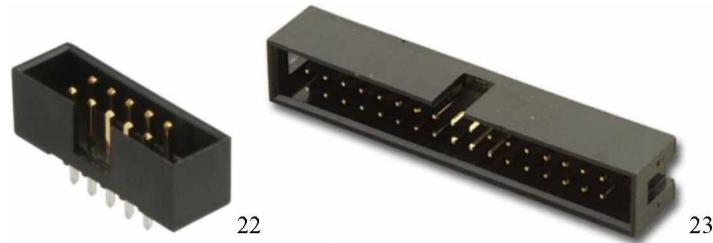
21

Part	Quantity	Type
JP1 <input type="checkbox"/>	1	3-pin polarized header block
JP2 <input type="checkbox"/>	1	2-pin header block

²⁰ [CN-PH-M3.jpg \(1200x1200\) \(doift4652t1in.cloudfront.net\)](#)

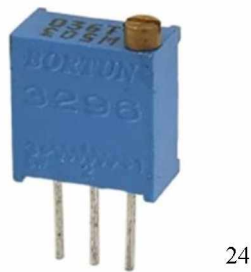
²¹ [2 Pin header_95408.1337689803.1280.1280.jpg \(800x600\) \(bp.blogspot.com\)](#)

Step 17: Solder SV1 and SV2. Have the center slot face the 40-pin socket.



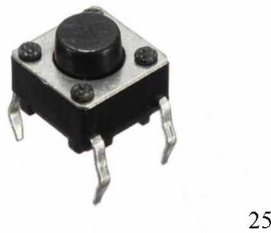
Part	Quantity	Type
SV1 <input type="checkbox"/>	1	10-pin polarized PCB header socket
SV2 <input type="checkbox"/>	1	34-pin polarized PCB header socket

Step 18: Solder P1, P2, and P3. There should be writing on the side of this part that indicates how much resistance it has. P1 should be 47k or 50k. P2 and P3 should be 10k.



Part	Quantity	Type
P1 <input type="checkbox"/>	1	Variable resistor 47k or 50k
P2 <input type="checkbox"/> , P3 <input type="checkbox"/>	2	Variable resistor 10k

Step 19: Solder the reset pushbutton S1.



Part	Quantity	Type
S1 <input type="checkbox"/>	1	Reset pushbutton

²² [10Pin-Box-Header-Male LRG.jpg \(640x640\) \(ventor.co.in\)](#)

²³ [SBH-34S.jpg \(504x308\) \(pacificcable.com\)](#)

²⁴ [41DzpvH7W9L_SX342 .jpg \(342x342\) \(images-amazon.com\)](#)

²⁵ [dfd075cb-35e6-4932-bf21-296a4163c925.jpg \(600x600\) \(alexnlid.com\)](#)

Step 20: Solder K1 (see following image). Have the side of the + sign (the polarity indicator in the picture below) face towards the 40-pin socket.

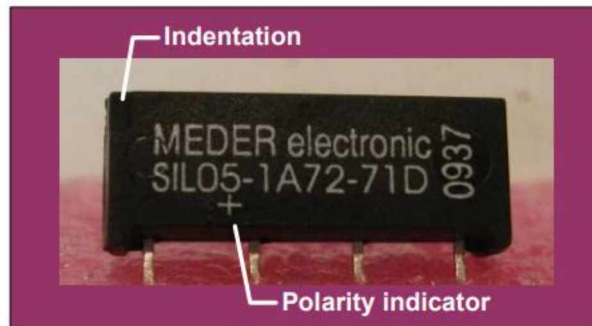


Figure 3.18: Polarity Guide for K1 (Image Courtesy of Reeve’s Engineers)

Step 21: Solder U6, U7, U8, U9, U11. These components look very similar. The checkboxes below have the specific names of these components. You can identify which component is which by the physical text written on the component.



26

Part	Quantity	Type
U6 <input type="checkbox"/>	1	MAX232 transceiver IC
U7 <input type="checkbox"/> , U9 <input type="checkbox"/>	2	NAND-Gate 74HCT00 logic IC
U8 <input type="checkbox"/>	1	Real time clock IC, RTC72421
U11 <input type="checkbox"/>	1	Op-amp IC, LM358N

²⁶ [IC0001_MED.jpg \(250x250\) \(rhydolabz.com\)](#)

Step 22: Solder OK1 and Q2.



27



28

Part	Quantity	Type
OK1 <input type="checkbox"/>	1	Opto-coupler CNY17F
Q2 <input type="checkbox"/>	1	Transistor, BC337

Step 23: Solder C19 and C20.



29

Part	Quantity	Type
C19 <input type="checkbox"/> , C20 <input type="checkbox"/>	2	Capacitor, 22pF

Step 24: Solder Q1. If it did not come with an insulating wafer, cut a small square from a piece of paper, and poke it through. This way the crystal is not touching the board directly.



30

Part	Quantity	Type
Q1 <input type="checkbox"/>	1	Crystal, 16MHz / HC49U-V

²⁷ [optocoupler-cny17f-2.jpg \(470x470\) \(electronic-center.hr\)](#)

²⁸ [BC337 General Purpose NPN Transistor-500x500.jpg \(500x500\) \(tu-eshop.com\)](#)

²⁹ [cp22pf-img_4531-2.jpg \(820x620\) \(solarbotics.com\)](#)

³⁰ [16mhz-crystal.jpg \(1100x1100\) \(edwinrobotics.com\)](#)

Step 25: Place U10 onto the 40-pin socket and push it in. Make sure the pins align before pressing in. Applying a bit of pressure might be necessary.



Part	Quantity	Type
U10 □	1	Microprocessor PIC16F877 IC

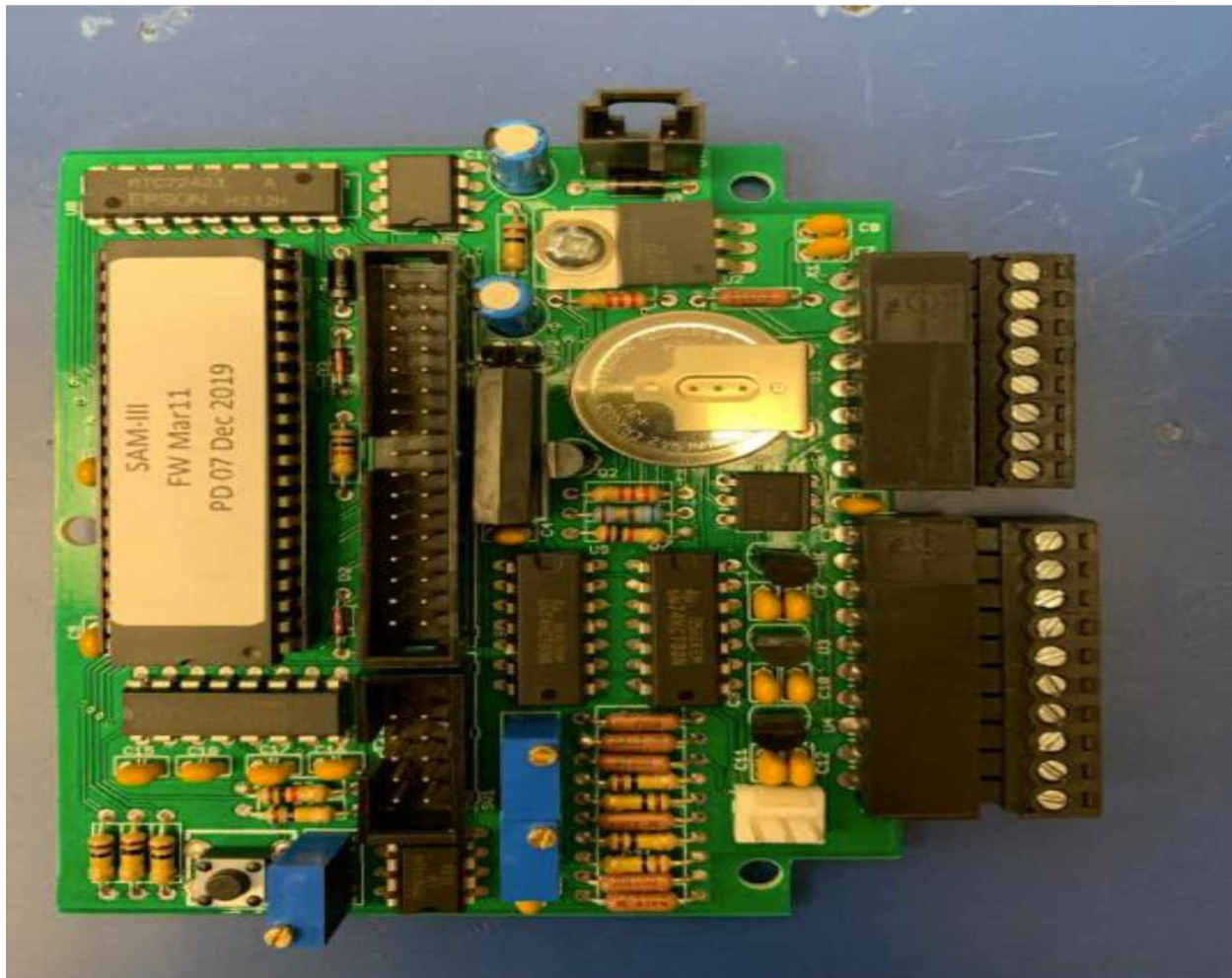


Figure 3.19: Finished Motherboard (Image Courtesy of Dogacan Ozturk)

Finished Motherboard

³¹ [Integrated-Circuits-ICs-Embedded-Micro-controllers-PIC16F877.jpg_350x350.jpg \(350x350\) \(alicdn.com\)](#)

Step 26: Find the display module and a pair of ribbon cables. These parts should already be assembled. If not, read the **NOTE** below.

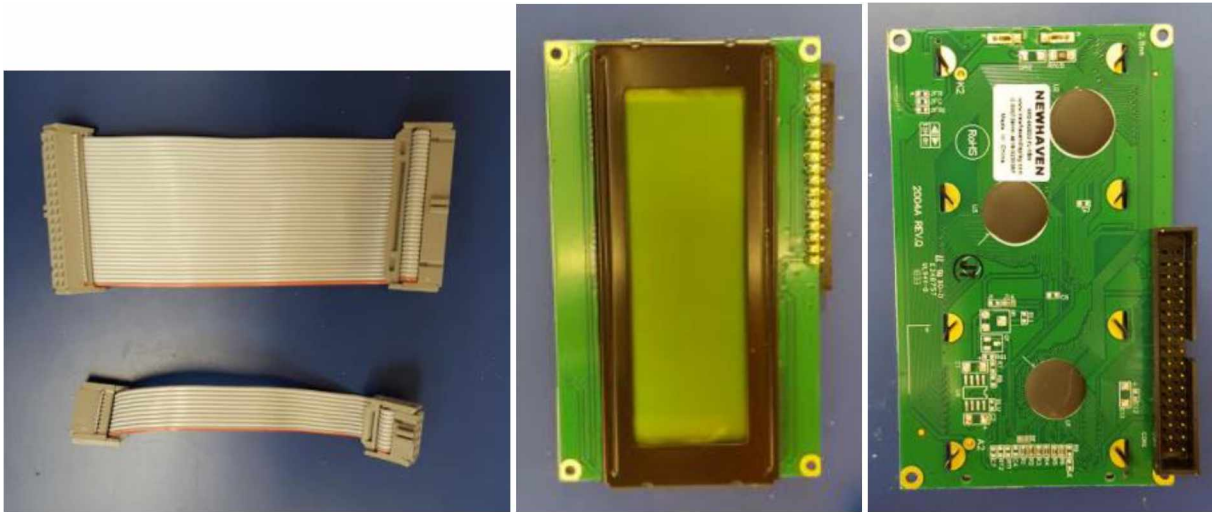


Figure 3.20: Ribbon Cables (left) and Display Module front and back (right)
(Image Courtesy of Austin Cohen)

NOTE: If the display module and/or the ribbon cables are not assembled, perform the following: Solder a 34-pin header to the display module and remove the last pair of pins to make sure it fits properly. For the ribbon cables, take the cables and run them through the cable clamp, tighten, and trim off the excess cable.

Step 27: Connect the display module and the keyboard to the motherboard. The wide cable goes to the display module and the thin cable goes to the keyboard. Refer to the image below.

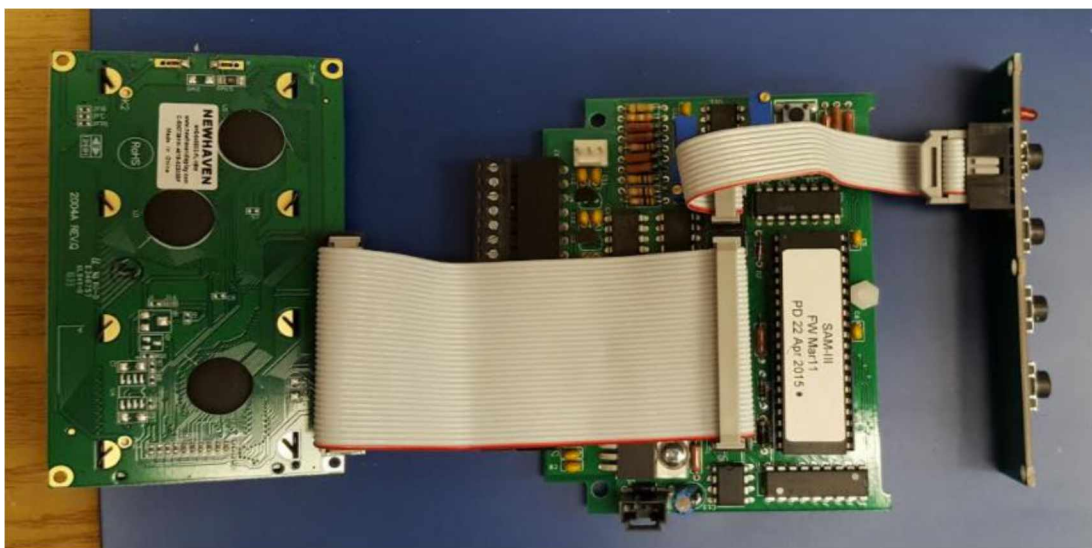
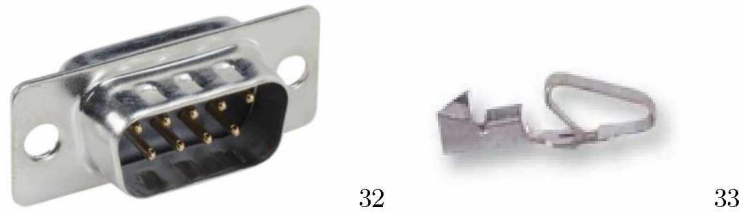


Figure 3.21: All Connections Established (Image Courtesy of Austin Cohen)

Step 28:



Part	Quantity	Type
JP4 <input type="checkbox"/>	1	DB-9M plug
JS1 <input type="checkbox"/>	1	Socket connector housing, white
<input type="checkbox"/>	3	Terminal contact, spring type
<input type="checkbox"/>	1	24 AWG wire, 15 cm long, red
<input type="checkbox"/>	1	24 AWG wire, 15 cm long, black
<input type="checkbox"/>	1	24 AWG wire, 15 cm long, green

Find the green, red, and black wires. Strip off half an inch of both sides of the wires. Solder the wires to the plug as shown below:



Figure 3.22: Soldered wires on Plug
(Image Courtesy of Austin Cohen)

- Solder green to 5
- Solder red to 3
- Solder black to 2



Figure 3.23: Wires in Housing
(Image Courtesy of Austin Cohen)

- Now solder the wires to the terminal contacts and plug them into the connector housing.

³² [241770.jpg \(200x140\) \(fullcompass.com\)](#)

³³ [241770.jpg \(200x140\) \(fullcompass.com\)](#)

➤ Finally, plug the housing onto the board:

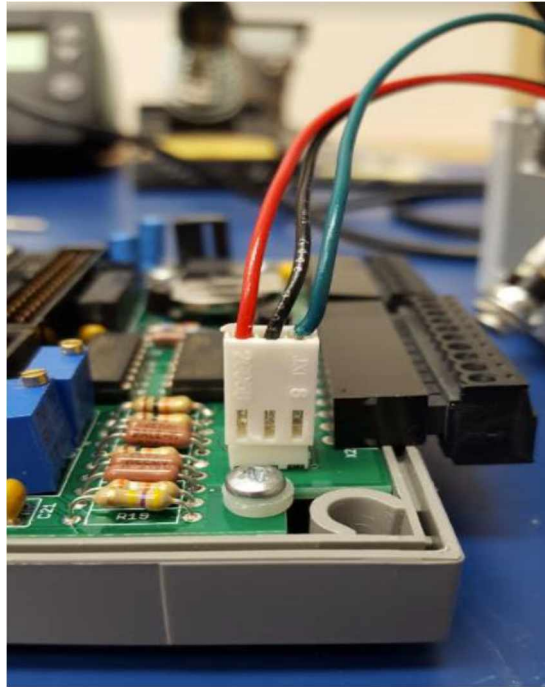


Figure 3.24: Connected Housing to Board (Image Courtesy of Austin Cohen)

Step 29:



34



35



36

Part	Quantity	Type
<input type="checkbox"/>	1	EIA-232 null modem cable
<input type="checkbox"/>	1	Header shorting block
<input type="checkbox"/>	1	AC power adapter, 12 Vdc, 200 mA

³⁴ Null Modem Cable (Photo by Austin Cohen)

³⁵ [HDSHOB_200.jpg \(200x204\) \(futurlec.com\)](#)

³⁶ AC Power Adapter (Photo by Austin Cohen)

- Take the header shorting block and insert it on top of JP2. This activates the internal clock.

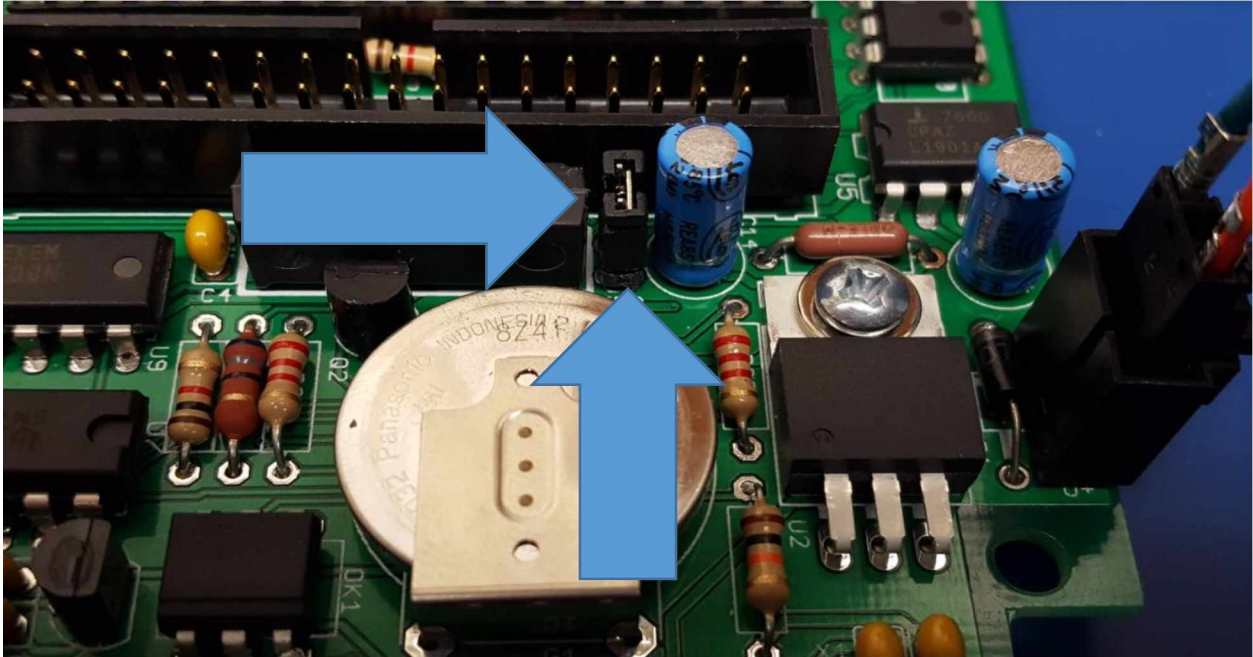


Figure 3.25: Shorting Block on JP2 (Image Courtesy of Austin Cohen)

- Plug in the ac power adapter.
- Take a small screwdriver and start turning the metal dial on the top of P3.

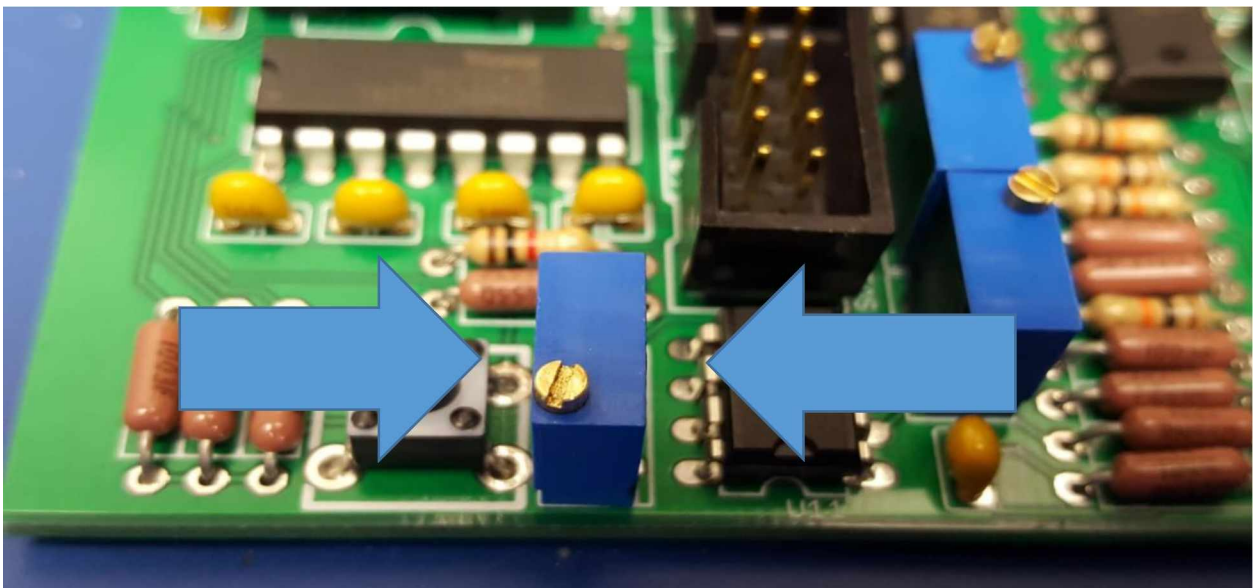


Figure 3.26: Variable Resistor P3 (Image Courtesy of Austin Cohen)

- Turn the dial Counter-Clockwise slowly until you see text appear on the screen OR the dial makes a click. If the dial makes a click, turn the dial Clockwise slowly until text appears on the screen. Make the text appear as dark as you can.



Figure 3.27: Turning P3 Dial (Image Courtesy of Joe Rm)

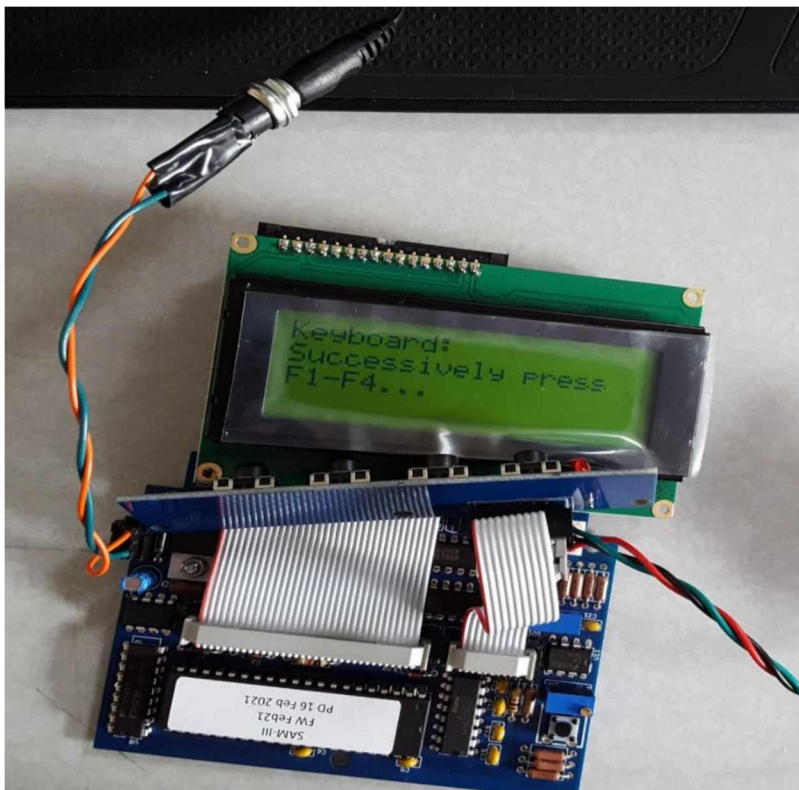


Figure 3.28: Initial Text Screen (Photo Courtesy of Joe Rm)

Step 30:

- Press all four buttons on the keyboard.
- Insert the null modem cable into the serial plug (the plug from Fig 3.22).
- If your computer does not have a serial port, use a serial to USB adapter to connect your computer to the magnetometer.
- If you are using a windows-based operating system (like Windows 10), download Tera Term or another serial reading software you choose.
- Tera Term: [Download File List - Tera Term - OSDN](https://osdn.jp/projects/teraterm/)

Tera Term Open Source Project

<https://ttssh2.osdn.jp/index.html.en> ▼

TeraTerm Project would have been developed terminal emulator "Tera Term" and SSH module "TTSSH". This software is open source software under BSD License. This is **Tera Term** Pro 2.3 succession version and is being officially recognized by the original author. Development is continuing in Project Pigeon OSDN. Download.

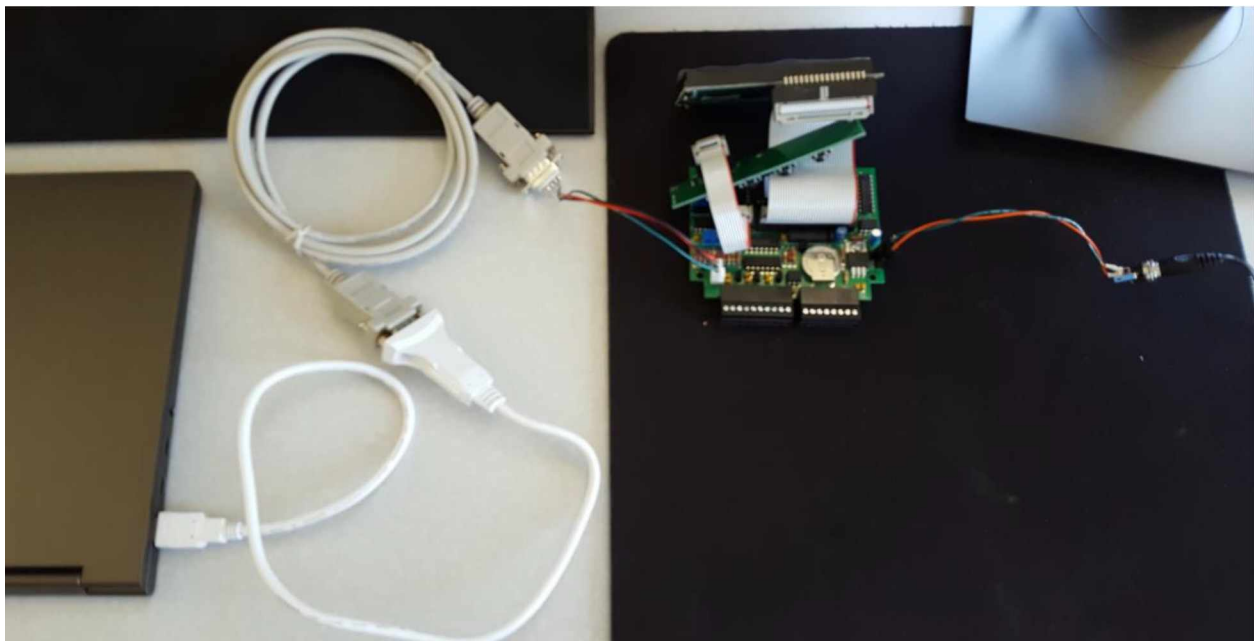


Figure 3.29: Connection Setup (Image Courtesy of Austin Cohen)

Step 31: Tera Term.

- After installing Tera Term, open up Tera Term. If you are having trouble, the path you need might look like this: C: → Program Files (x86) → teraterm → ttermpro. The ttermpro is an application that should yield the following window:

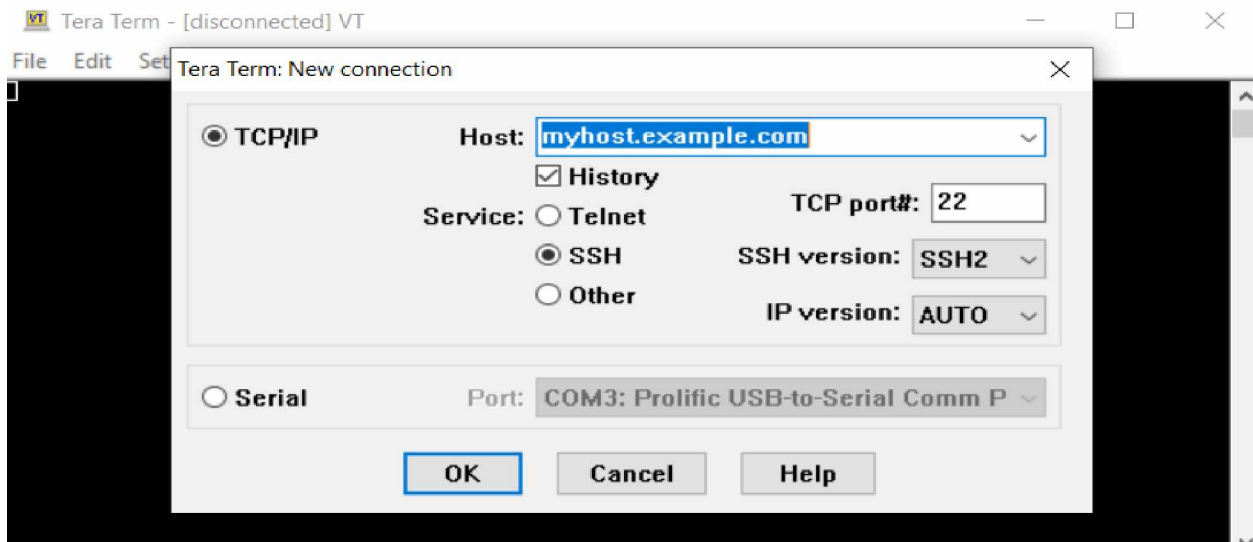


Figure 3.30: Initial Tera Term Window (Image Courtesy of Austin Cohen)

- Click on the Serial option

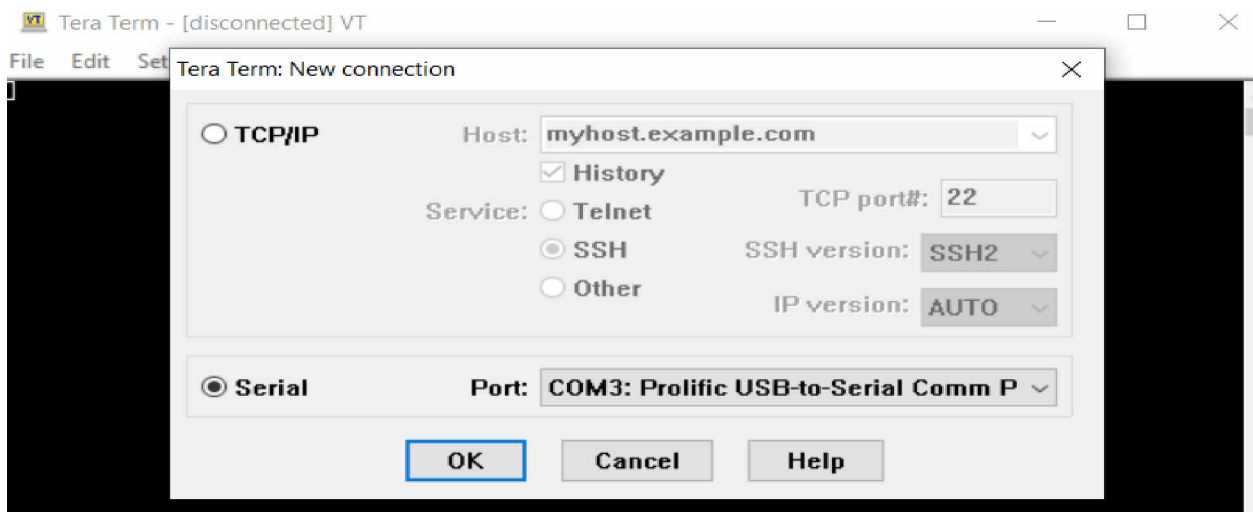


Figure 3.31: Tera Term Serial (Image Courtesy of Austin Cohen)

➤ Click OK

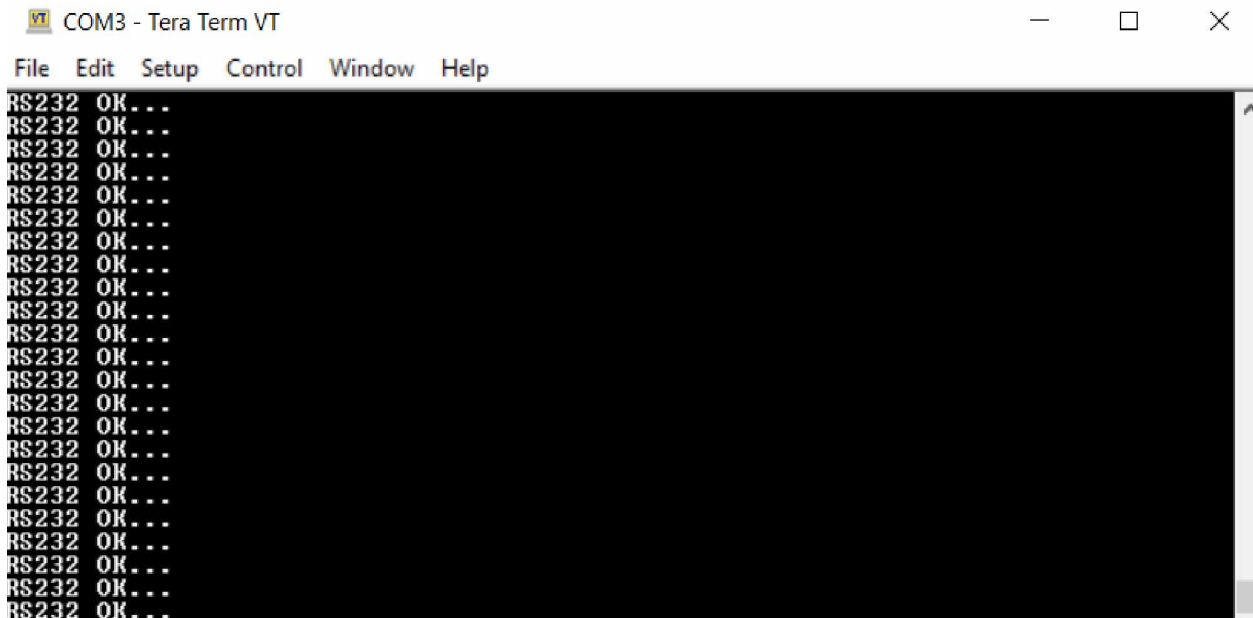


Figure 3.32: OK..... (Image Courtesy of Austin Cohen)

- If you see all the OK's, press the far-left button on the keyboard (F1). If you do not see all the OK's, try restarting Tera Term.

Step 32: Setting the clock

- Now the screen on your kit should look like this:

```
00.01.00 00:05:56
Clock:
Press F1 if clock
is running
```

Figure 3.33: (Image Courtesy of Revee)

- Press F1 if the clock is indeed running.
- The kit will now ask you to set the day, month, year, etc. Set up the date to follow UTC. Alaska is UTC -8, so 10:00 am in Alaska is 1800 UTC. You can also use time-and-date.com or another clock website. The instructions on how to change the date should be seen on the kit's screen. NOTE: You cannot change the seconds, but they are set back to zero when you change the minutes.

Step 33: Testing the hardware

- The next screen should look like this:

```
Alarm switch:  
Relay switches in  
1s-interval. Press  
F1 to confirm.
```

Figure 3.33: (Image Courtesy of Revee)

- You should hear a faint chirp or click near the board about every second or so.
- The next screen asks you to apply a voltage to the digital input. Do not bother with this. Press F1 and continue. The screen should say test aborted.
- Now your screen should look like this:

```
analog output  
P1: gain P2: offset  
F1 = OK F2 = 1/2Umax  
F3 = Umax F4 = Umin
```

Figure 3.34: (Image Courtesy of Revee)

- For this part you will need a multimeter and a small flat head screwdriver.
- Set the multimeter to 20 V (direct current):

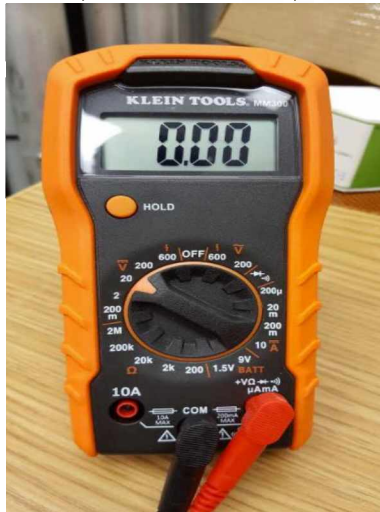


Figure 3.35: Multimeter (Image Courtesy of Austin Cohen)

- Refer to the following image to see where to put the multimeter leads (Note: I have removed some of the parts to make it easier to see where to put the leads):

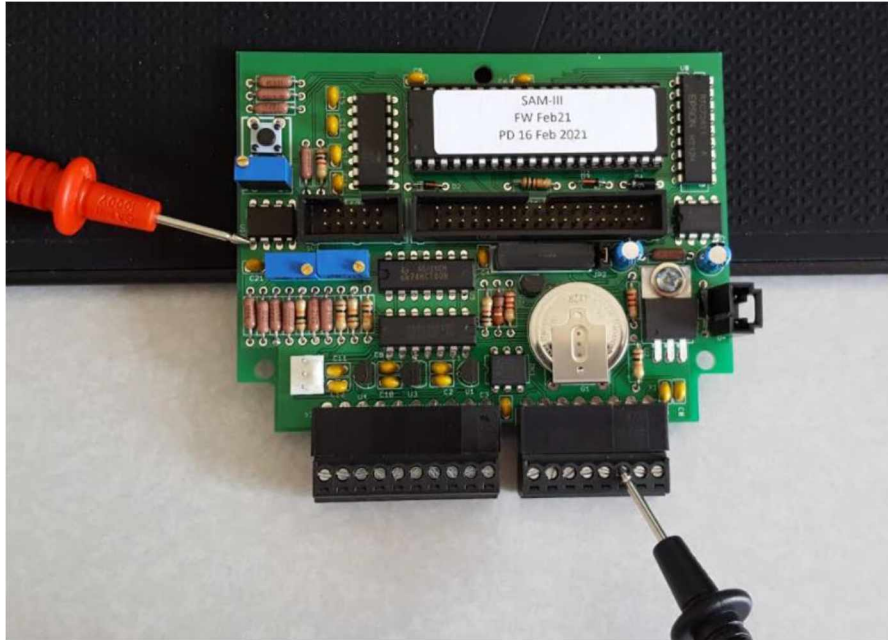


Figure 3.36: Lead Placement Part 1 (Image Courtesy of Austin Cohen)

- You might need another person for this step. While the multimeter leads are in place, Press F3 on the keyboard (Umax). Turn the dial on top of P1 until the multimeter reads 5V.

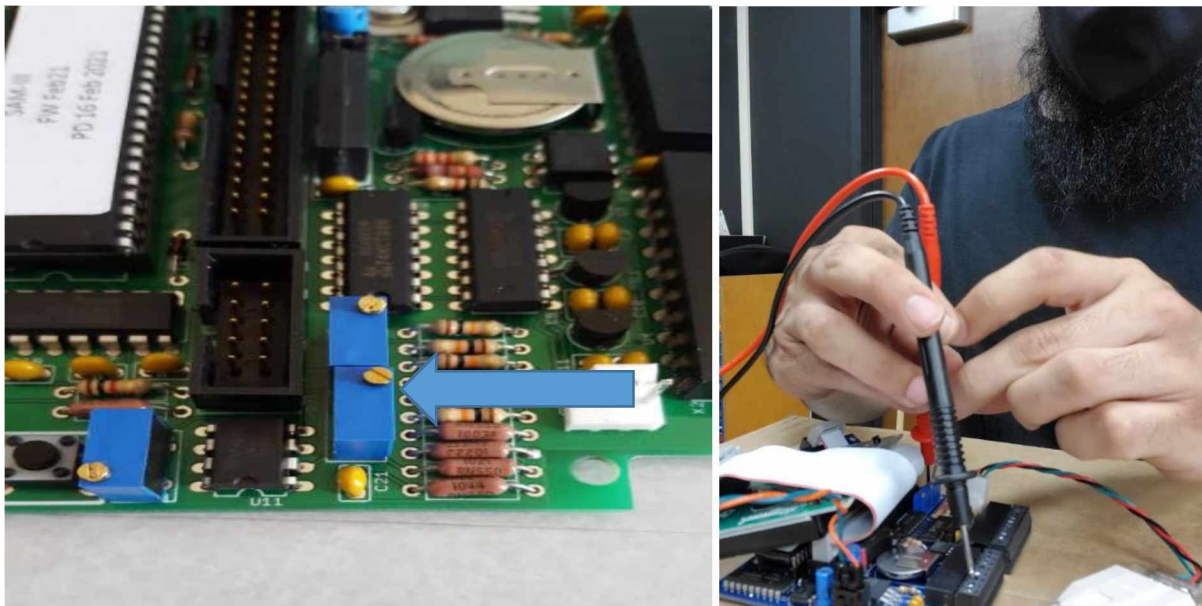


Figure 3.37: P1 (Image Courtesy of Austin Cohen and Joe Rm)

- Now take the red positive lead and move it to the pin left of the black negative lead:

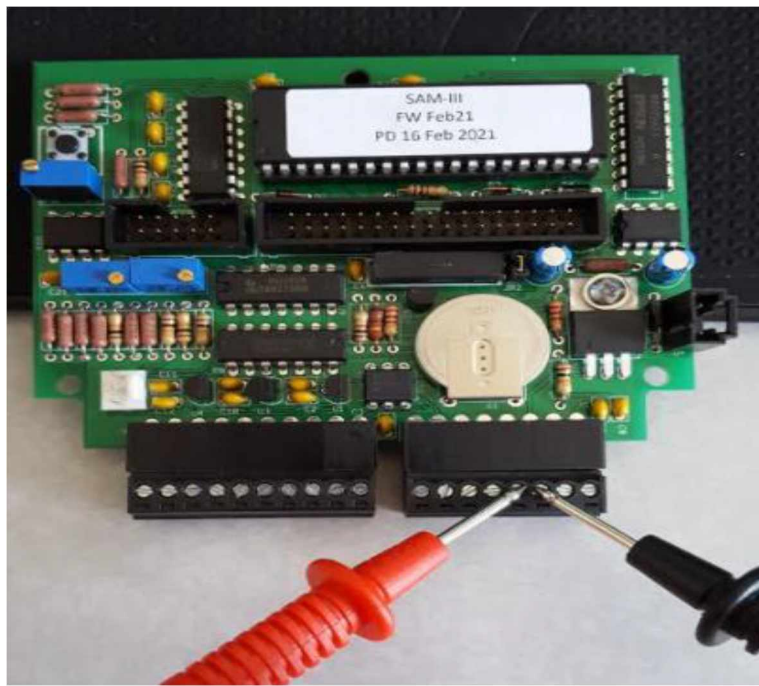


Figure 3.38: Lead Placement Part 2 (Image Courtesy of Austin Cohen and Joe Rm)

- Press F4 on the keyboard (Umin) and turn the dial on P2 until the multimeter reads 0V.

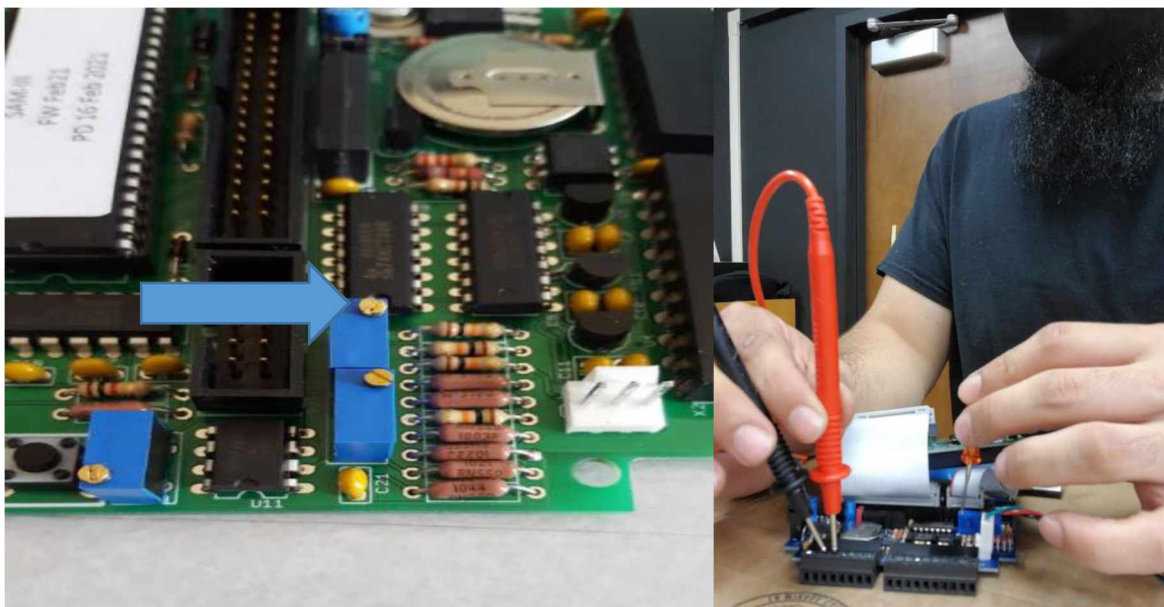


Figure 3.39: P2 (Image Courtesy of Austin Cohen and Joe Rm)

- Repeat the previous steps until the multimeter reads 5V for P1 and 0V for P2 consistently. When finished Press F1.
- Next the display will ask you to “Initialize EEPROM with default parameters?”. Select yes (F1).

Step 34: Downloading Software

- Find the USB with the sticker that says “SAM-III Documents and Software.



Figure 3.40: USB (Image Courtesy of Austin Cohen)

- Insert the USB and find the “Software-Firmware” file.

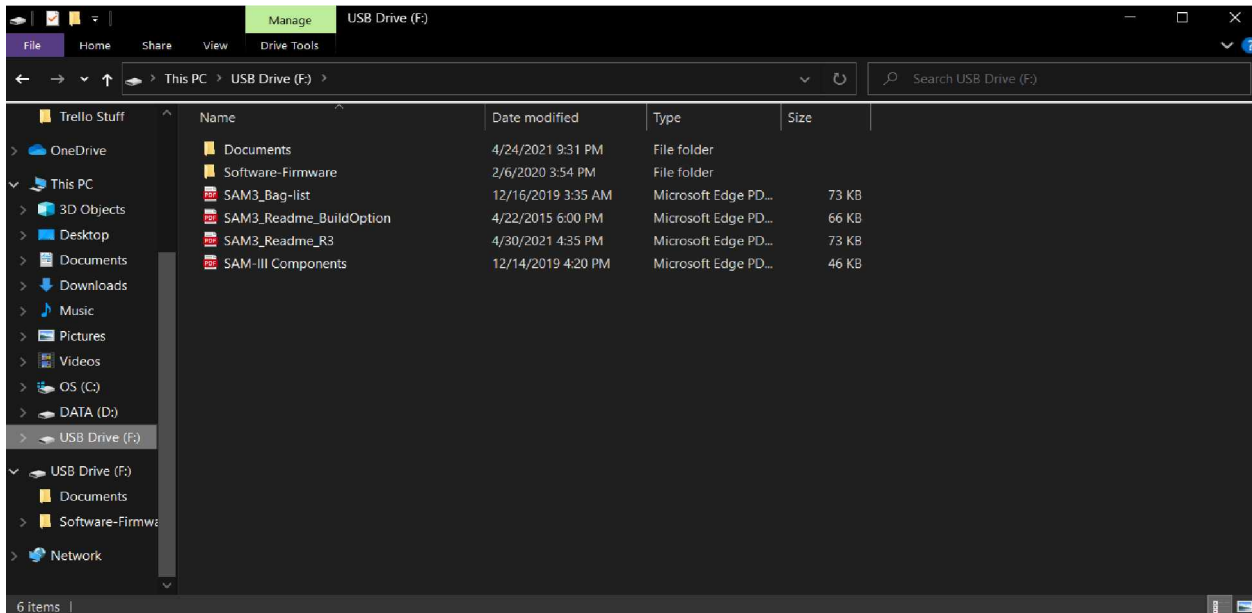


Figure 3.41: USB Files (Image Courtesy of Austin Cohen)

➤ Follow this path:

Software-Firmware → SAM3 Firmware → PIC_Downloader

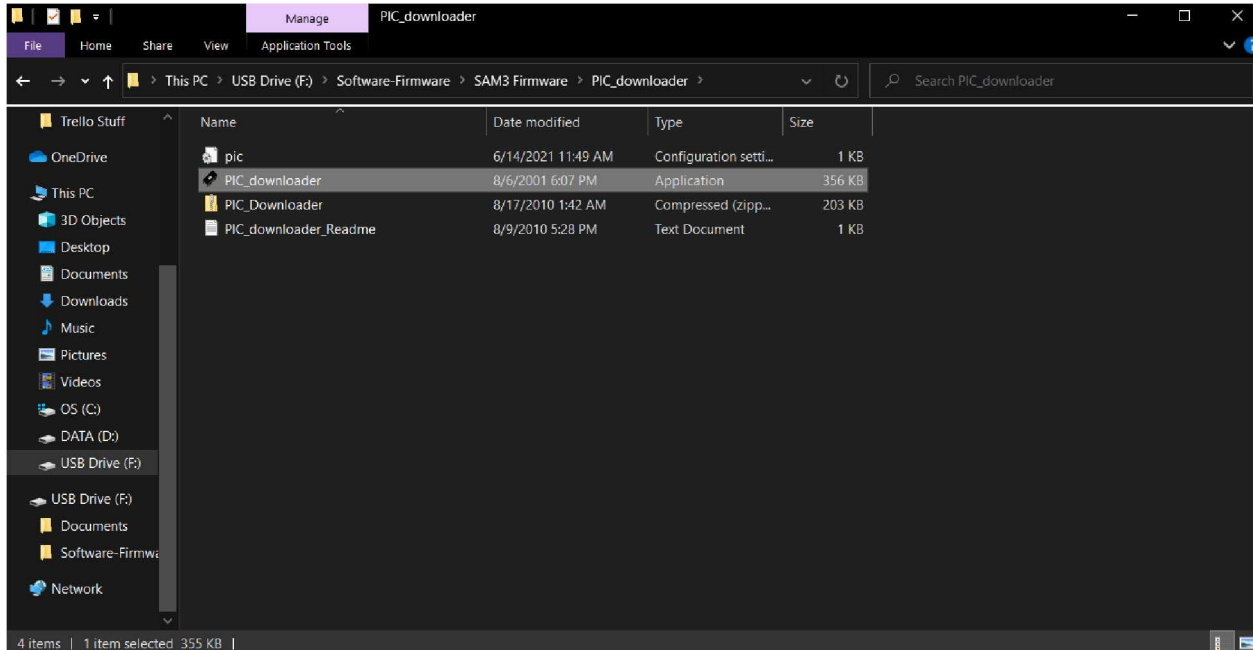


Figure 3.42: PIC_Downloader (Image Courtesy of Austin Cohen)

➤ Open the PIC_downloader application.

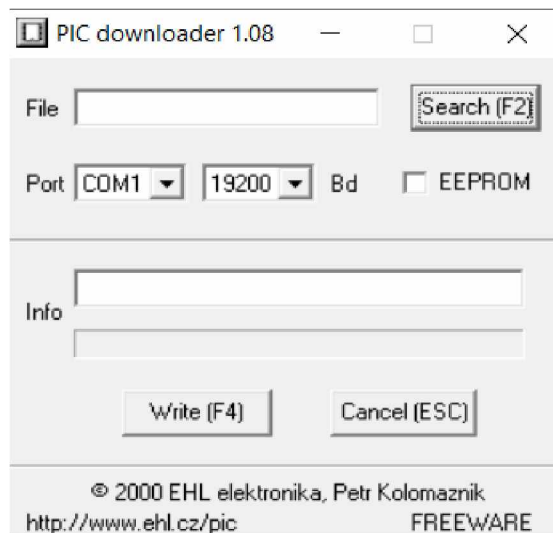


Figure 3.43: PIC_Downloader Application (Image Courtesy of Austin Cohen)

- Search for the SAM3_ENG.HEX file. Use this path:

USB Drive → Software-Firmware → SAM3 Firmware → SAM3_ENG.HEX

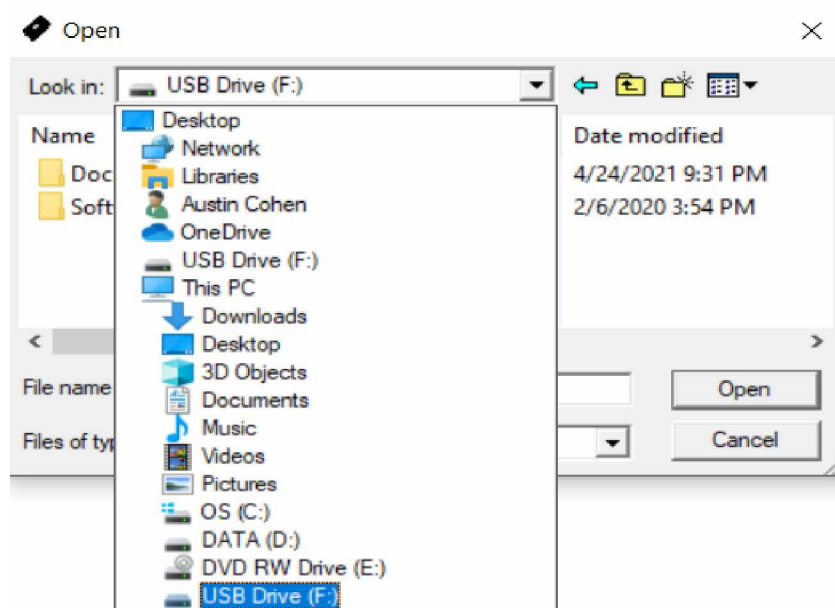


Figure 3.44: File Search (Image Courtesy of Austin Cohen)

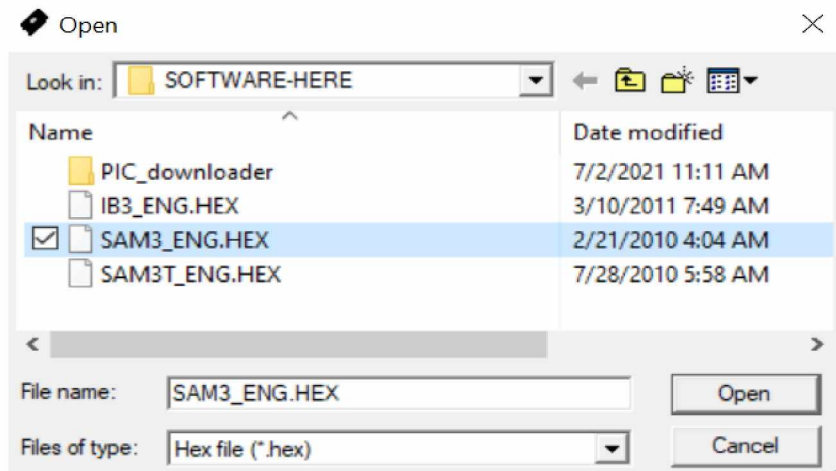


Figure 3.45: HEX File (Image Courtesy of Austin Cohen)

- Set the COM to the right port by using device manager. Your comm port may be different.

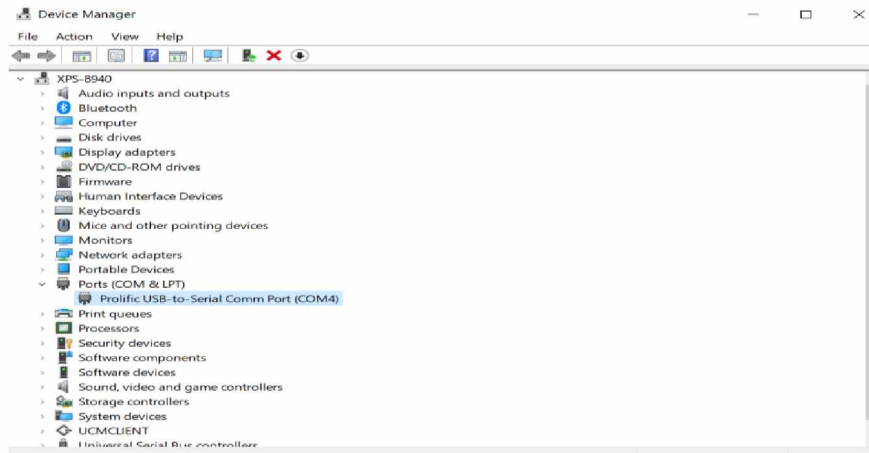


Figure 3.46: Device Manager (Image Courtesy of Austin Cohen)

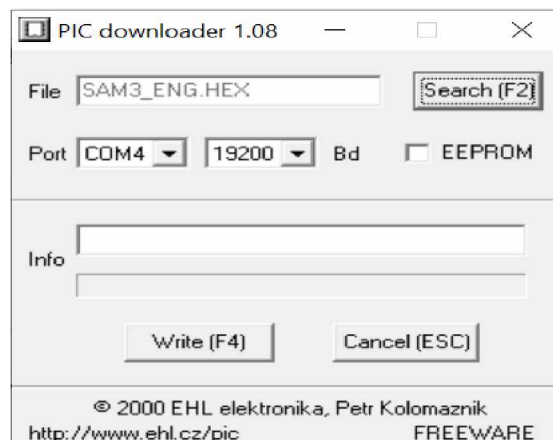


Figure 3.47: Set the COM (Image Courtesy of Austin Cohen)

- Leave the EEPROM box unchecked.
- Now click “Write” and the program will start to install the software.
- After the program reads “All OK !”, the display on your kit should start to look like the following:



Figure 3.48: Display (Image Courtesy of Austin Cohen)

References

- Abell, G. O., et al. (1987). *Exploration of the Universe (5th ed)*. Saunders College Publishing.
- Byun, W. E., et al. (2016). *Fluxgate Magnetometer*. MIT.
- Garriott, R. (1969). *Introduction to Ionospheric Physics*. Academic Press.
- Gombosi, T. I. (1998) *Physics of the Space Environment*. Cambridge
- Hines, C.O., et al. (1965). *Physics of the Earth's Upper Atmosphere*. Prentice Hall.
- Kelley, M. C. (2009). *The Earth's Ionosphere (2nd ed)*. Academic Press.
- Kivelson, M.G., Russell, C. T. (1997). *Introduction to Space Physics*. Cambridge
- Menk, F. W., Waters, C. L. (2013). *Magnetoseismology*. Wiley-VCH
- Reeve, W. D. (2018). *SAM-III Construction Manual*. Anchorage, AK: SAM.
- Seeds, M. A. (1995). *Horizons: Exploring the Universe*. Wadsworth Publishing Company
- Smith, W. C., et al. (2019). *The Space Weather Underground: A Student-Built Array of Ground Based Fluxgate Magnetometers in Northern New England*. New Hampshire.

[Earth's magnetosphere | NOAA / NWS Space Weather Prediction Center](#)

Image Sources

- [BE-01-1022-800x800.JPG \(800×800\) \(xcluma.com\)](#)
- [3mm Red-6-1-2-800x800.jpg \(800×800\) \(cytron.io\)](#)
- [s-l1000.jpg \(1000×1000\) \(ebayimg.com\)](#)
- [diodes2.jpg \(1024×768\) \(autodesk.com\)](#)
- [dc930148-e56d-48bb-9a34-2f2ebc2ec2af.jpg \(600×600\) \(mikroelectron.com\)](#)
- [RD1K.jpg \(1280×600\) \(circuitspecialists.com\)](#)
- [Voltage-regulator-7805-5v-800x800.jpg \(800×800\) \(potentiallabs.com\)](#)
- [da78105-250x250.jpg \(250×250\) \(hobbytronics.co.uk\)](#)
- [a-1385.jpg \(500×500\) \(taydaelectronics.com\)](#)
- [10uF-25V-Radial-Lead-Aluminum-Electrolytic-Capacitors.jpg \(1100×1100\) \(ardustore.dk\)](#)
- [31137108_1_800x.jpg \(800×640\) \(shopify.com\)](#)
- [s-l640.jpg \(640×495\) \(ebayimg.com\)](#)
- [CR2032_1GU_93872.1441763387.1280.1280.jpg \(800×800\) \(bigcommerce.com\)](#)
- [0050579403 Molex | Connectors, Interconnects | DigiKey](#)
- [1-794607-1 - Amp - Te Connectivity - Contact, Micro MATE-N-LOK Series, Socket \(newark.com\)](#)
- [coaxial power jack, 2.1 x 5.5 mm, panel mount - Bing images](#)
- [dil-socket-40-wide-500x500.jpg \(500×500\) \(hobbytronics.co.uk\)](#)
- [CN-PH-M3.jpg \(1200×1200\) \(dojft4652t1in.cloudfront.net\)](#)
- [2_Pin_header_95408.1337689803.1280.1280.jpg \(800×600\) \(bp.blogspot.com\)](#)

- [10Pin-Box-Header-Male_LRG.jpg \(640×640\) \(ventor.co.in\)](#)
- [SBH-34S.jpg \(504×308\) \(pacificcable.com\)](#)
- [41DzpvH7W9L_SX342.jpg \(342×342\) \(images-amazon.com\)](#)
- [dfd075cb-35e6-4932-bf21-296a4163c925.jpg \(600×600\) \(alexnlid.com\)](#)
- [IC0001_MED.jpg \(250×250\) \(rhydolabz.com\)](#)
- [optocoupler-cny17f-2.jpg \(470×470\) \(electronic-center.hr\)](#)
- [BC337 General Purpose NPN Transistor-500x500.jpg \(500×500\) \(tu-eshop.com\)](#)
- [cp22pf-img_4531-2.jpg \(820×620\) \(solarbotics.com\)](#)
- [16mhz-crystal.jpg \(1100×1100\) \(edwinrobotics.com\)](#)
- [Integrated-Circuits-ICs-Embedded-Micro-controllers-PIC16F877.jpg_350x350.jpg \(350×350\) \(alicdn.com\)](#)
- [241770.jpg \(472×265\) \(fullcompass.com\)](#)
- [HDSHOB_200.jpg \(200×204\) \(futurlec.com\)](#)
- [751930main_pia16938-946.jpg \(946×710\) \(nasa.gov\)](#)
- [517890main_Earth-Magnetosphere.jpg \(800×509\) \(nasa.gov\)](#)
- Reeve, W. D. (2018). *SAM-III Construction Manual*. Anchorage, AK: SAM.
- Dogacan Ozturk

Added in original format

Appendix D: Optimization techniques in the assembling, testing, and deployment for SAM IV Magnetic induction Data Collection Vessels. A Capstone Report by Joe Reyes-Mora.

1. Abstract.

The Space Weather Underground project (SWUG) is an outreach project focused on improving the understanding of space weather by high school and undergraduate students. It is emphasized on enhancing understanding of space weather by assembling and deploying SAM III and IV and their corresponding research deployment vessels. The project also introduces students to basic data monitoring and analysis tasks. This report was built as a sequence to the first volume: “SWUG Magnetometer Manual” created by Austin Cohen and supervised by Prof. Hyunju Connor in the Capstone Report titled: “Space Weather Underground Project” released in the spring of 2021. It provides background information about the SWUG project as well as a detailed research vessel assembly guide composed of basic instructions to complete a research vessel by a student with minimum to no assistance required. The report ends with a brief description of the project’s current progress and proposed future work in the short to midterm time ranges.

2. Introduction

This Capstone report consists of the following sections: i. A brief background on the SWUG project, ii. The current progress and starting point of this stage of the project, iii. A detailed introduction to the SWUG deployment vessels and possible sources of data discrepancies, and iv. A step-by-step guide to assemble the SWUG research vessels and their corresponding sensor enclosures. Finally, the report will culminate with a description of the deployment strategy, future plans, and goals for the team.

3. Background

A. SWUG History.

The Space Weather Underground project (SWUG) is part of a Cooperative Agreement granted by the National Science Foundation in collaboration with the University of Alaska Fairbanks and the Geophysical institute (grant #1920965). The project has matured since its launch in late 2019. However, the education and outreach component of the project stays firm: To create an array of magnetometer data collection vessels to measure the changes in magnetic field in the ground. This array is composed by vessels that can be assembled with tools and equipment accessible to high school level students with the proper guidance.

B. Prior Work

During his senior year as an Undergraduate Student. Austin Cohen developed a didactical assembly guide based on the official SAM III/IV magnetometer assembly guide provided by Reeve Engineers. While Reeve Engineers' assembly guide is highly technical and fully detailed, most of the language is directed towards engineers or individuals with a background in engineering and it required simplifications considering the needs of the SWIG program and high school students. The SWUG Magnetometer Manual consists of a start to finish guide for the assembly of the SAM III/IV magnetometer including an introduction to soldering and lab safety, culminating in sensor testing and calibration.

C. Starting Progress

With the help of several high school students, teachers, and members of the SWUG team, a mix of 13 SAM III and IV devices were assembled, calibrated, and tested. Out of which only one was defective/damaged. This was accomplished during the spring and summer of 2020.

All these devices were built to be deployed in the field, a strategy needed to be developed to create deployment vessels with all the required components for the least amount of maintenance and interaction. Due to the data sensitivity which will be described below, it was crucial that all the deployment vessels were made as independent and reliable as possible while keeping costs low.

4. An Overall Picture of SWUG Magnetometer Deployment Vessels

A. SAM IV quick overview:

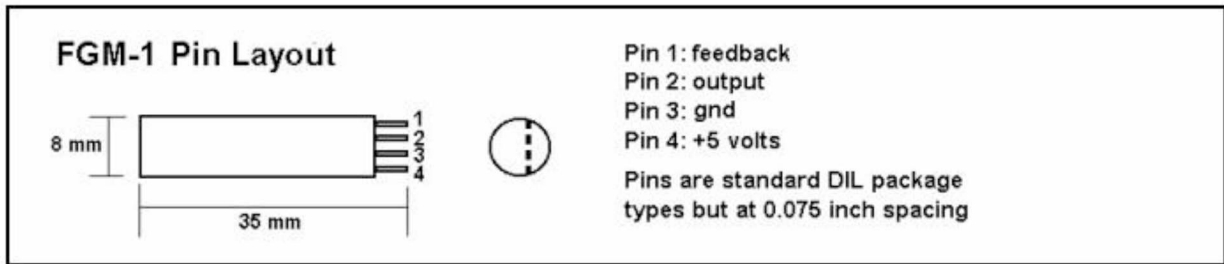
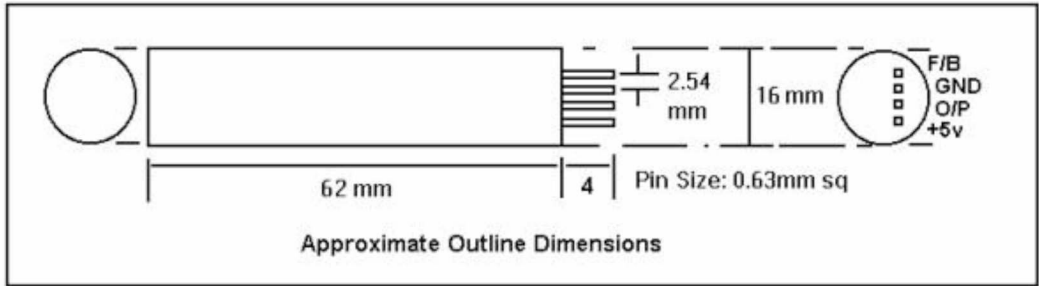
The SAM-IV or Simple Aurora Monitoring (4th edition) kit is very similar in every way to the SAM-III except for a higher quality PCB and Keyboard modules as well as an improved enclosure. The Simple Aurora Monitor is a semi-professional Geo-magnetometer designed by Dirk Langenbach and Karsten Hansky.

In a few words, the SAM is a signal processing station, that converts the electrical signals from the sensors into readable data in real time that can then be sent and collected with a data collection device (computer) and analyzed graphically. This data can then be used to generate larger models and achieve a broader understanding of the nature of Space Weather.

B. Sensor Details

The Sensors calibrated for the SAM are called Fluxgate sensors. Which, in a few words, are densely packed coils (around .2mm wire) (around 4000 turns/meter). These coils are often made by materials that are extremely reactive or sensitive to changes in magnetic field. The sensitivity ranges around the +/- 50 micro-Tesla range. These sensors work with a 5v input provided by the SAM and around 12mA of current.

By always keeping a constant magnetic field on the sensors, any minor disturbances in that field will be registered as electromagnetic variations and generate a signal that can be monitored by the SAM box and then processed as data.



Finally, the recommended manufacturer operating temperature is 0-50 C. This was a major challenge to overcome, and several implementations were done to achieve this as close as possible in the harsh weather conditions in Alaska.

5. Possible sources for data discrepancies, current challenges

A. Temperature variations

Fluxgate sensors are known to have temperature variation issues. While the sensors are stable at a consistent temperature, rapid change in temperature could generate spikes in the data. This can be controlled by adding insulation to the sensors and slow down the change in temperature equilibrium.

B. Soil conditions

Due to weather in Alaska, all underground stations must be buried before the ground is completely frozen. While the sensors are factory supported at 0 C. The drastic changes in temperature are more damaging to the data than the cold weather itself. An alternate option is having a heat source or extensive insulation to provide a more regulated temperature environment. Both approaches will be discussed in the next section.

C. Moving magnetic fields.

There are many sources of perturbations around the environment all the time. Even something small as a dog or a cat can trigger a spike in the data and produce inconsistent results. Due to the sensor's precision, it is recommended to completely bury the vessel. Both approaches were made to compare data results.

D. Moving charges

Moving charges from components and even sensor cables could potentially interfere with the data collection. To avoid this issue, all the magnetometer sensor axes are pointed against any sort of possible source of interference.

E. Instrument/vessel faults

Not all instruments are perfect and technical problems can always arise. However, there are ways to reduce the risk of failure and target the possible points of breakage is crucial to keep a smooth operation.

6. Vessel Assembly Guide

Overview

A. General assumptions for this guide:

This guide was built as the second volume for the SWUG project, following the "UAF SWUG SAM Construction Manual" written by Austin Cohen and supervised by Prof. Hyunju Connor. There will be some reference to the content described in the first volume of the guide. It's assumed that the student successfully completed a SAM III magnetometer and is familiar with the basic concepts of soldering and electric engineering required to complete such a task.

B. Sensor Enclosure (pictures of completed Enclosures)

The sensor Enclosure is the first part of the assembly process and contains all sensors and cables required to collect a quality data sample. The enclosure is composed of a solid PVC body, and it holds the sensors as well as the cables that transmit the data.

C. Deployment Vessel

The deployment vessel will be the second part of the assembly process. It contains all necessary electronic components to collect and record data from the buried sensors. This guide describes the assembly process of two different types of deployment Vessels designed for different deployment applications.

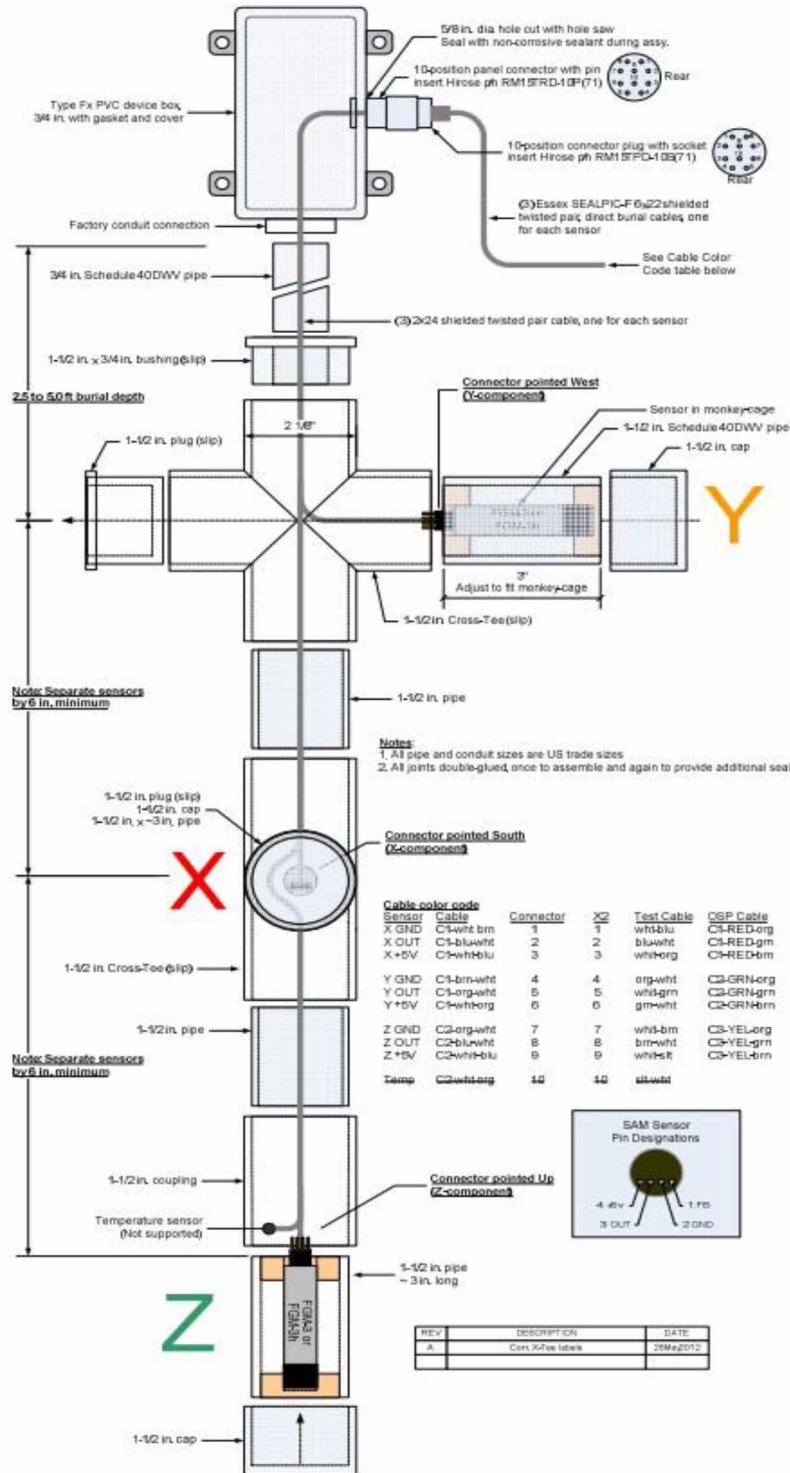
D. Reeve Engineers' guide for sensor enclosures (brief description of Manual for Enclosure)

Below is a proposed sensor enclosure model by Reeve Engineers, this model was used as reference to create our own. Several Materials remain the same, but some lab adaptations were made to better accommodate the weather demands and environmental challenges presented in Fairbanks and surrounding areas.

Refer to the following diagram for a basic idea of the sensor enclosure.

SAM-III Construction Manual

Buried Sensor Fixture – Three-sensor installation, Typical (all components in USA trade sizes)



E. Materials, Tools, and Components

Sensor Cable

- (3 conductor 18 – 22 g cable) * 3
- Shrink tubing
- Capacitors (from SWUG Manual,) 10nF and 10uF
- Sensor Cable Tips (insert Details) (provided in kit)
- Zip ties, cable management
- Labels (label maker)

Tools/Equipment:

- Soldering Kit and Solder
- Screwdriver
- Pliers and Wire Cutters
- Wire Stripper
- Personal Protective Equipment (mask, gloves, eye protection)
- Ruler or Measuring Tape
- SAW (PVC PIPE)
- File (for PVC pipe)
- Drill and Drill bit kit
- Measuring tape
- Permanent marker
- Pliers
- Clippers
- Heat gun/hair drier

Sensor Enclosure:

- Axis Fluxgate FG-3+ Magnetometer Sensors (3)
- PVC PIPE (quantity, type)
- PVC Box (Anchor Type Only)
- PVC Joints (quantity, type)
- PVC Glue • Sensor Cable
- Sensor Cable capacitors
- Sensor Cable Heat Shrink tubing (types, uses)
- Sensor Cable end tips (specifics, type)
- Label Maker (or labels)
- Zip ties or other type of cable management
- Wall Insulation (specifics), Quantity
- Insulation spray foam

Deployment Vessels:

- Sensor Cable Extension (type 2 vessel) (3 conductors) (3 Cables per unit)
- PVC plug (for type 1 vessel)
- Sensor cable plug (3 way * 3)
- Power chord extension (cable) (type 1)
- Power Strip
- Raspberry pi 3 or 4
- Protective equipment (masks, eye protection)
- Label Maker (or labels)
- Component plastic box
- Zip ties or other type of cable management
- Packing foam (optional)
- PVC box
- Ethernet Cable (new version for data retrieval)
- Ethernet Cable Extension
- Pelican Box
- Temperature Sensor
- Insulation
- Padding Foam
- PVC Cap (for whole)
- Power Strip
- Extension Cord

F. Step 1

Sensor Enclosure Assembly

As mentioned previously, this guide describes two different types of sensor enclosures, which will be referred to as “L type” and “Anchor Type” sensor enclosures because of their shape.

L type Sensor Enclosure



Step 1.1 Gather Materials

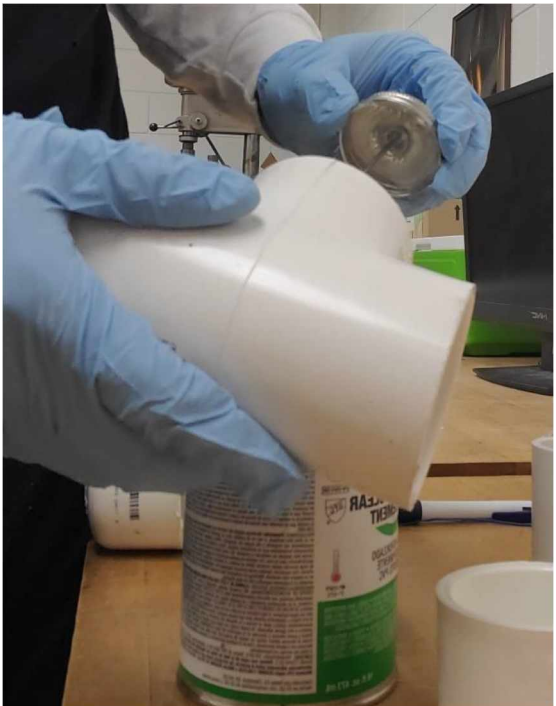
To build the L type sensor enclosure, we will start with the body. Gather the following materials and equipment: PVC pipe, joints and glue, hand saw, measuring tape, permanent marker, and protective equipment. This part requires the use of a hand saw, so please ask for help if needed.

Step 1.2. Prepare Enclosure

Using the measuring tape, mark and cut two 15 cm PVC segments, and three 8 cm PVC segments as shown in the picture below.



Use the PVC glue to join the PVC parts that were cut in the previous step and main elbow joints included in the kit, do not close the enclosure yet, we need to keep the sensor holes open to complete the next steps.





Step 1.3 Sensor Cable

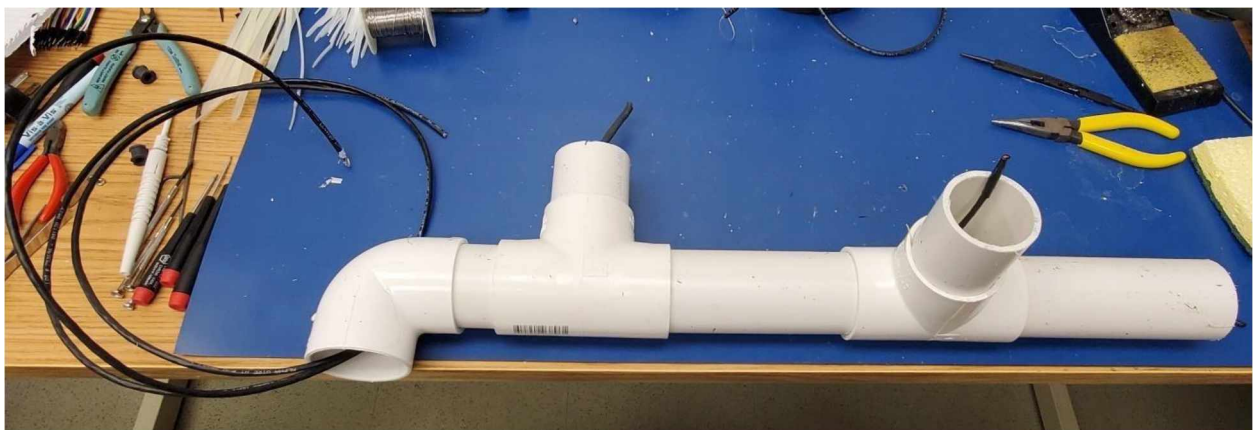
The sensor cables are a very important part of the process and need to be built carefully. The process is similar for both enclosures as they only vary in length.

Step 1.3.1

To complete the sensor cables, gather the following materials and equipment: Sensor cable, cable capacitors, cable extensions, heat shrink tubing, solder and soldering kit, wire cutter, wire stripper and pliers.

Step 1.3.2

Using the wire cutter, cut three cables to lengths matching distances inside the PVC enclosure. Make sure that there is at least 15 to 20 cm of cable outside the vessel as we will need it to plug in the SAM device. The typical length for the wires is of 60 cm, 45 cm, and 30 cm. However, this may vary slightly depending on each enclosure. Make sure all the cables outside the enclosure are about the same level.



Step 1.3.3

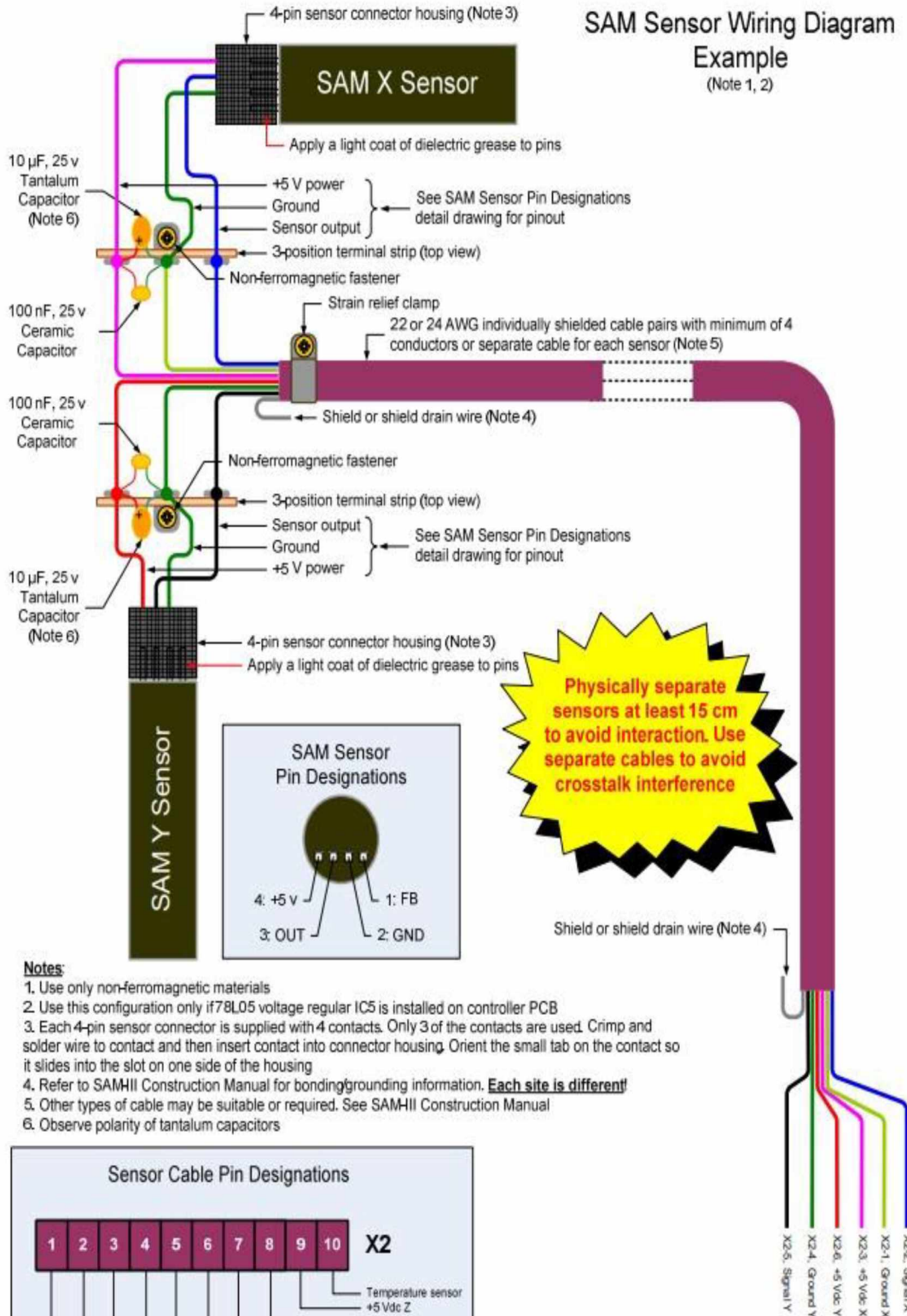
From now on, we will work on each cable independently. Cut the cable again about 10 to 15 cm from one end in to create a high pass filter and reduce noise in our data. This end will be the one closest to the sensor, so feel free to adjust the length and ensure the filter is inside the vessel to prevent any chance of exposure.



Refer to the following diagram for a full picture of the Cable Sensor Wiring Diagram

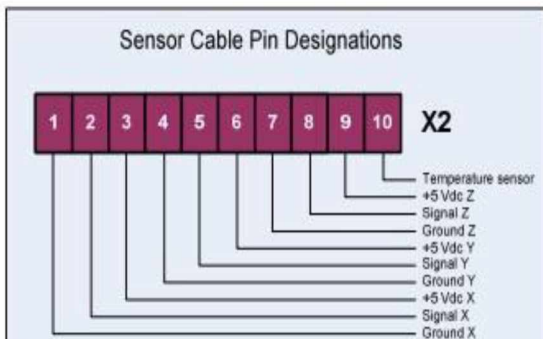
SAM Sensor Wiring Diagram Example

(Note 1, 2)



Notes:

1. Use only non-ferromagnetic materials
2. Use this configuration only if 78L05 voltage regular IC5 is installed on controller PCB
3. Each 4-pin sensor connector is supplied with 4 contacts. Only 3 of the contacts are used. Crimp and solder wire to contact and then insert contact into connector housing. Orient the small tab on the contact so it slides into the slot on one side of the housing
4. Refer to SAMIII Construction Manual for bonding/grounding information. **Each site is different!**
5. Other types of cable may be suitable or required. See SAMIII Construction Manual
6. Observe polarity of tantalum capacitors



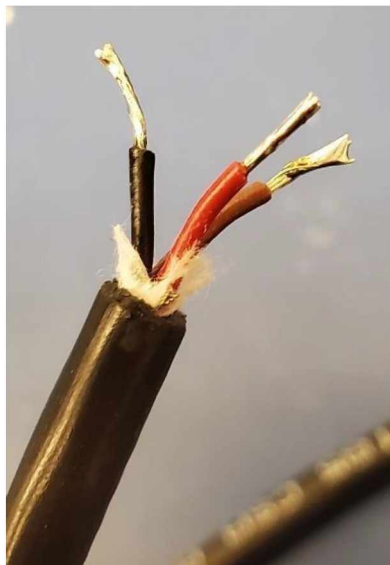
Step 1.3.4

We will now prepare the cable to create our filter. Using the wire stripper, strip all sides of the cable and each wire independently. Leave about 3 cm of exposed wired and make sure all ends are about the same length.



Step 1.3.5

Turn on the soldering kit around 400 C and use a small amount of solder on each end of the wires to make an easy connection. (Show Picture) We will also use an even smaller amount of solder in each of the ends of the capacitors. Do not attach the capacitors yet, only prepare them for the next step.



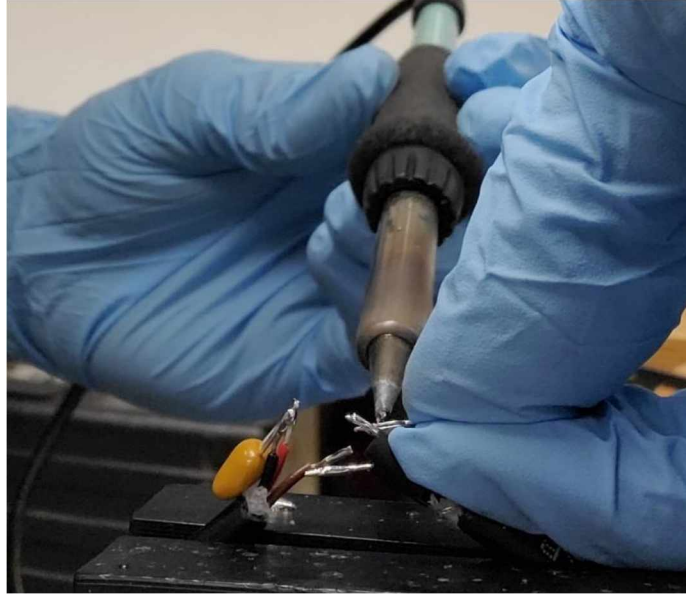
Step 1.3.6

Measure and cut heat shrink tubing. Three different kinds of heat shrink tubing will be provided in your kit. We will need the smallest tubes for the independent sensor conductors, medium for the complete sensor cable and the largest one for the combination of the cables. Cut nine 2 cm pieces of the small tubing, and three 5 cm pieces of the medium size tubing. We will pre-install the tubing before each step of soldering to ensure a proper seal, use a bench vise if needed.



Step 1.3.7

Carefully proceed to solder the capacitors to our cable. The bigger capacitor is polarity sensitive, and you must make sure to connect the positive sides together. Please look at the reference below and ask for help if needed. We will first solder the large capacitor to the positive and negative cables and proceed with the smallest one to make it simpler. We will then connect the signal cables together. This step might be challenging, and it is recommended to use a bench vise or an extra hand.



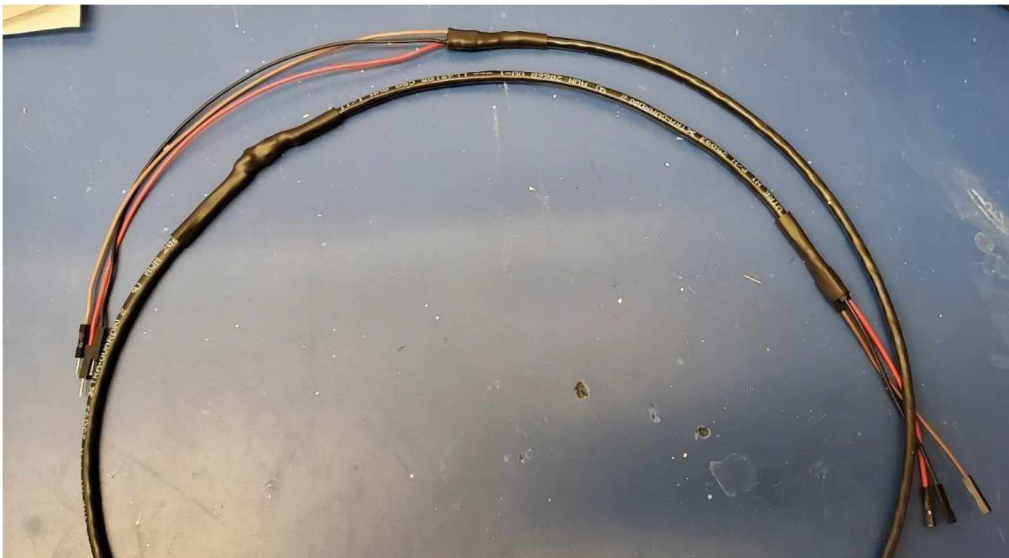
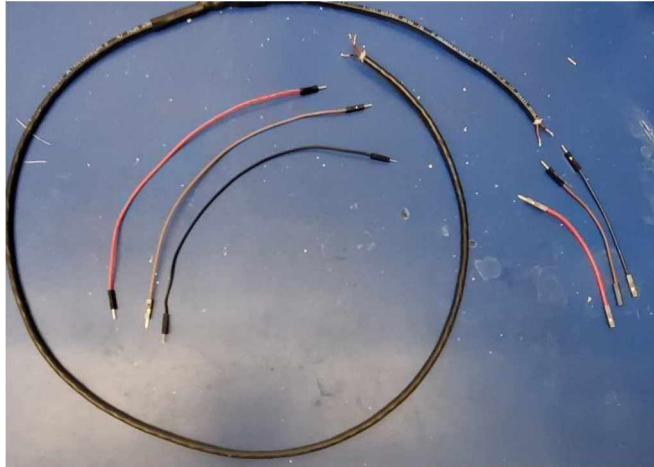
Step 1.3.8

We will now cover our soldered joint with the heat shrink tubing, try to cover as much of the exposed are as possible and ensure the cables are independent from each other. Now, use the heat gun or hair dryer to Install heat shrink tubing. Start with the small ends first, then use the medium size tubing to cover the entire filter. If the medium size tubing does not fit, use the large tubing instead of compressing the filter.



Step 1.3.9

The final step of the sensor cable is attaching the cable extensions. Use the provided cable extensions in your kit for each side of the cable. There are two different kind of cable extensions, one is designed to fit the sensors, and the other one to fit the SAM box. The extensions are color coded to match the sensor cables. Make sure to use the hollow ones on the side closer to the filters as these will be plugged in directly into the sensors. Proceed to solder each of the extension cables to the ends of the cable and cover with heat shrink tubing, similar to the previous step.



Step 1.3.10

Repeat steps 1.3.3 – 1.3.9 for the remaining cables to complete the full 3 axis sensor cable. Use the largest heat shrink tubing provided to cover both ends of the cable and ensure a proper sealing. Label all cables with their corresponding axes (X, Y, Z) Please refer to the enclosure diagram provided above to ensure proper labeling.



Step 1.4 Sensor Enclosure Assembly process

Step 1.4.1

Gather all the following materials and equipment to complete the sensor enclosure: PVC sensor enclosure (completed in Step 1.2), three sensor cables (completed in Step 1.3), 3 Fluxgate sensors, a small 6" x 9" piece of insulation, insulation foam, PVC glue, large heat shrink tubing, heat gun/hair dryer, cable ties.

Step 1.4.2

Connect the sensor cables with their corresponding sensors and wire them through the PVC enclosure that was completed in Step 1.2.



Step 1.4.3

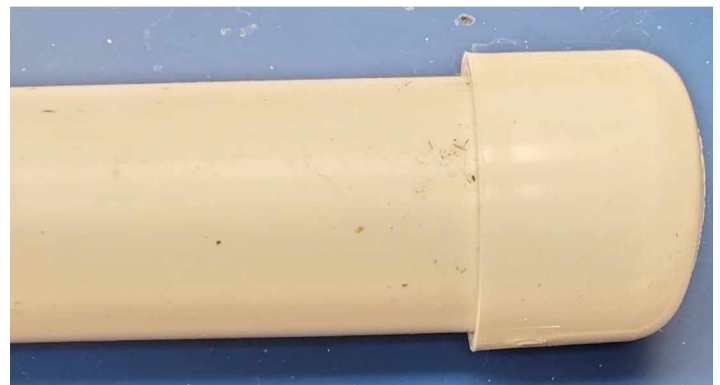
A small layer of approximately an inch of insulation will be used to slow the rate of cooling and keep the sensors in a centered position inside the sensor enclosure.

Cut a small piece (1"x2"x4") of insulation for each sensor, Wrap the insulation around a sensor while already in its final location and secure with 2 cable ties, creating a "sleeping bag" shape around the sensor.



Step 1.4.4

Insert the sensor in the PVC enclosure and seal it by applying glue around the PVC plug and twisting around to create a complete seal (picture). Then repeat this process for the remaining sensors inside the enclosure.



Step 1.4.5

Once all sensors are sealed, install the larger heat shrink tubing at the end of enclosure to add flexibility and weather resistance to the cable. Quickly test your sensor connections with the SAM box to ensure

the cables are working properly before completely sealing the enclosure. Now use the spray foam insulation at the end of the enclosure to create a full seal. This sensor enclosure is now complete and ready for testing.



Anchor Type Sensor Enclosure (Fairbanks, Poker)



Step 1.1 B Gather Materials

The steps for building an Anchor Type enclosure are very similar to an L-type enclosure with a few differences. Gather all the materials and equipment mentioned in Step 1.1. In addition, grab an extra piece of PVC Pipe $\frac{3}{4}$ inch in diameter, the PVC box and extension cable 3-way plugs included in your kit.

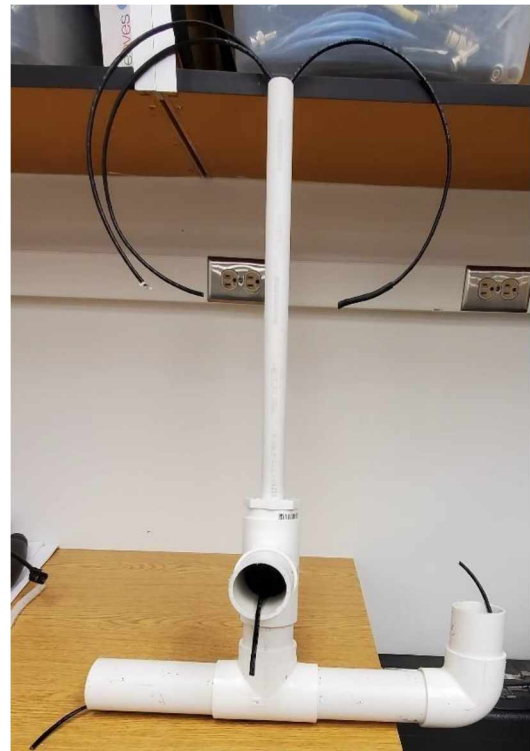
Step 1.2 B Prepare Enclosure



Repeat measurements and cuts from step 1.2. In addition, Measure a cut about 1m of the thinner PVC pipe. This will be the neck of the enclosure. Do not attach yet, this will be done at the end. Use PVC glue to assemble the base structure of the enclosure, with the joints provided for the Anchor enclosure type.

Step 1.3 B Sensor Wires

Repeat the same procedure as Step 1.3 to complete the sensor cables. The only difference in this process is the length of the wires themselves. Make sure to allow an extra 1.25 meter of length at the end of the enclosure to accommodate for the enclosure neck that will be buried underground. Additionally, there is no need to install the extension cables at the end of the sensor cable and only install the extension cables needed to connect the sensors themselves. The cables will be directly attached to the extension plugs connected to the PVC Box. This part of the process will be explained in detail in the continuing step.

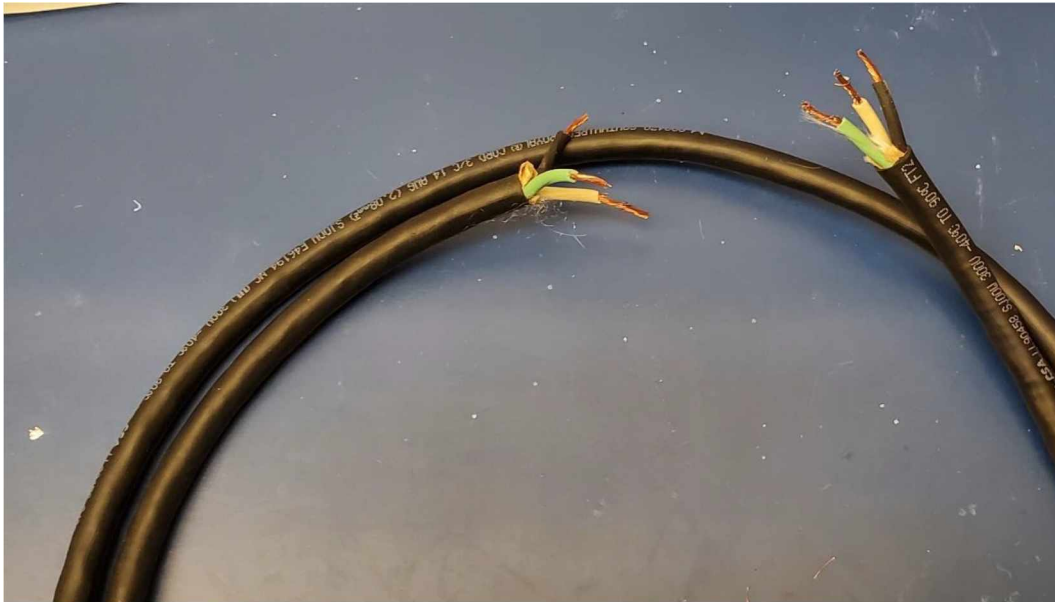


Step 1.4 B Wire Extension Cables

This step is specific for this sensor enclosure type. There will be 3 wire extension cables that will be plugged in from the indoor location of the SAM box to the sensor enclosure which will be buried underground.

Step 1.4.1 B

Measure and cut the long extension cables to equal lengths up to 50 m (tested value). Now, we'll prepare the cables in a similar way as the sensor cables. Use the wire stripper to cut and strip the extension cables. In parallel, cut eighteen 1cm pieces of small heat shrink tubing (one for each side of the cable), and six 8cm pieces of the large tubing accordingly



Step 1.4.2 B

Prepare the ends of the cables with a small amount of solder in each of the tips, exposing about 0.5 cm of cable on each tip to ensure a proper connection. Preinstall heat shrink and plug hardware before soldering the cable to the plugs, then solder the extension cables to end plugs. The orientation of the plugs is not important if you remain consistent. It is recommended to use X with number 1 or the letter A, Y with 2 and Z with 3 correspondingly.

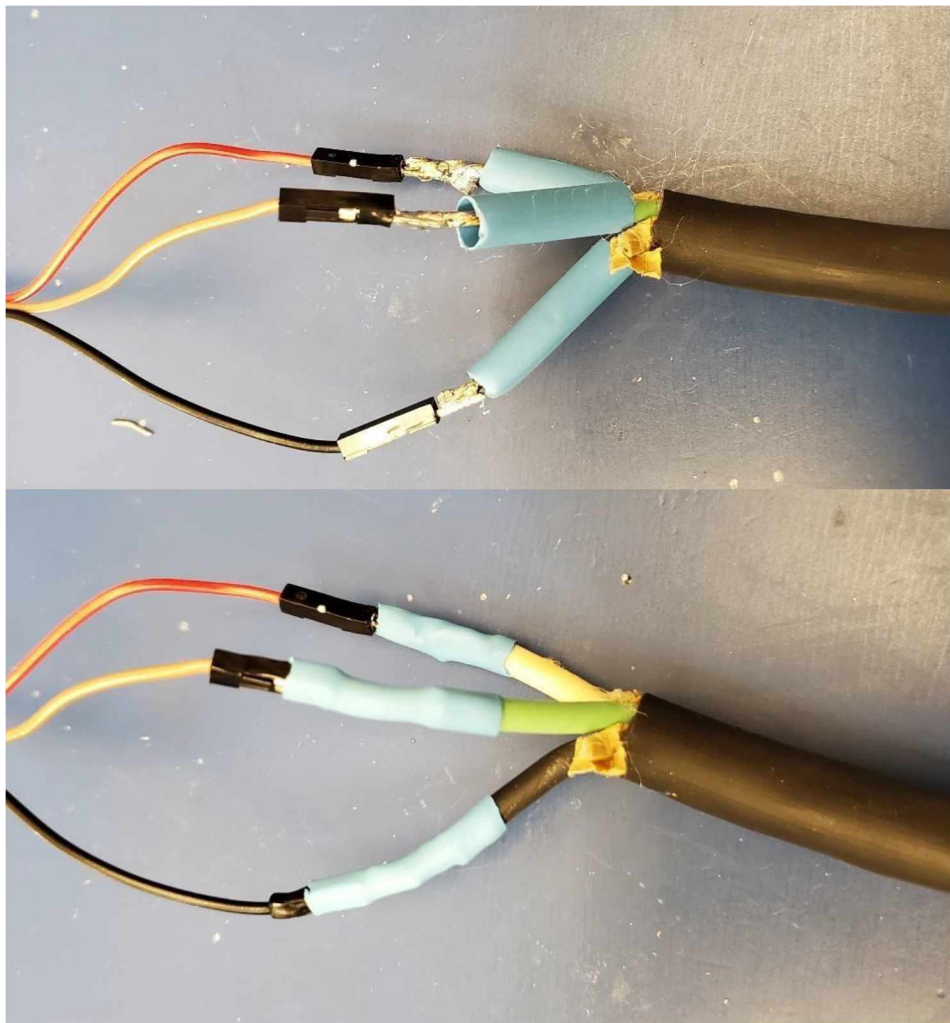


Step 1.4.3 B

Cover the soldered joints with the heat shrink tubing and use the heat gun or hair dryer to complete the heat shrink installation. Then proceed to cover all cables with the larger tubing and complete the cable by finishing the plug hardware installation.

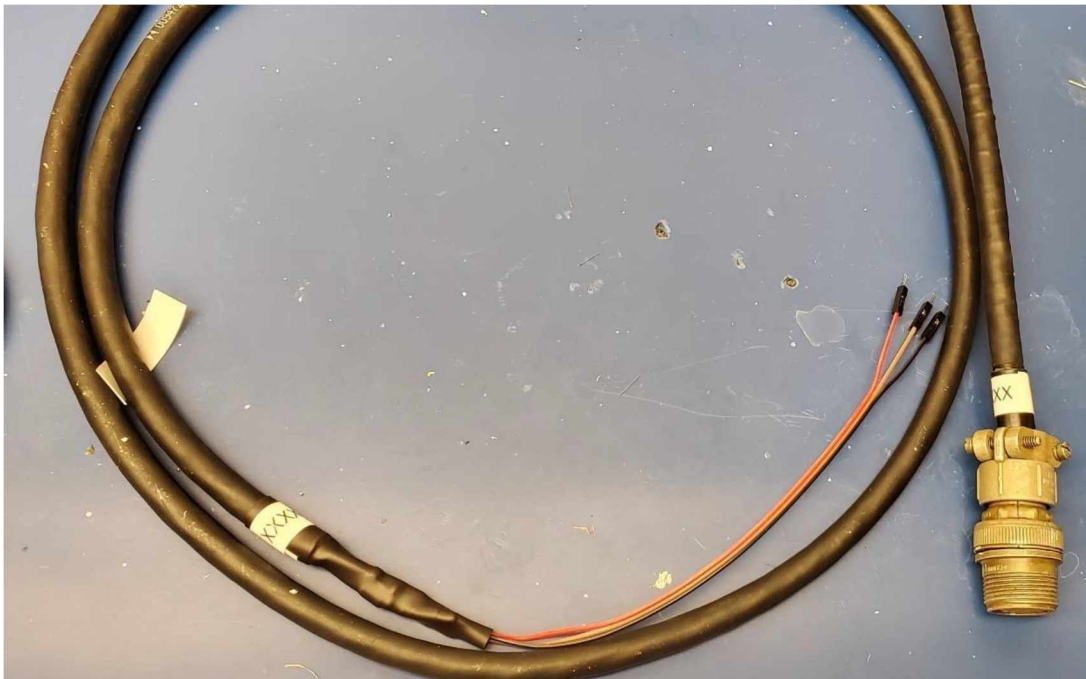


At the other end of the cable, install the short wire extension tips that directly connect to the SAM box as done in Step 1.3 for the L-type enclosure.





Complete Sensor Extension Cable

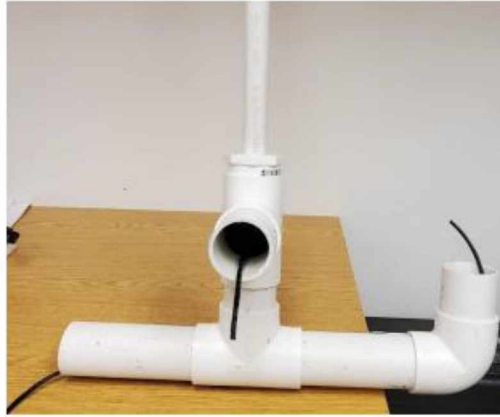


Step 1.5 B Assembly process for Anchor Type Sensor Enclosure

The assembly process is quite similar to the L-type sensor enclosure. The main difference is the installation of the neck of the enclosure as well as the PVC box installed at the top.

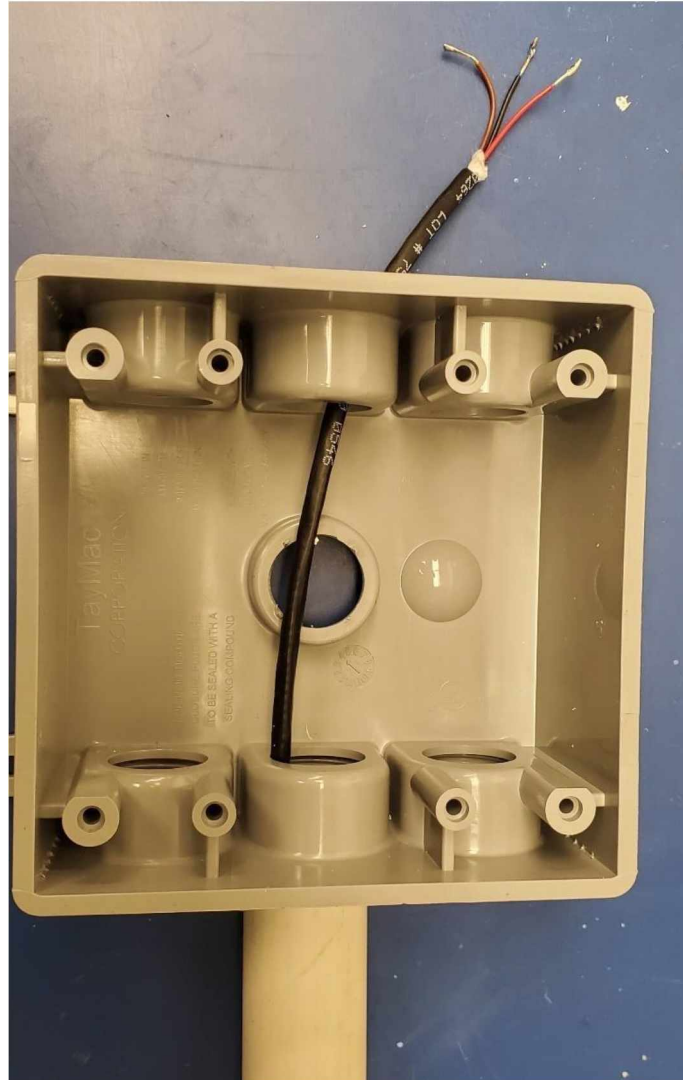
Step 1.5.1 B

Repeat steps 1.4.1 to 1.4.4 for the L-type enclosure, the only difference in this process is the location of the sensors, pay attention to the picture below to make sure all your sensors are in the right direction.



Step 1.5.2 B

Now we will proceed to install the neck and box of the enclosure. First, attach the neck of the enclosure to the PVC adapter provided using PVC glue and adapter. Make sure to guide wire through neck of enclosure and pull it through the end. There should be an extra 10 cm of extra cable after installing the neck. If this is not the case, cut the neck to have an approximate length of 8 to 12 cm of sensor cable to install the cable plugs.



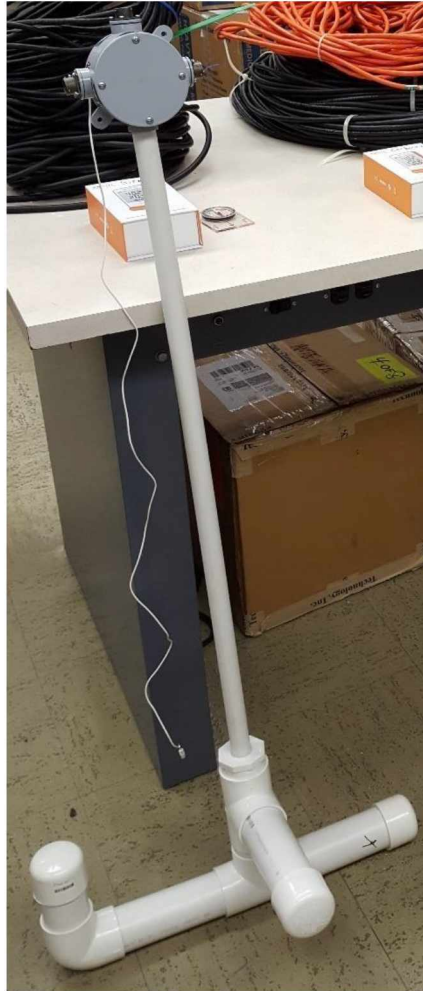
Step 1.5.3 B

Use a small amount of solder to connect the sensor cable to the plugs. Make sure to preinstall the heat shrink tubing on each cable to ensure proper sealing. Complete the installation by installing the heat shrink tubing after soldering the cables to the plugs. Double check the pattern of connection to ensure consistency along the device.



Step 1.5.4 B

Check connections, perform a quick test with the SAM box to ensure everything is working as expected and proceed to seal the PVC box. This enclosure is now ready for further testing and deployment.



G. Step 2

Research Vessel Assembly

Vessel type 1 Assembly

This Vessel was designed to fit the L-type sensor enclosure. The vessel is meant to be completely buried or insulated for regular weather. It is power chord based, which means that the only requirement for it to function and collect data is power. While sacrificing data accessibility unless a network connection is possible, the signal could be extended for as long as needed depending on the deployment area which makes this vessel better adapted to a wider deployment range under the right conditions.

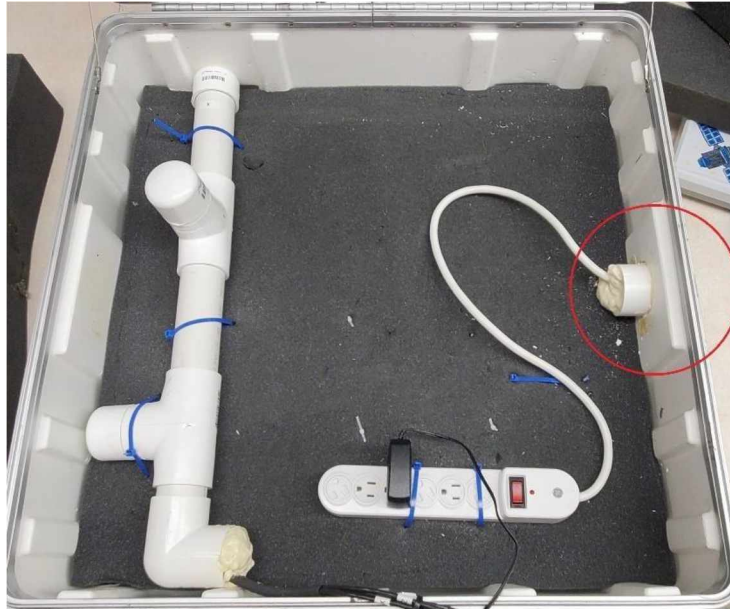
There are five simple steps to complete the Vessel:

Step 2. 1

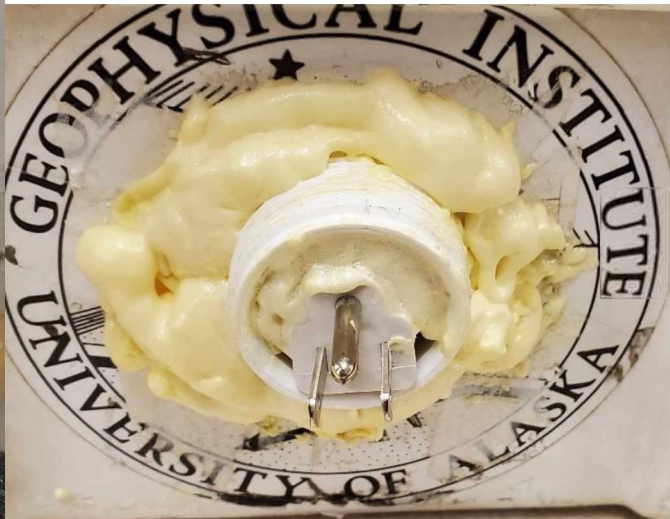
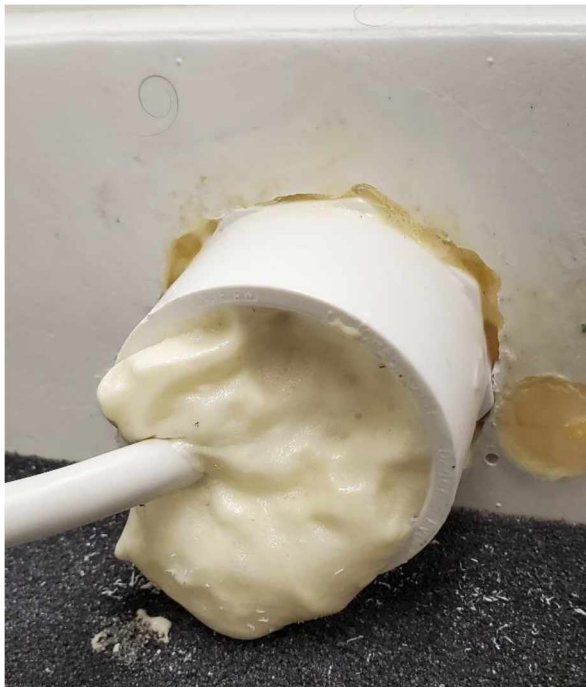
Gather all required materials and equipment required to complete the vessel: Pelican Box, SAM III, serial cable, USB adapter, L-Type sensor enclosure, temperature sensor, component plastic box, power strip, power extension cord, network cable and extension (when needed), Raspberry pi, zip ties, PVC plug, insulation foam and packing foam. Don't forget the power adapters for both the SAM III and Raspberry pi. For this task, we will also need the power drill, 2-inch drill bit, scissors, and protective equipment. Please ask for assistance if needed.

Step 2. 2.

We will now prepare the pelican box for deployment. Use the drill bit provided to make a hole in one of the sides of the pelican box (As shown in the picture below). In addition, make sure the hole goes through the foam to have a direct connection within the inside and outside of the box.

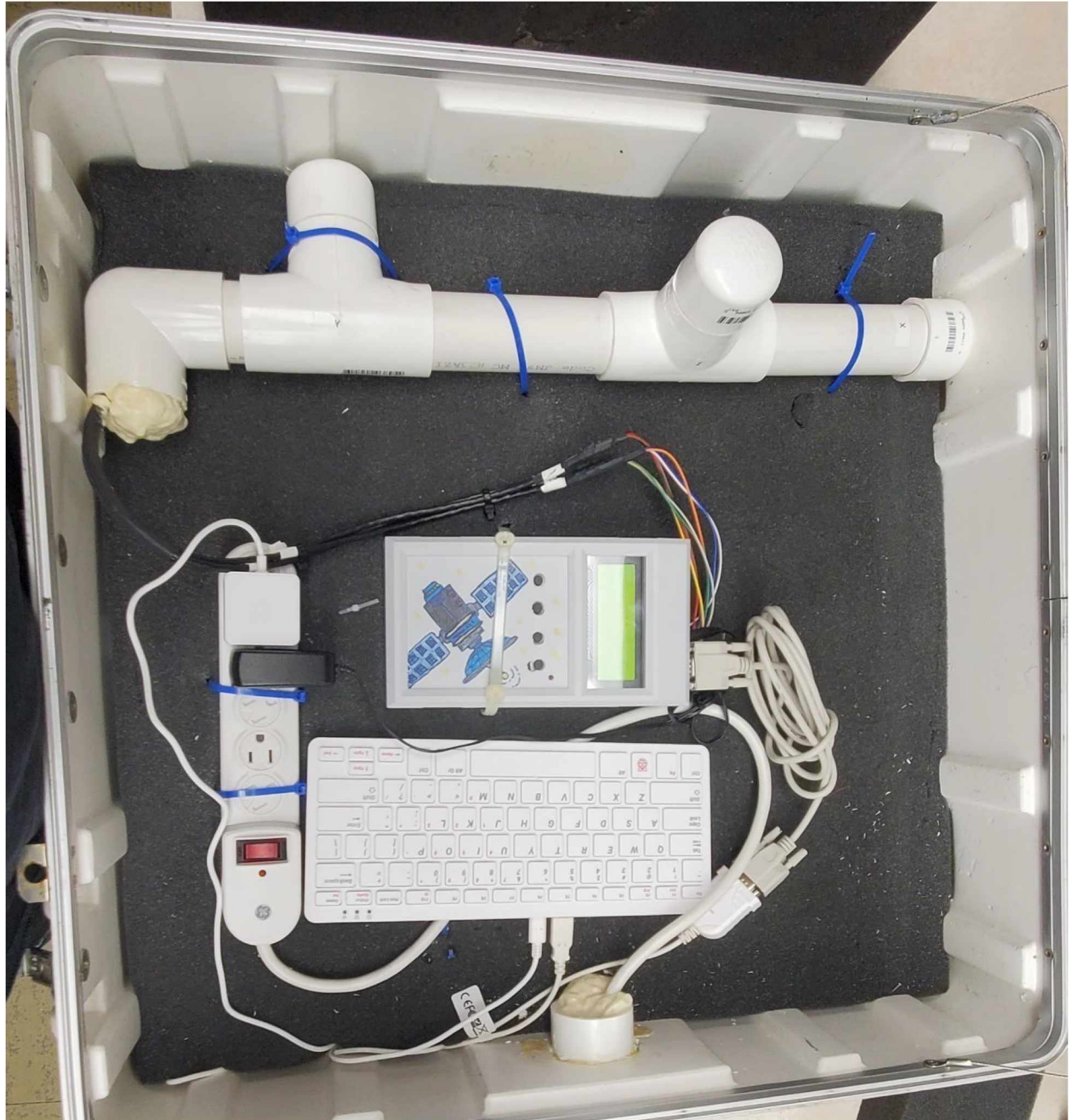


Lastly, insert the PVC plug in the hole and seal it with PVC glue as well as insulation foam. Make sure to secure the powers strip plug inside the seal as well as the network cable (if applicable).



Step 2.3

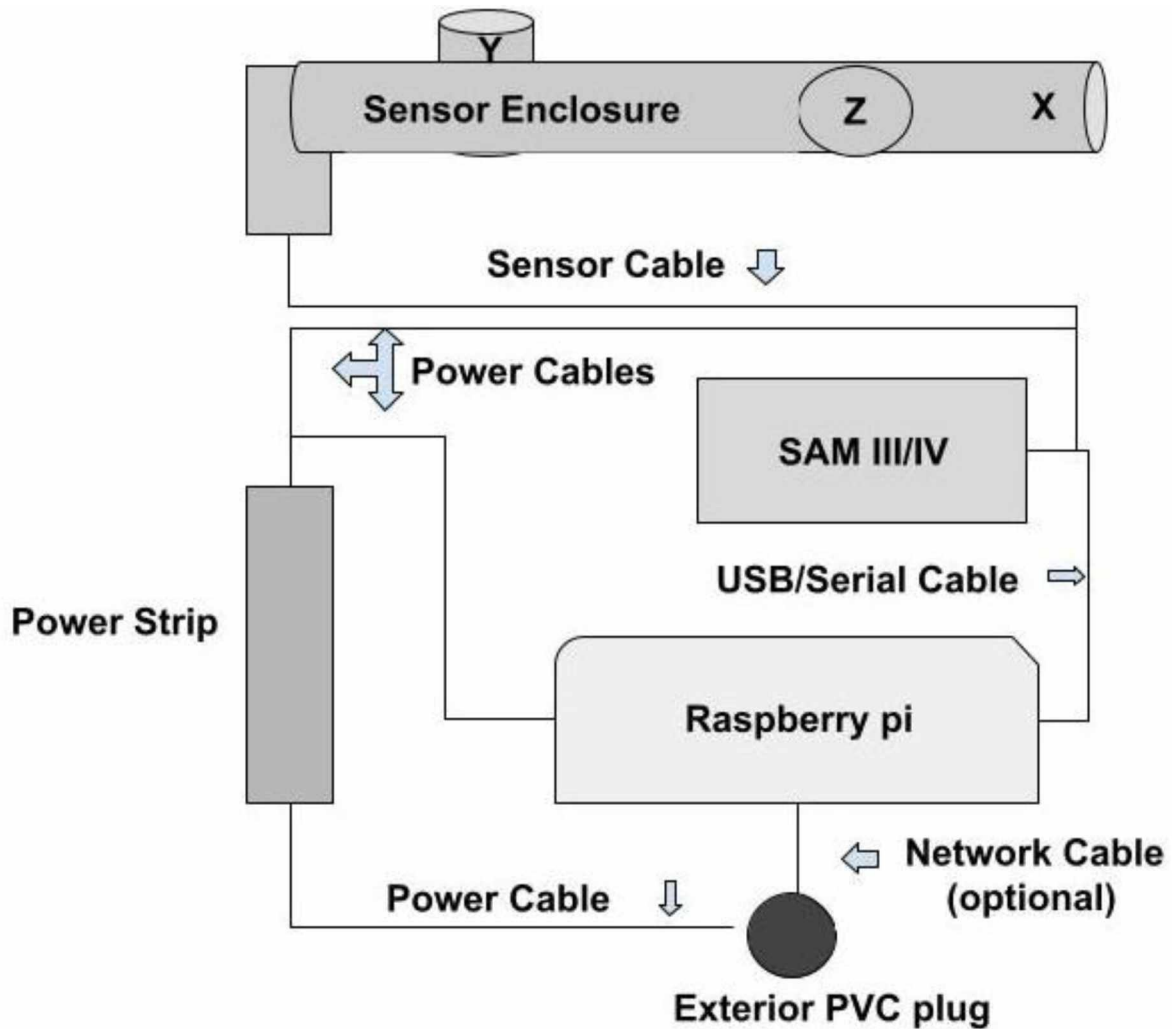
Now, using the cable ties. Install the L type sensor Enclosure, SAM III, Raspberry pi and power strip as shown below. Make sure that all the sensors are pointing away from the electronic components to avoid any sort of interference. After installing the major components, plug in the power adapters, serial cable, network cable (if applicable) and sensor cables to their corresponding locations as shown in the picture below.



Step 2.5

Ensure that all cables are properly plugged in and power on the vessel. If the SAM is displaying data for all axis, and the Raspberry pi turns on, the device is ready for initial data collection testing and deployment.

Type 1 Deployment Vessel Diagram



Advantages:

- Less Expensive To build
- Faster Building time (lower Personnel Cost)
- Easier to transport
- Longer possible range from power source when no remote access capabilities
- Possibility of adding remote access with network cable from the source.
- Fully buried, allowing weather resistance for all components but reducing to manual • Data collection or remote access only when Ethernet Plug is available to router or switch
- Smaller probability of data noise due to short length of sensor cables.

Disadvantages:

- Remote data access capabilities under testing
- Only optimal for accessible areas and overall good weather (not in AK) unless a heat source is added (heat pad, fan) which would increase the operative and power cost as well as sources of possible noise.
- The weather must be optimal for proper burial of the vessel. Which limits the season in which such vessels could be installed. So remote data access is crucial for this vessel to work as the complete vessel needs to be buried.

Possible Places of Deployment:

- Places with medium to warm weather (above 0 C)
- Experimental (1st data trial) places with increased length from power source.
- Places where data doesn't need to be picked up right away (record an event in a remote area.

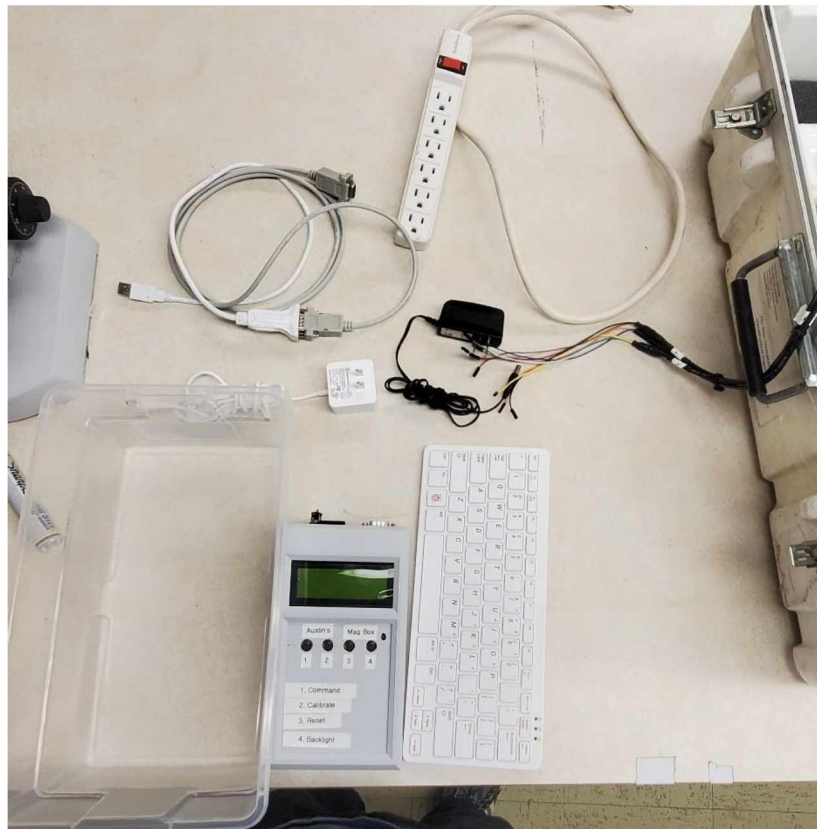
Vessel Type 2 assembly (Poker/Fairbanks) (Cerberus / Hydra)

This research vessel was designed to work with the Anchor type vessel. Only the sensors are buried, electronic components are stored in a small plastic box located in a warm place (above 0 C) with network access if possible. The sensors signal is transmitted via the sensor extension cables that were built in Step 1.4 B to accommodate different deployment conditions. Although this vessel requires a warm place and network connection, it has a higher potential for remote data access capabilities and live data monitoring.

To complete this vessel, there are three steps to follow:

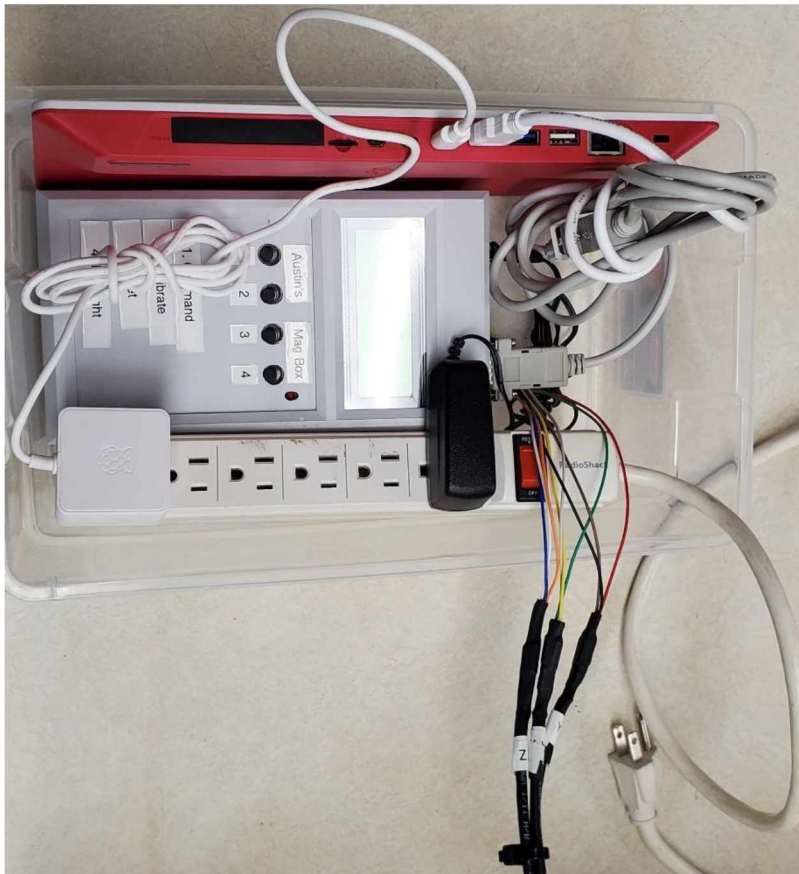
Step 2.1 B

Following the guidelines for the type 1 Vessel, gather all required materials mentioned above except for a pelican box and L-type sensor enclosure, as this deployment vessel does not require a box and we will be using the Anchor Type sensor enclosure. In addition, grab the sensor extension cables that we made in step 1.4 B.



Step 2.2 B

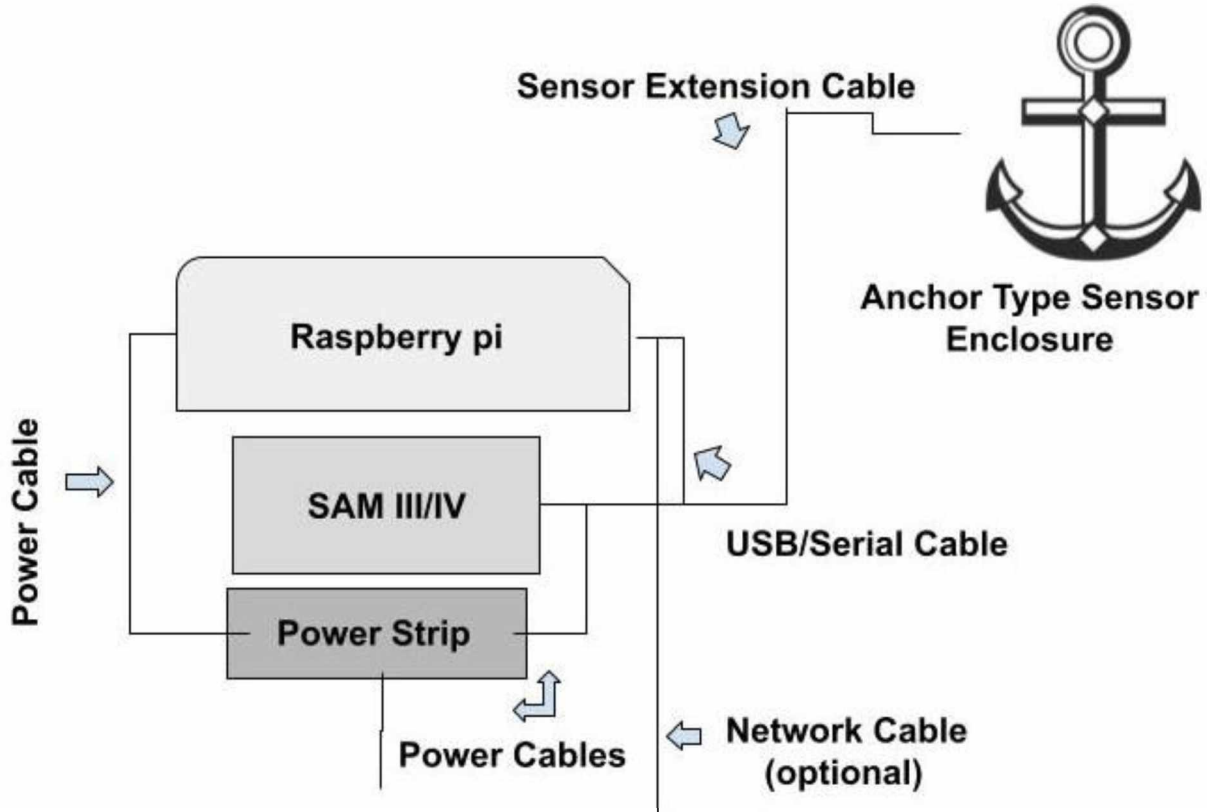
Prepare the Anchor Type sensor enclosure: make sure PVC box is properly attached and all sensor cable 3-way plugs are properly installed. Simultaneously, in the plastic box provided, install the SAM III, Raspberry pi, and the power strip. Make sure all electronic components are properly installed and connect the network cable to the Raspberry pi, if possible, to allow remote data access.



Step 2.3. B

Test vessel and prepare for deployment: attach the sensor extension cables to their corresponding 3 way plugs and ensure that each cable is connected to the right axis in the SAM box (see picture). Ensure all cables are properly connected and turn on device to test signal. If the SAM is displaying data for all 3 sensors, the vessel is ready for data collection testing and deployment.

Type 2 Deployment Vessel Diagram



Advantages:

- Remote collection capabilities
- Live data capabilities currently in test
- Data could also be easily manually retrieved by accessing electronics in a warm, enclosed environment.

Disadvantages:

- Increased cost due to the extension cables, larger risk of failure due to more components working together
- Range from power source is limited to range of the extension cables. Leading to a shorter range of deployment from a warm access point. However, there's a higher chance of developing remote access since all electronic components are always accessible.
- Increased probability of data noise due to longer sensor extension cables.

Places of possible deployment:

This type of vessel is aimed to be deployed at research stations, universities, or high schools with internal heated space for the electronic components as well as network access for remote data monitoring.

Due to hostile environments, the sensors can be buried and withstand hostile environments. Sensors are limited to shorter deployment distances since the extension cables are more expensive than power cords to extend the deployment range.

7. Overall Deployment Strategy

The deployment strategy consists of five stages that will be performed by members of the SWUG team, Highschool students and teachers.

A. SAM IV assembly

The assembly of the SAM III and IV kits will be done by members of the SWUG team as well as high school students and teachers. This part of the process will completely rely on the “SWUG Magnetometer Manual “.

B. SAM IV kit initialize, testing, settings.

The SAM IV will be tested by both the students and teachers, with supervision from the SWUG team to assist with any sort of issues regarding testing. The “SWUG Magnetometer Manual” contains all necessary details to initialize and test the devices. However, issues can always arise, and it is recommended to have open contact with members of the SWUG team to ensure this part of the process flows smoothly.

C. Sensor testing, Calibration.

Similar to part b, the fluxgate sensors will be tested and calibrated by the students and teachers according to the instructions provided in the SAM construction guide. Members of the SWUG team will check all sensors to ensure they are properly calibrated and provide consistent data samples.

D. Sensor Enclosure

The sensor enclosure assembly guide is meant to be fully understood by high school level students and teachers. However, supervision is recommended to ensure students are working in safe conditions. Help might also be required in certain parts that could present a bigger technical challenge. The SWUG team will also perform overnight and weekend testing of all completed sensor enclosures before completing the deployment vessels to ensure data quality every time.

E. Deployment Vessel build

Both types of research vessels are designed to be assembled following simple instructions. Supervision is also suggested at the time of initialization to ensure all components are working correctly. The SWUG team must check all components are installed correctly and the data is collectable and transmittable.

8. Current Deployment Progress

Bellow is a list of current deployment locations of Research Vessels.

A. Locations

- i. Farmers Loop, (Fairbanks AK)
- ii. Poker Flat (Poker Flat Research Range, Fairbanks AK)
- iii. Reichardt Building (Troth Yeddha Campus, Fairbanks AK) iv. Eagle River (Eagle River, Alaska)

9. Current Data Collection Progress

A. Manual

Manual data collection is fully functional and tested. Current work is focused on refining data samples and reducing noise.

B. Remote

First trials for remote data access are currently being worked on. Vessels will be accessed via ethernet cable or Wi-Fi through the Raspberry pis.

C. Live streaming

The construction of a data Center has been proposed with the intention of accessing live data plots. This part of the project is on the early stages and will be completely covered in the third volume of this guide.

10. Current and Future Work

The SWUG team is currently working in building and deploying as 8 more deployment vessels for a total of 12 deployments across Alaska. We are also working on refining the quality of our data to ensure all these vessels provide the best possible data samples. The future work will be focused on deploying all available vessels as well as creating a data center to collect and analyze data as well as a data archive to store such data to be used for further analysis and assist machine learning models along the MAGICIAN team.

11. References.

- Abell, G. O., et al. (1987). *Exploration of the Universe* (5th ed). Saunders College Publishing.
- Byun, W. E., et al. (2016). *Fluxgate Magnetometer*. MIT.
- Cohen, A. et al. (2021) *UAF SWUG SAM construction Manual*. University of Alaska Fairbanks.
- Garriott, R. (1969). *Introduction to Ionospheric Physics*. Academic Press.
- Gombosi, T. I. (1998) *Physics of the Space Environment*. Cambridge
- Hines, C.O., et al. (1965). *Physics of the Earth's Upper Atmosphere*. Prentice Hall.
- Kelley, M. C. (2009). *The Earth's Ionosphere* (2nd ed). Academic Press.
- Kivelson, M.G., Russell, C. T. (1997). *Introduction to Space Physics*. Cambridge
- Menk, F. W., Waters, C. L. (2013). *Magnetoseismology*. Wiley-VCH
- Reeve, W. D. (2018). *SAM-III Construction Manual*. Anchorage, AK: SAM.
- Seeds, M. A. (1995). *Horizons: Exploring the Universe*. Wadsworth Publishing Company
- Speake & Co. Limited (2018) *FMG Series Magnetic Field Sensors*
- Smith, W. C., et al. (2019). *The Space Weather Underground: A Student-Built Array of Ground*

Added in original format

Appendix E: Comprehensive Manual for the SWUG Multi-Deployment-Vessel. A
Manual by Jonah Barkley-Griggs

Construction

The device consists of a 4"-6" length section of a 6" diameter PVC pipe, inserted into a PVC cap at one end and a PVC threaded adapter at the other. These off-the-shelf components are permanently sealed and made waterproof using PVC cement. To that end, using at least two layers of thread sealant tape and generous application of pipe-dope on a threaded cap has been successful in holding back water. With the cap's recess obverse to the side facing you, apply the tape primarily on the bottom and in a counterclockwise fashion¹. This reduces the chance of the tape bunching up and ensures the tape will fully contact the threads of both the cap and adaptor. Pressure fit into the threaded cap is the first and most important printed component called the sensor housing². Three sensors, wrapped in fiberglass insulation, are held within the housing. The insulation keeps the sensors in place and provides thermal protection. Markings on the top of the cap indicate the direction of each sensor. Another component called the Alignment Plate can be printed to give a more precise indication of the sensor's orientation³. This is done so the vessel can more easily be positioned with 'x' facing north. And a third component called the separator may be printed to hold the SAM PCB and insulate the exposed pins⁴. This component also helps space out the other parts, reducing interference. The sensor cables⁵ should be cut to a length which allows them to twist around each other while the cap is being screwed in. Secure the cables to the sensors with jumper cables and wrap the area in tape as this joint is susceptible to disconnect during assembly.

In the bottom cap of the vessel, a hole is drilled just large enough to accommodate the RJ45 plug⁶. Alternatively, the hole can be made smaller if one has the tools required to assemble the cable after threading it through the hole⁷. However, a hole the size of the RJ45 jack is small enough that this appears to be unnecessary. After the short CAT 5 cable is threaded through the hole, an extension cord/splitter with three receptacles on one end is prepared by cutting it into three pieces: one cable and both ends⁸. The side of the cord with three receptacles rests in the base while the rest of the attached cord is fed through the hole in the bottom cap. The two ends of the power cable are then soldered together, discarding the middle wire. The pipe is then inserted into the base for test fitting. If the hole is not low enough, it may be necessary to drill out a slot for the wires. For waterproofing use epoxy, silicone, or expanding foam to seal the hole. Silicone designed to seal fish tanks has proved the most reliable of these options. PVC cement can then be applied to the connection between the cap and pipe⁹. At this stage, one should test if it is possible to fit the 3D printed separator through the hole in the threaded adapter. The separator is designed with some compliance, but if the separator cannot fit, one should place it in the pipe before continuing to the next step. If this is unnecessary, assembly will be easier if

¹ See [Fig10 pg8](#)

² More information on [page 3](#). Schematic at [pg11:b](#)

³ Schematic at [pg11:a](#)

⁴ Schematic at [pg10](#)

⁵ Three Wires of equal length should be constructed in accordance with *Optimization techniques in the assembling, testing, and deployment for SAM IV Magnetic induction Data Collection Vessels B:1*

⁶ See '[Detailed Assembly Instructions. Making and Sealing the Cable Passthrough](#)' for more information. B:2

⁷ See [fig11 pg8](#)

⁸ See [fig7 pg8](#)

⁹ For more information on the usage of PVC cement, refer to '[Detailed Assembly Instructions. Usage of PVC Cement](#)' pg7

the separator is left outside until a later step. Next, the threaded adapter is attached with PVC cement⁹. Apply pipe dope to the threads of the adapter where the cap will interface. There should be no gaps in the application. At this stage, if not already done thread tape is applied to the cap¹⁰. Using a vice or wrench, tighten the cap onto the vessel. The waterproofness of the vessel should be tested in each assembly by fully submerging the vessel in water for two minutes or more¹¹. If waterproofing is not achieved, increase the amount of sealant. If this is unsuccessful, refer to the ‘Leaks’ entry in the ‘Maintenance and Troubleshooting’ section of this manual¹². Once sealed, the device is re-opened, and the power cables for the mini pc and SAM PCB are plugged into the extension cord. Shortening the internal power cables is optional but decreases the space required and makes cable management easier. The sensors are connected to their wires and tightly wrapped in fiberglass insulation. They are placed in their slots and checked to make sure they are oriented properly and unlikely to move. Zip ties can then be fastened around the channels in the sensor housing ensuring the sensors do not come out. This assembly should be placed into the cap with careful attention to orientation. To facilitate this, the 3D printed alignment plate has a narrow slot which should run parallel to the ‘x’ sensor slot¹³. Marking where the ‘x’ sensor is orientated on the lid ensures redundancy if the alignment plate is separated.

The power, ethernet, and USB-to-serial and temperature sensor¹⁴ connectors are then plugged into the 3.8x3.8x0.78 inch fan-less mini-computer. Anything which needs to be done via USB can be done at this stage. The power button will remain accessible until the vessel is closed. The computer is configured to automatically start up and begin sending data to the server when plugged in. There are multiple methods to connect to the device once it is closed, some include Remote Desktop Protocol, SSH, or VNC software. The PC rests at the base of the vessel with the serial cable wrapped around it. The SAM is then screwed into the separator, insulating the contacts. This assembly sits atop the PC with the sensor cables attached. If there are problems with crosstalk, one can tape a layer of aluminum foil to the side of the printed sensor housing which faces away from the threaded cap. This would provide extra magnetic shielding against the alternating currents generated by the components and power cable. Aluminum should not interfere with the sensor data. Alternatively, one could wrap the foil over the components on the lower half. However, the foil may be crumpled and moved to one side by the wires when screwing in the cap.

Before screwing in the cap, the screen and keyboard are attached to the PCB to check if all sensors are connected properly. Remove the screen and keyboard before completing assembly.

When closing the vessel, it is important to counter twist the cables. Experimentation has revealed that even when this is done, the cables are liable to become detached from the sensors, so it is important to make sure all are still attached by checking the computer’s incoming data post-assembly.

¹⁰ [Fig8 pg8](#)

¹¹ [Fig12 Pg8](#)

¹² The Leaks section is located on [page 5](#)

¹³ [Fig9 pg8](#)

¹⁴ More details on the temperature sensor in Chapter 4, Section 4.3 *Design, calibration, and experiments to improve feasibility of student-built magnetometers for heliophysics research*

Deployments

The device can be deployed as a surface vessel or a buried vessel.

To account for instability in a surface deployment scenario, two simple structures have been developed to level the device when deployed on a surface. Both structures consist of a board and four pegs. In one design, the pegs are glued on to the board such that they support the sides of the vessel, thus keeping it vertical¹⁵. In the event that the previous design is not suitable, the pegs can be attached closer together with the device resting atop¹⁶. Strong adhesive is used to secure the bottom of the device to the stilts. This design should only be used on a flat surface, and only serves to prevent rocking of the vessel.

When deploying as a buried vessel, the structure is unnecessary as the hole itself may keep the device vertical. A small trench must be dug from the hole to accommodate the power and ethernet cables. This prevents the power cable from coming too close to the sensors. It is advised that one check the magnetometer and temperature data before burying the device. Use of ethernet and power extension cords is highly encouraged as it distances the vessel from any buildings.

The device is preconfigured to work with Ethernet. To deploy, first plug the device into an ethernet port, then plug in the power. The device will connect to the server and VPN automatically establishing a remote connection. To use SSH, log into the VPN server to see the new IP address for the device. Data collection is started with the command 'service gima_launch start'. Re-enter the command to test if the device is collecting. If the computer says it is starting to collect data the second time, an error has occurred¹⁷. It is advised that one check the data values on deployment of the vessel, as returning to the deployment site may be inconvenient and errors may be discovered when looking over the values¹⁷.

3D Printed Sensor Housing

The prototype for the 3D printed sensor housing consisted of a 162.4 mm diameter disk, 38.1 mm thick with two 38.1x70 mm rectangular holes positioned such that the sensors could be arranged to maximize the distance between their tips. Semi-circular gutters run along one face of the rectangular holes. These exist to accommodate the wires protruding from the FGM3 sensors. Protruding from one of the circular faces of the disk is a cylindrical shaft 52.1 mm in diameter and 40 mm in length. A 38.1 mm diameter hole in the shaft goes through the entire object to accommodate the third FGM3 sensor. The filament used was 159 grams of HPLA. The print time was 14 hours, 46 minutes. When printed, the model was printed upside-down to eliminate the need for scaffolding and therefore reduce complexity. In theory, this version could be easily reproduced with clamshell injection molding methods.

The second version had improvements based on new ideas and practical tests with the working print. Additional holes in the larger cylinder were made to increase the speed of the print and reduce material waste. The high structural rigidity of the prototype print exceeded expectations suggesting that there was excess material. Other changes include a reduction in the thickness of the larger disk from 38.1 mm to 26 mm with a step down to a radius of 73.03 mm at 21 mm from the top. This was done for two reasons. First, this also reduces the time of the print and the amount of filament necessary for the print. Second, the threaded adapter component has

¹⁵ See [Fig5](#)

¹⁶ See [Fig6](#)

¹⁷ See '[Maintenance and Troubleshooting](#)' for instruction on handling errors.

an inner lip that interfered with the original prototype. To make the initial prototype fit, modifications to the lip were necessary. And part of the printed shaft needed to be cut off. These changes should eliminate the need for these modifications resulting in easier and faster assembly. Other design changes include a reduction in the radius of the internal hole in the shaft and a reduction in the lesser dimensions of the rectangular cutouts to 26 mm. This was done because the size of the holes was found to be excessive, thus requiring extra insulation and lowering the tolerance for the distance between the sensors. The outer radius of the shaft was also reduced to 32 mm. This is a reduction in the overall wall thickness which increases clearance and reduces material use at a negligible cost to rigidity. Two additional holes were added 4 mm from the outer edge of the rectangular holes. 2 mm deep trenches run along the top side of the disk 90 degrees to the rectangular holes. They originate from the new holes and continue toward the center of the disk. These features were added to accommodate zip ties if the pressure from insulation proves insufficient to hold the sensors in place long-term. The zip ties add reliability to the design without becoming an obstacle to maintenance. The total height of the design has also been reduced from 78.1 mm to 67 mm due to excess room in the shaft of the original design. To reduce confusion when orientating the sensor housing, axes labels were added to the ends of the sensor slots. All these changes serve the dual purpose of reducing the print times and amount of filament necessary.

The latest version built upon these principles and included a minor adjustment to sensor placement as governed by geometric principles for maximizing the distance between sensor tips. It uses 159g of PLA and takes 10h though results may vary depending on one's printer setup and slicer.

Interference Experiments

The vessel was fully assembled and set up to collect data overnight with a solenoid aimed at it to provide a stable magnetic field. The data gathered had variations of $\sim \pm 43$ nT measured at various intervals. Potential sources for the measured variations include devices in the room, wiring in the walls of the room, cable crosstalk, crosstalk from the PCB to the cables, crosstalk from the pc, and interference from the power chords.

In a similar experiment, the crosstalk was measured at $\sim \pm 5$ nT. This experiment was performed in a more controlled environment and the pcb, computer, and power source were distanced from the sensors. The relative position of the sensors to each other was approximately the same in both experiments. The Z sensor was ~ 97 mm from the Y sensor and ~ 80 mm from the X sensor. The distance between the Y and X sensors was ~ 103 mm.

In a third experiment, a layer of aluminum foil was added to the bottom of the printed component. The vessel was set collecting data next to a box magnetometer. A solenoid was run at 12 volts and 2 amps to provide a stable magnetic field. The interference measured was $\sim \pm 0.25$ nT in both the prototype and the box.

Maintenance and Troubleshooting

The vessel was designed with maintenance in mind. The largest barrier to maintenance and troubleshooting is the watertight lid. This is why it is important to do checks on the system before the lid is closed. If an error does occur after closing the lid, the first step is to remotely restart the device. This can be done with the command 'reboot'.

If the issue is not resolved through this process, in-field maintenance may be necessary. For in-field maintenance, bring: a multimeter, ~2mm flathead screwdriver, Phillips screwdriver, keyboard, SAM screen, USB to Serial to SAM adapter assembly, electrical tape, pipe dope, thread tape, spare zip ties, a cutting implement, a compass, and disposable gloves. If available, it may also be useful to bring a large wrench (large enough to fit around the square top of the screw-on cap), as the cap may be difficult to unscrew.

Failed Connection: If the device is showing up on the VPN software, it must be connected to both ethernet and power. If it has not connected to the VPN, check both cables and make sure they are connected properly. Also, check the router and the solder joint in the power cable. If all are properly connected and functioning the computer may have to be reprogrammed. When removing the computer check for evidence of water ingress into the vessel. If there is any moisture check all other electrical components for damage and locate the source of the leakage. For further information, continue to the next paragraph. If the cap was removed, use the compass to re-orient the vessel.

Leaks: Common points of water ingress are the threads, joints between the pipe and adapter or cap, and the cable hole. If the threads are leaking, increase pipe dope and or thread tape as needed. If the joints between the pipe and cap or adapter are suspected to be leaking, adding silicone sealant to the outside edge of the suspected joint may solve the issue. Take care to make sure the silicone completely covers the gap between the inside edge of the cap or adapter and the pipe. If the cable hole is leaking, add more silicone to the inside and outside of the vessel at the point of the wire's entry. Take care to seal the underside of the wires and the space between them.

Gima Launch Start failure: First try rebooting the device. If rebooting the device was unsuccessful, use the command “\$ dmesg | grep tty” to list terminals communicating with the computer. Identify the port connected with the SAM, it may be listed as something similar to “ttyUSB0”. Follow with the command “\$ cat /dev/[port leading to SAM]”. This command should display the input from the SAM, if no data is being displayed, proceed to the ‘Missing Data’ section. Otherwise check if the data follows this format “dd.mm.YY HH:MM:SS: X,####,Y,####,Z,####”. If it does not, the SAM may be running the incorrect firmware version. Please use the firmware version from the website to rectify the issue.

Missing Data or Data Errors: Open the device and press the reset button on the SAM PCB. If this does not fix the issue, attach the SAM's screen, and restart the SAM. If the screen does not display any data, the SAM may not be receiving power or the PCB may be damaged.

Otherwise, unplug the serial connector from the SAM and plug in a serial connection to your computer. Use serial port reading software (example: Tera Term) to read the data coming from the SAM. If the data looks normal, there may be an issue with the serial adapter assembly in the vessel. Check all the wires in the cable for continuity and shorts using a multimeter and proceed from there. If all the connections are sound, refer to the SAM manual¹⁸.

If your computer is not receiving any data, the serial connector on the SAM may be damaged. Check the solder joints and wires for breaks and shorts.

If the serial cable is wired correctly and the data is incomplete or abnormal but being received, check the connection between the SAM and the sensors. The areas of the wire most prone to breakage are the connection to the SAM, the capacitor assembly, and the connection to

¹⁸[SAM-III Construction Manual](#)

the sensors. It may be necessary to cut the zip ties and remove the sensors to check the sensors or the connecting wires for damage. If this is done, take note of which sensor belongs in each axis. After closing the device, use the compass to re-orient the vessel.

Incorrect timekeeping: The clock data in the output file is produced by the computer which is synchronized with an online clock. The SAM PCB also has timekeeping capabilities and if the software is not properly configured, it may be reporting the SAM time instead of the computer time. It is also possible that the computer time is not functioning properly. These issues may manifest as clock drift. If the clock data is consistent but offset, the computer may be set to local, or daylight savings time as opposed to UTC. The exact cause can be diagnosed remotely. The issue may be possible to fix remotely, or it may be necessary to recover the computer from the device and do a full reset.

Detailed Assembly Instructions

Tools List:

Vice
Gloves

Snippers
Screwdrivers

Drill
3D Printer

File

Making and Sealing the Cable Passthrough:

- 1) Mark a location near the base of the PVC cap.
- 2) Drill multiple small holes in the PVC cap such that the outer edges are slightly larger than a RJ45 connector.
- 3) Use snippers to cut out the material between the holes. The resulting hole should be vaguely rectangular.
- 4) Test that the RJ45 connector can fit in the hole. If not, use a file to expand the hole. If necessary, drill more holes.
- 5) Use a file to remove any burs created.
- 6) Thread the ethernet cable and power cable through the hole. To fit the power cable through the hole, cut it in half. Place the receptacle end of the power cable inside the cap and push the severed end through the hole and past the RJ45 connector.
- 7) Pull enough of each cable into the base to attach all components. Then tape the cables in place.
- 8) Put liquid silicone under, around, between and above the wires such that there are no gaps.
- 9) Before the silicone dries, join the PVC pipe to the PVC cap using PVC cement.
- 10) After the pipe and cap are joined, make sure both sides of the hole are completely sealed with silicone.

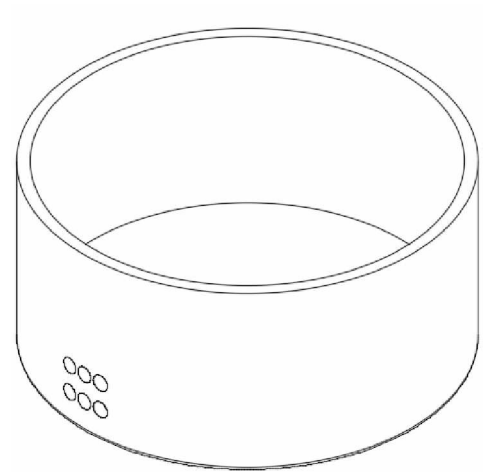


Figure 1

Usage of PVC Cement:

1) First, saturate the primer brush with primer. Press it against the **inside** wall of the can to reduce dripping. Then apply the primer to the inside wall of the PVC cap (Fig 2). It may be necessary to dip the brush in the can again.

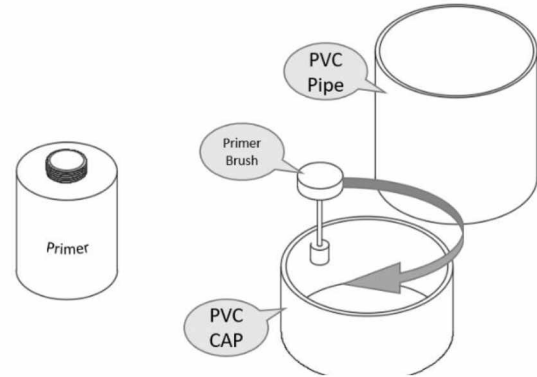


Figure 2

2) Next, re-saturate the brush with primer. Press it against the inside wall of the can to reduce dripping. Then apply the primer to the **outside** wall of the PVC pipe (Fig 3)

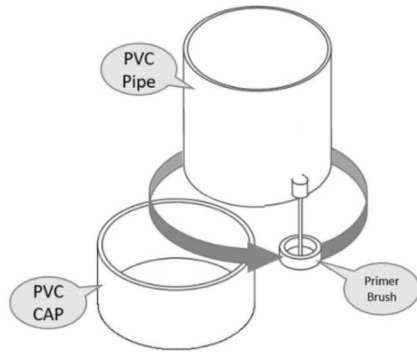


Figure 3

3) Repeat steps 1 and 2 using PVC cement instead of primer.

4) Quickly press the PVC pipe into the PVC cap. The pipe should pinch the cables and the silicone should mold itself around the pipe, creating a better seal. *after this step, test fit the separator*

5) Saturate the primer brush with primer. Press it against the inside wall of the can to reduce dripping. Then apply the primer to the **inside** wall of the PVC Adapter wherever the pipe will touch the surface. (Fig 5).

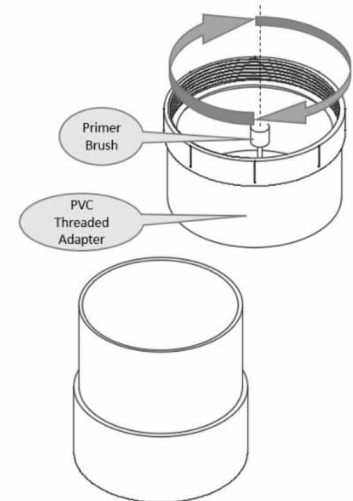


Figure 5

6) Saturate the Primer brush and press it against the inside wall of the can. Apply the primer to the **outside** wall of the PVC pipe where the two components will overlap (Fig 4).

7) Repeat steps 5 and 6 using PVC cement instead of primer.

8) Quickly press the two components together ending at the desired length.

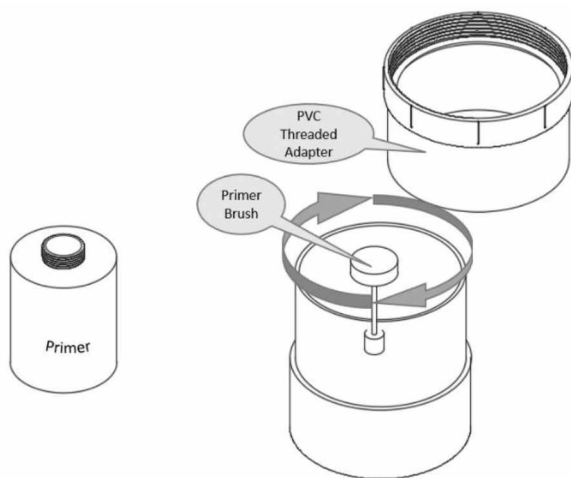


Figure 4

Cost Breakdown:

Variable Costs (Estimated Maximum):			Fixed Costs (Exact; per Device):	
Item	Unit cost	\$ per Device	Item	Cost \$
PVC primer	1.19 \$/oz	0.10	4-40 3/4" bolts & nuts x3	0.52
Thread tape	0.52 \$/roll	0.26	Solderless jumper wires	0.78
Pipe dope	2.70 \$/oz	0.45	Zip ties	0.80
Silicone	0.99 \$/oz	0.49	RJ45 coupler	1.83
Gloves	0.26 \$/pair	0.52	Power cable	2.51
PVC Cement	0.64 \$/oz	0.64	3d printed components	3.89
Heat-Shrink	0.55 \$/piece	3.29	Short CAT 5 cable	9.97
6inØ PVC Pipe	7.04 \$/ft	3.52	6inØ PVC threaded lid	10.98
Insulated cable	5.09 \$/ft	15.27	Temperature PCB & sensor	18.31
Labor	5 hrs	~ 65.00	6inØ PVC end cap	17.98
Fiberglass Insulation	0.82 \$/ft ²	<0.01	6inØ PVC adapter	23.28
Electric tape	1.83 \$/roll	<0.01	Power extension cord	28.57
			150 ft CAT 5 cable	46.97
			Computer	82.79
			SAM-III kit	400.00
Total cost: ~738 USD (as of April 2023)				

Other Figures

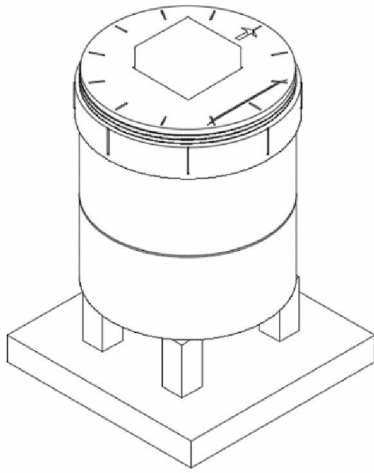


Figure 10

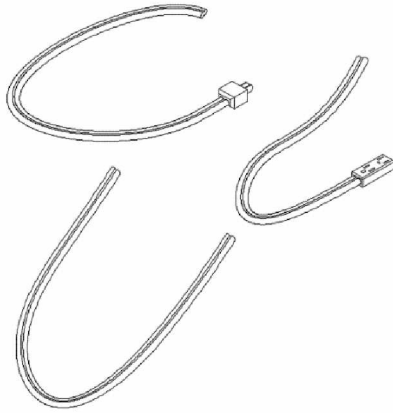


Figure 9

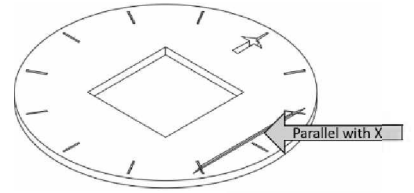


Figure 6



Figure 10 a

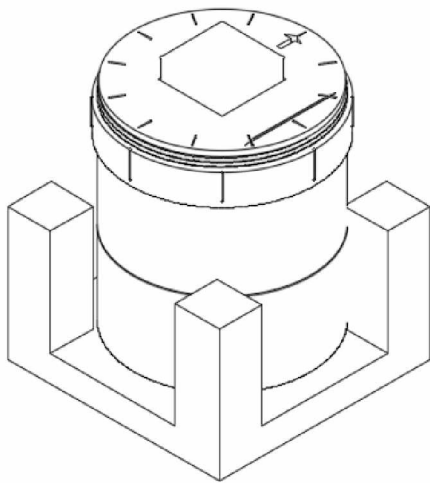


Figure 8



Figure 11

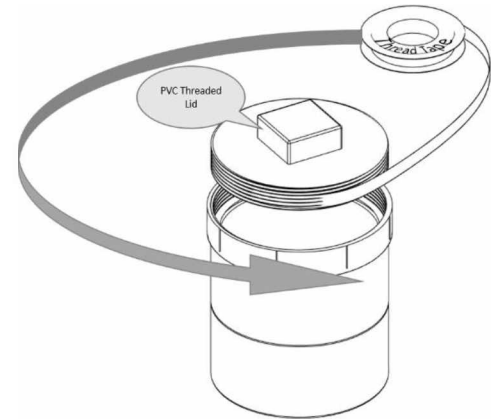
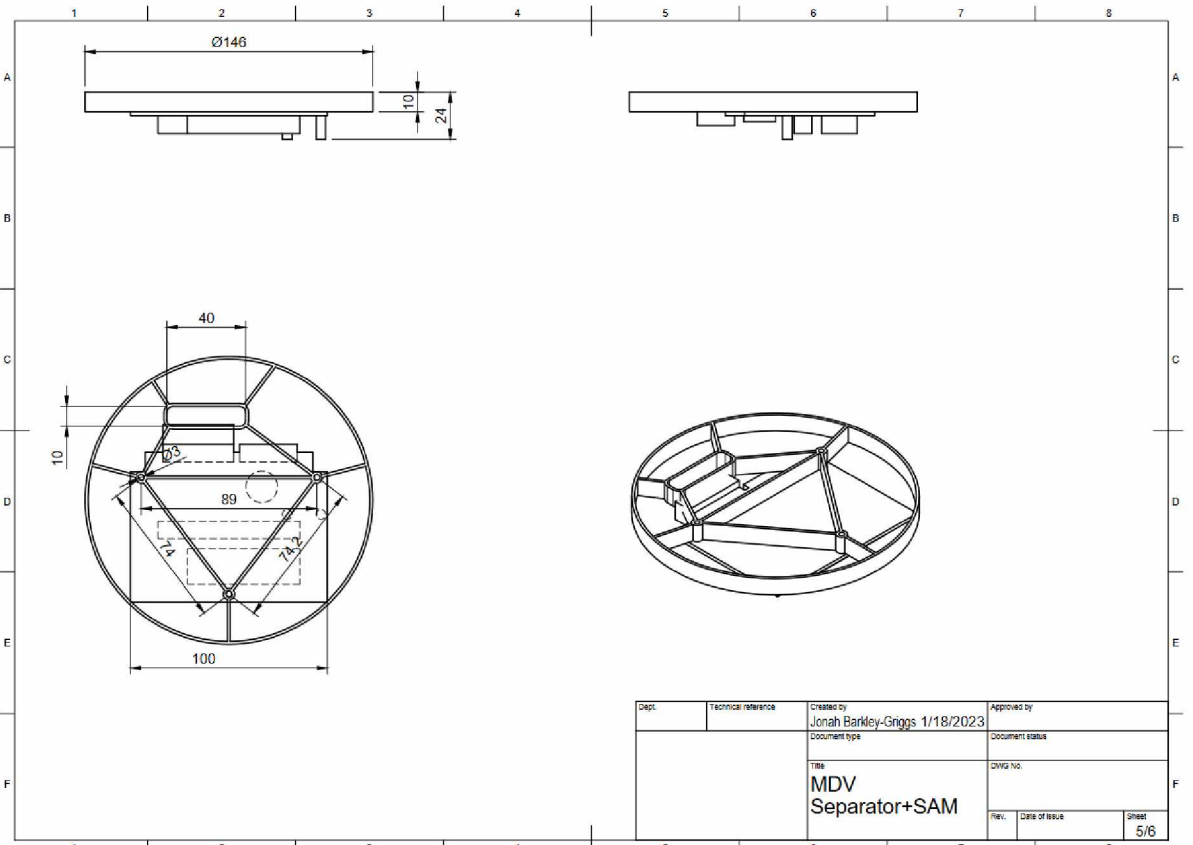
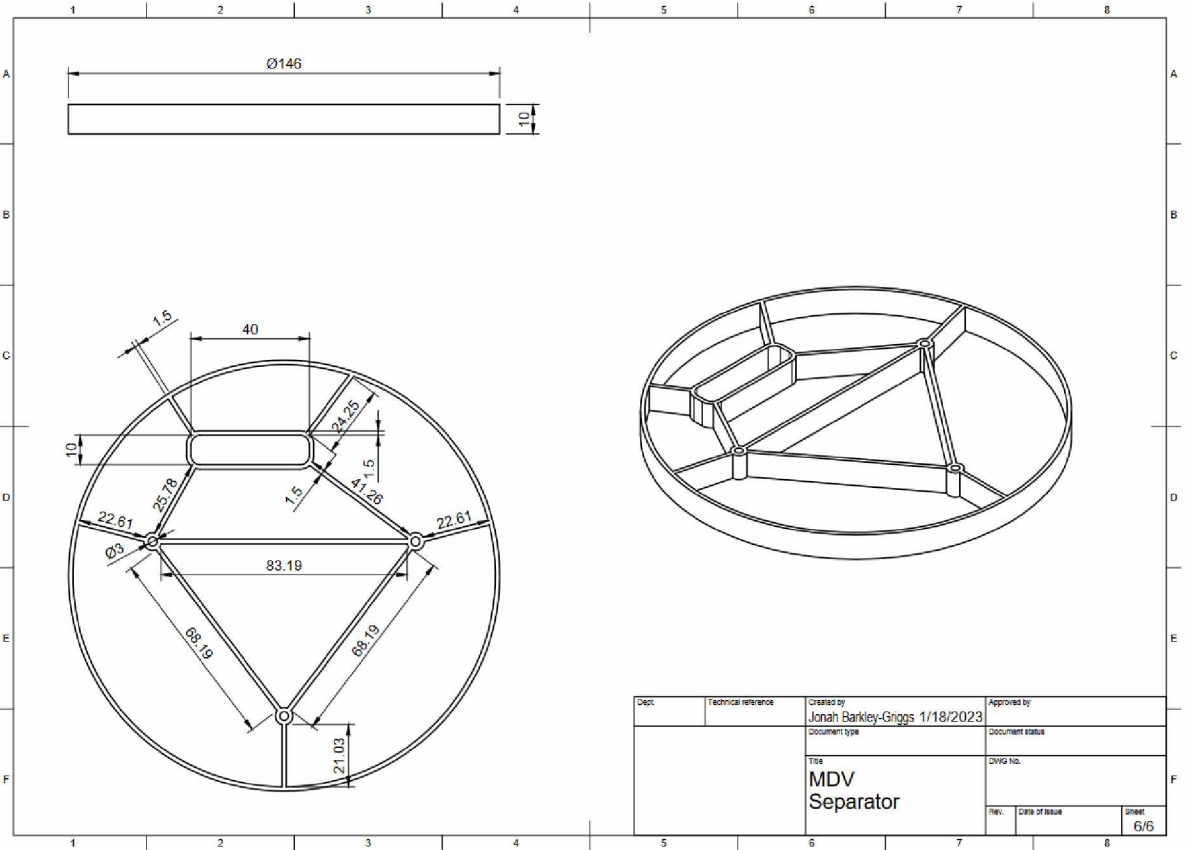


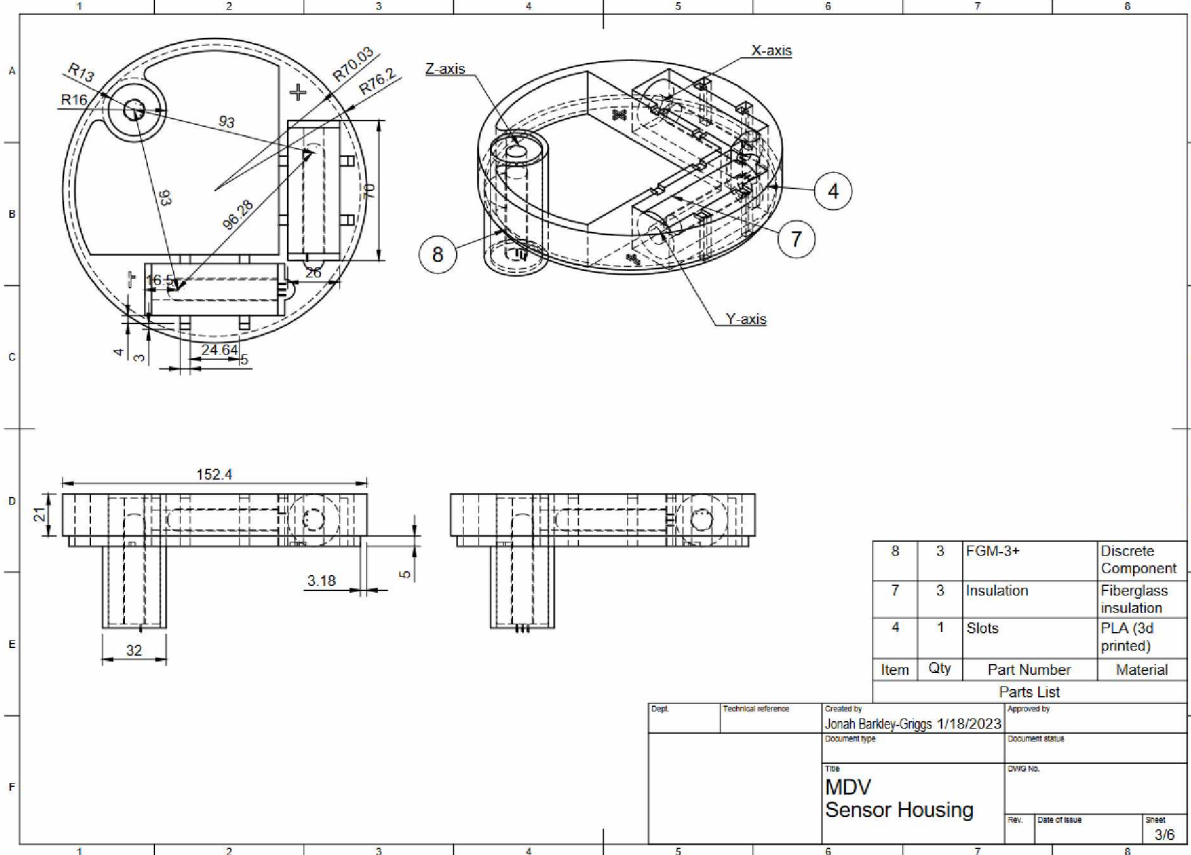
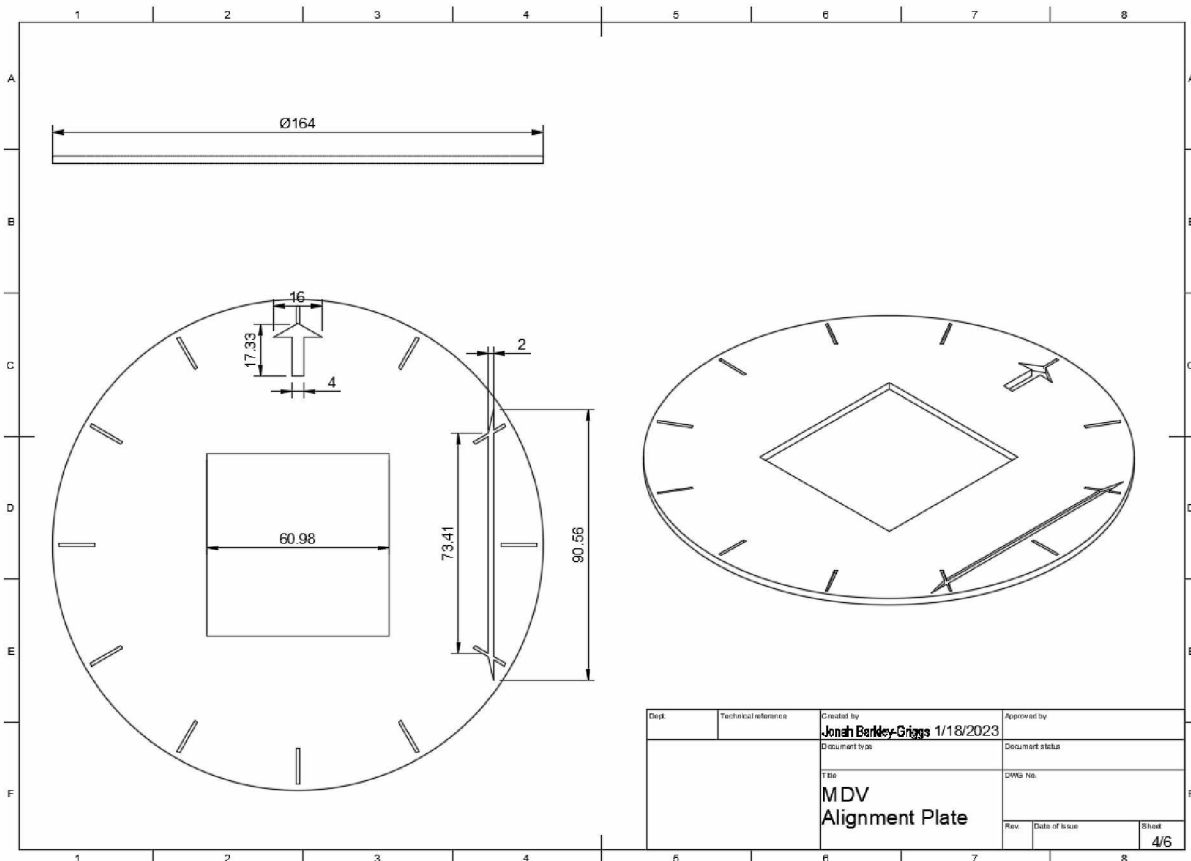
Figure 7 b

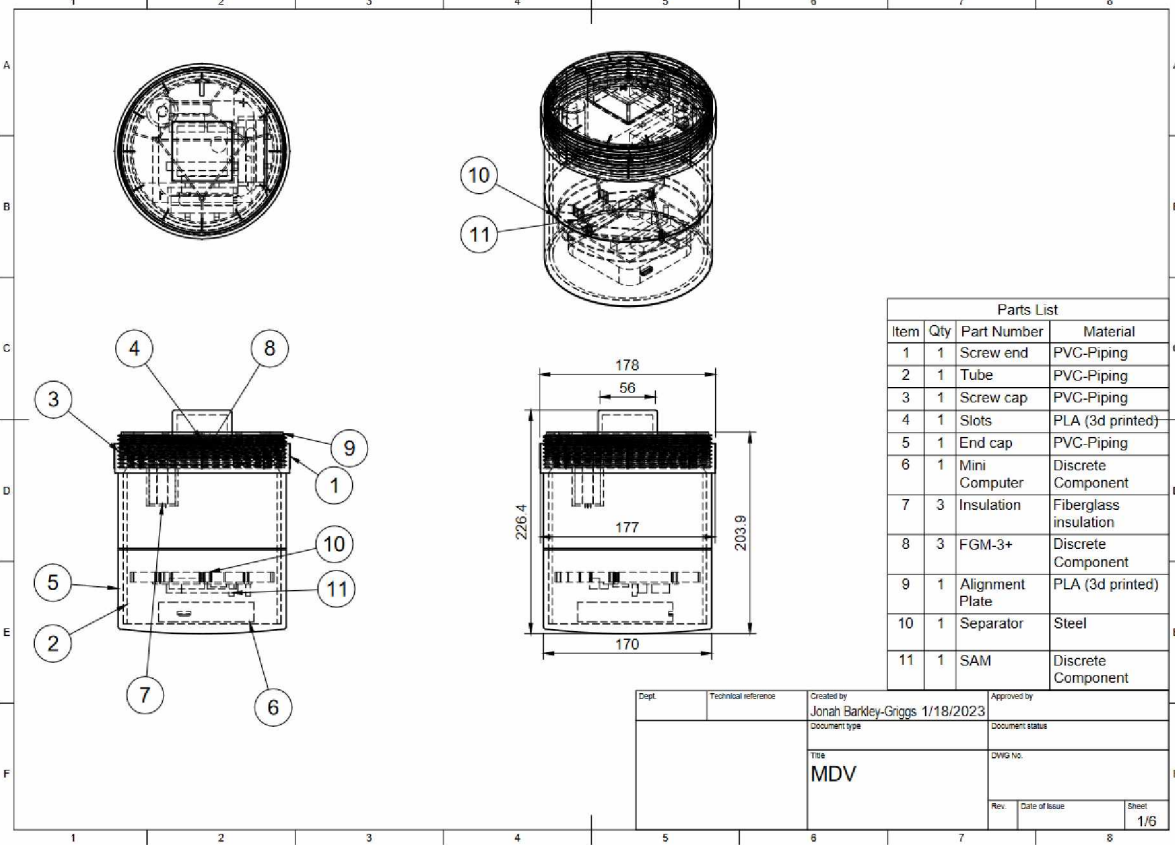
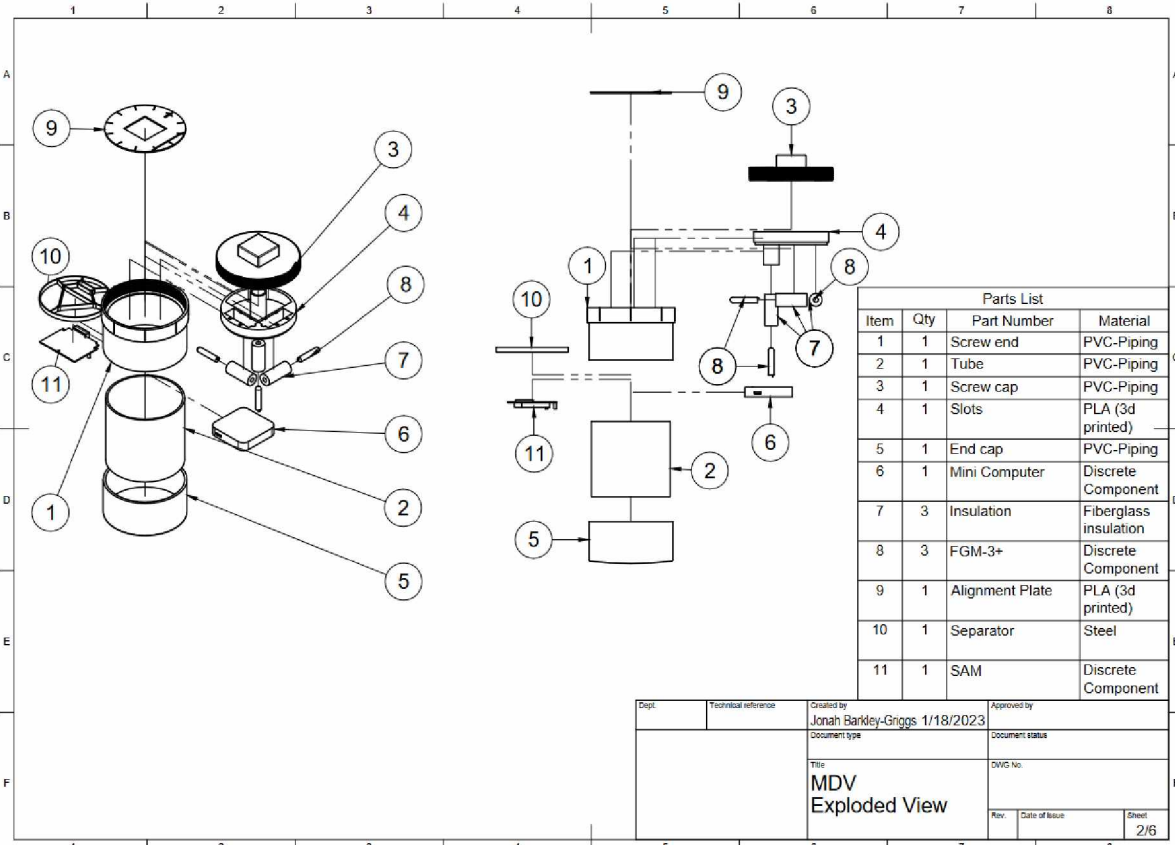


Figure 12

Schematics:







References:

Reeve, W. D. (2018). SAM-III Construction Manual. Anchorage, AK: SAM.

Chapter 4, Section 4.3 of Cohen, A. (2023). Design, calibration, and experiments to improve feasibility of student-built magnetometers for heliophysics research. University of Alaska, Fairbanks.

Reyes-Mora, J. (2021). Capstone Report: Optimization techniques in the assembling, testing, and deployment for SAM IV Magnetic induction Data Collection Vessels. University of Alaska, Fairbanks.

